RESEARCH INTO THE PROPERTIES OF LATERITIC GRAVELS AND THEIR IMPACT ON PAVEMENT DESIGN

PETER NG'ANJO

A thesis submitted to the Faculty of Engineering,
University of Stellenbosch, in partial fulfilment of the requirements
for the degree of Master of Science in Engineering

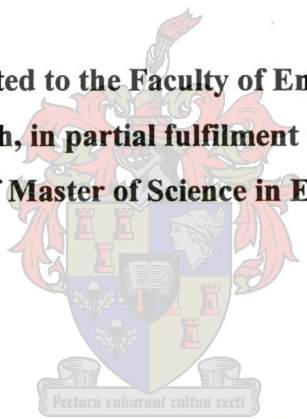

Study leader
Prof. MFC van de Ven

Internal examiner
Prof. F. Hugo

External examiner
Dr. P.J. Strauss

Stellenbosch, October 2000

Declaration

I, the undersigned, do hereby declare that the work contained in this thesis is my own original work and has not been submitted previously in its entirety or in part at any university for a degree.

Signed:

Date:

Abstract

Laterites are used extensively in the tropics as road building materials in unbound base, sub-base layers and in surface layers. However, most base course specifications usually require the provision of crushed and graded stone or stabilized base and often exclude the general use of as-dug laterites or other naturally occurring gravels. Various field studies in the past have clearly indicated that many lateritic gravel deposits can be used successfully as base course materials in roads carrying low to medium traffic without incurring additional maintenance costs and with considerable cost savings in pavement construction rehabilitation.

Further research is needed for the more precise definition of the relationship between laterite characteristics, traffic loading, environment, and pavement performance. In this study, extensive use was made of static and cyclic triaxial testing to investigate the fundamental behaviour of a lateritic gravel material. The tests produce information for characterizing the shear strength, stress-strain properties and behaviour under repeated loading. The gravel was sourced from stockpile at Malans Transport borrow pit at Maaitjies Kuil near Cape Town. Testing was conducted on the material both as granular material and stabilized with cement and foamed bitumen. Testing was done under various conditions of stress, moisture and compaction. The resilient modulus of the lateritic gravel was found to be affected by moisture and compaction apart from the stress condition. Well known models were used to characterize the stress-dependent resilient modulus. A model for prediction of permanent deformation was developed which together with the resilient modulus model were applied to the design of a light pavement structure composed of lateritic gravel base.

Samevatting

Lateriete word wydverspreid gebruik in die trope as 'n padbou materiaal. Die materiaal word gebruik in ongebonde kroonlae, stutlae en oppervlaklae. Die meeste spesifikasies vir kroonlae vereis dat gegradeerde gebreekte klip of gestabiliseerde materiaal in die kroonlaag gebruik word. Die spesifikasies maak nie voorsiening vir lateriet en gruis wat natuurlik voorkom nie. Verskeie veldstudies in die verlede het duidelik getoon dat lateritiese materiaal met sukses gebruik kan word in die kroonlae van paaie wat ligte tot medium verkeer dra. Lateriete kan gebruik word sonder addidionele onkoste vir instandhouding en daar is merkbare kostebesparings wanneer plaveisels rehabiliteer word.

Die verhouding tussen lateriet eienskappe, verkeerslas, omgewingsinvloede en plaveisel werkverrigting moet beter gedefinieer word deur verdere navorsing. In hierdie studie is omvattend gebruik gemaak van eenmalige en herhaalde belasting drie-assige toetse om die fundamentele gedrag van lateritiese materiaal te definieer. Hierdie toetse se resultate lewer inligting oor die skuifsterkte, spanning-vervorming eienskappe en gedrag onder herhaalde belasting.

Die gruis wat gebruik is, is verkry vanaf 'n materiaalopslag by die leengroef van Malans Transport te Maaitjies Kuil naby Kaapstad. Die materiaal is getoets as granulêre materiaal en gestabiliseer met sement en skuim-bitumen. Die toetse is gedoen onder verskillende toestande van spanning, voginhoud en verdigting.

Daar is bevind dat die veerkragtigheidmodulus van die lateritiese gruis nie net deur die aangewende spanning beïnvloed word nie, maar ook deur die voginhoud en verdigting van die materiaal. Welbekende modelle is gebruik om die spannings-afhanklike gedrag van die materiaal te karakteriseer. 'n Model is ook ontwikkel om die permanente vervorming van die materiaal te voorspel. Die twee modelle vir die veerkragtigheidsmodulus en permanente vervorming is gebruik om 'n ligte plaveiselstruktuur mee te ontwerp wat 'n lateritiese kroonlaag bevat.

To my mother

Acknowledgements

I would like to thank the following people and organisations:

NUFFIC, for the postgraduate scholarship

Prof. van de Ven, for his valuable guidance and supervision of this thesis

Prof. F. Hugo, for the vital suggestions

Dr. P.J. Strauss, for the worthwhile comments

Kim Jenkins and Andrè Smit, for help with the MTS machine

The geotechnical laboratory team, for lending a hand

All colleagues at ITT, for their interest and moral support

"....to the King eternal, immortal, invisible, the only God, be honour and glory for ever and ever. Amen." 1 Timothy 1:17

Contents

List of figures

List of tables

List of symbols and abbreviations

a_l	Layer coefficient
AASHTO	American Association of State Highway and Transportation Officials
c	Cohesion
CBR	California Bearing Ratio
CLT	Cyclic load triaxial test
DSN	Design Structural Number
E	Elastic modulus
ESAL	Equivalent Standard Axle (80 kN)
ITS	Indirect Tensile Strength
LL	Liquid Limit
LVDT	Linear variable displacement transducer
N	Number of load cycles
OMC	Optimum moisture content
MDD	Maximum Dry Density
MTS	Materials Testing System
PL	Plasticity Index
PI	Plasticity Index
S	Soil Support Value
SATCC	Southern Africa Transport and Communication Commission
UCS	Unconfined Compressive strength
Mr	Resilient modulus
F	Safety Factor
S/R	Silica/sesquioxide ratio
ε	Strain
ϕ	Angle of internal friction
γ	Density
ν	Poisson's ratio
σ	Stress

1 INTRODUCTION

1.1 Background

Laterites occur widely across the tropics where climatic conditions favour their formation. They are used extensively in the tropics as road building materials in unbound base, sub-base layers and in surface layers. However, base course specifications in most countries usually require the provision of crushed and graded stone or stabilized base and often exclude the general use of as-dug laterites or other naturally occurring gravels. Various field studies in the past have shown that many of the laterite deposits can be used successfully as base course materials under a wide range of circumstances with considerable cost savings in pavement construction and rehabilitation and without incurring additional maintenance costs.

Pavement design procedures in use in most countries in the tropics are for most part empirical and have largely been adopted from those developed in the temperate zone countries. This means such design procedures apply to the environmental and loading conditions under which they were developed. Transfer of such methods to different environments, materials and axle loading lead to inadequate designs or over design. Analytical design methods, now in increased use, offer the opportunity for more realistic designs but require a more fundamental understanding of the properties of the materials and response under loading. Using laboratory cyclic load triaxial testing, the fundamental stress-strain properties of granular materials and their behaviour under repeated loading can be investigated. In a triaxial test, testing can be done under different conditions of stress, moisture and compaction to simulate conditions in a real pavement structure. Results from static and cyclic load triaxial testing yield fundamental parameters that describe the shear strength, resilient stiffness and resistance to permanent deformation of granular materials providing inputs to analytical design methods.

1.2 Objectives

To study the properties of laterite gravels and demonstrate the application of the results to design of pavement structures, with particular reference to the Zambian environment.

1.3 Methodology and Scope

The test programme comprised mainly laboratory tests for material characterization on lateritic gravel and triaxial testing in the MTS machine (Materials Test System, described in Chapter 5) of the Civil Engineering Department at the University of Stellenbosch. Because of the large quantity of material needed for triaxial testing, gravel only from one stockpile was used for the test programme. The size chosen for the triaxial specimens was 150mm diameter by 300mm high. Tests were conducted on the gravel both as unstabilized material and stabilized with cement and foamed-bitumen. Results from the tests were used to develop models for resilient stiffness and permanent deformation providing input to mechanistic design of a model pavement structure composed of a lateritic granular base under a thin bituminous surfacing.

A 4 weeks visit to Zambia was done during which road design related information and information on the road delivery network was collected. In Zambia lateritic gravel remains an important road building material. Therefore, this research partly focused on the Zambian situation so that results would be of relevance to pavement design and construction in Zambia. However, attempts to transport large quantities of laterite required for triaxial testing from Zambia to South Africa proved difficult because of the high cost. As a result a lateritic gravel had to be sourced from a nearby burrow pit at Maaitjies Kuil in CapeTown which was considered a suitable substitute.

The structure of the research programme is shown diagrammatically in Figure 1.1.

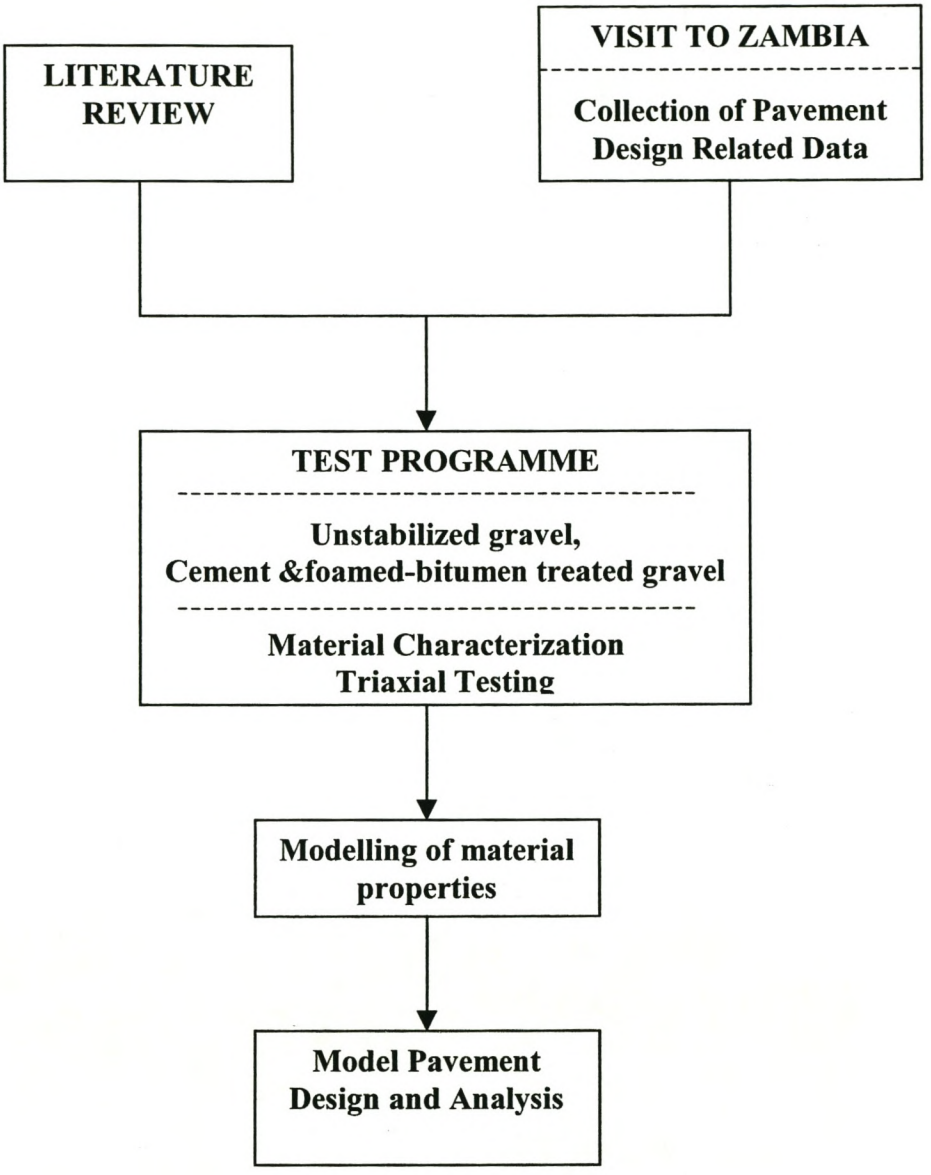

Figure 1.1 Structure of the research programme.

1.4 Outline

Firstly, a review of the literature on lateritic soils and gravels is given in Chapter 2. Chapter 3 describes the mechanical behaviour of granular materials and models used to characterize this behaviour. In Chapter 4, information on the Zambian road delivery network, common pavement structures and road building materials, is given. The test programme is described in Chapter 5 followed by a presentation and analysis of results in Chapter 6. Further analysis is done in Chapter 7 with the modelling of the stress dependent resilient modulus and development of a permanent deformation model. These models are then applied to design a model pavement structure. Conclusions and recommendations are presented in Chapter 8. At the end, Appendices provide extra information referred to in the report.

2 LITERATURE REVIEW

2.1 Introduction

During the last 30 years, various laboratory and desk studies have been made of the properties of lateritic soils and gravels. Limited field studies of roads using non-standard base materials have also been reported. Most of this work on lateritic soils and gravels done in the past has concentrated on standard tests to characterize the material properties. The common tests used are shown in Table 2.1.

Table 2.1 Standard tests for characterizing granular materials.

Test	Reason for Test
Atterberg limits	Component analysis
Particle size analysis	Component analysis
Proctor density	Compaction
CBR	Strength test
Degradation tests like Los Angeles Abrasion test	Durability

Most of the standard tests are empirical in nature. This means the knowledge of the engineering properties or performance in road construction of these materials is limited to the conditions under which such experience was gained. Studies on lateritic soils have often gone into details to describe the nature of the laterization process and its implication on the engineering properties and performance in road construction. This chapter reviews available literature on laterites from definition and laterization process to the engineering properties, testing and evaluation procedures, specifications, design and construction. Not much work has been done using more fundamental testing techniques like cyclic load triaxial testing to determine the resilient and permanent strain properties of laterites. Cyclic load triaxial testing is described in detail in Chapter 5.

2.2 Definition, genesis and nature of laterite soils

2.2.1 Definition

Laterites are essentially products of tropical and sub-tropical weathering. The higher proportion of sesquioxides of iron (Fe_2O_3) and aluminium (Al_2O_3) relative to other chemical components is a feature characteristic of all grades of laterite soils. The term 'laterite' is often used loosely in most places. Buchanan(1807) first used the term 'laterite' to describe a material which hardens irreversibly on exposure to air. Since then various authors have distinguished laterites on the basis of silica-sesquioxide ratio $SiO_2/(Al_2O_3 + Fe_2O_3)$. Winterkorn (94) proposed distinction according to silica-sesquioxide ratio, S/R, as outlined in Table 2.2.

Table 2.2 Identification of laterite, lateritic soil and non-laterite

$S/R = \frac{\%SiO_2/60}{\%Al_2O_3/102 + \%Fe_2O_3/160}$	
<1.33	True laterite
1.33 - 2.00	Lateritic soils
> 2.00	Non-lateritic

One definition of laterite which seems to have gained wide acceptance is that attributable to Alexander and Cady (8), which states that:

"Laterite is a highly weathered material, rich in secondary oxides of iron, aluminium or both. It is nearly void of bases and primary silicates, but it may contain large amounts of quartz and kaolinite. It is either hard or capable of hardening on exposure to wetting and drying".

The irreversible hardening process in laterite soils seems to consist mainly of crystallisation of the amorphous iron oxides, and dehydration (8). Most of the controversies on the definition and nomenclature of laterite materials are insignificant from the engineering point of view. While it is important to recognise the differences

between laterite and non-laterite, the fact remains, that the true consideration for identification and evaluation of laterite soils for engineering purposes is not "what is its name", but what are its significant engineering properties and behaviour (52). Maignien (51) and Remillon (73) proposed that laterite be used to describe all reddish residual and non-residual tropically weathered soils, which genetically form a chain of materials ranging from decomposed rock through clays to sesquioxides rich crusts.

2.2.2 Laterization

The most important factors in the process of tropical weathering and laterization in order of importance probably are (58):

1. Climate
2. Topography and drainage conditions
3. Bedrock and parent material associations

Lateritic soils form in different parent materials whether these be transported soils or in situ weathered rock. The effects of parent rock is more pronounced in the initial stages of weathering, but during the later stages other pedologic factors predominate. There are many differences of opinion on the exact processes involved in the formation of laterite. The generally accepted principles are that their formation results from the progressive hydrolysis of the primary minerals silicates, i.e. of the rock forming minerals such as feldspars, ferromagnesian minerals, etc The following steps are involved in their formation (59):

(a) The leaching and removal, in the ground water, of soluble bases such as potassium, sodium and calcium, etc and also silica in the form of silica acid. There is a consequent enrichment of iron, manganese and alumina compounds
(b) In the wet season, the iron compounds in the parent material, which are more mobile than the alumina compounds are reduced to their mobile ferrous state in the ground water. During the dry season the capillary rise (also lateral seepage) brings these ferrous compounds into contact with the atmosphere just below the surface of the soil. They are then dehydrated and oxidised into ferric compounds

which are relatively immobile in the soil moisture. The amorphous compounds thus accumulate between the soil particles and then develop into concretions.

Table 2.3 illustrates the phenomena of leaching, replacement and relative enrichment.

Table 2.3 Changes in chemical composition due to weathering (after (67)).

	A			B			C		
	a	b	c	a	b	c	a	b	c
SiO_2	60.7	45.3	-15.4	71.5	55.1	-16.4	51.3	16.1	-35.2
Al_2O_3	16.9	26.6	+9.7	14.6	26.1	+11.5	15.2	29.1	+13.9
$FeO+Fe_2O_3$	9.1	12.2	+3.1	2.3	6.3	+4.0	14.3	31.9	+17.6
CaO	4.4	0.0	-4.4	2.1	0.2	-1.9	9.6	0.02	-9.6
MgO	1.1	0.4	-0.7	0.8	0.3	-0.5	5.6	0.06	-5.5
K_2O	4.3	1.1	-3.2	3.9	0.14	-3.8	0.6	0.06	-0.5
NaO	2.8	0.2	-2.6	3.8	0.05	-3.7	2.1	0.05	-2.0
H_2O	0.6	13.8	+13.7	0.3	10.4	+10.1	0.3	20.2	+19.9
Total	99.9	99.6		99.3	98.6		99.0	97.5	
S/R	4.54	2.24		7.59	3.14		3.59	0.55	

a. parent material

b. product of weathering

c. difference between a and b

A. Kaolinitic weathering of an intermediate gneiss, Virginia

B. Kaolinitic weathering of an acid granite-gneiss, Minnesota

C. Lateritic weathering of dolerite, Guyana

S/R Silica-sesquioxide ratio

+/- Gains or losses.

Comparing in Table 2.3 the intense laterite weathering (column C) to the moderate kaolinitic weathering (columns A and B), a more intense leaching of SiO2, CaO and MgO is characteristic of the lateritic weathering. The relative content of iron ($FeO+Fe_2O_3$) of the material is increased due to this intense leaching; in column C a far larger increase in iron can be observed as compared to columns A and B.

Table 2.4 gives results of chemical and physical test results on 10 typical Zimbabwean laterites.

Table 2.4 Chemical and physical test results on 10 typical Zimbabwean laterites (After Van der Merwe(89)).

	Banks-Staple-ford 1	Salisb-ury Gilling ham 2	Salisb-ury Airport 3	Mtoko-Mozam -bique border 4	Salisb-ury Enterp-rise 5	Lundi-Beit Bridge 6	Eastern Border 7	Bulaw-ayo Airport 8	Gwelo-Umvu-ma 9	Fort-Victoria Roswa 10
Loss on ignition	5.8	6.5	7.1	5.8	6.4	3.0	9.1	5.7	4.8	8.6
Al_2O_3 (%)	16.9	16.9	21.4	17.7	18.0	7.7	34.9	26.3	11.1	25.4
Fe_2O_3 (%)	10.3	9.1	9.8	11.2	11.7	13.7	11.3	5.0	10.4	12.1
SiO_2 (%)	63.8	66.0	58.2	61.1	58.7	67.3	43.0	62.0	68.9	52.3
Other oxides,%	1.3	1.5	2.6	1.6	1.9	8.3	1.0	1.5	2.0	1.6
S/R	2.34	2.54	1.87	2.11	1.98	3.14	0.93	1.98	3.20	1.39
pH	6.6	7.1	6.8	6.5	6.5	6.7	6.2	5.8	6.0	5.8
Plasticity Index	3	NP	6	4	NP	NP	9	5	NP	7
Liquid limit	17	-	22	16	-	-	25	23	-	22
<37.5 mm and >2.36 mm (%)	46	44	44	47	60	47	52	48	25	56
< 75 µm (%)	15	16	19	14	12	12	34	15	20	13
< 2 µm (%)	5	2	9	5	4	6	9	10	3	5
Triaxial class*	3.0	3.0	2.4	3.2	2.7	2.8	2.7	3.1	3.1	2.5
10% FACT	5.2	4.2	3.6	2.6	4.9	8.6	4.5	5.4	4.6	4.8

d'Hoore (26) distinguished between two types of accumulation for laterite deposits:

1. Relative accumulation owing their concentration to the removal of more mobile components, and
2. Absolute accumulation owing their concentration to the physical addition of material.

It is important to distinguish for engineering purposes the difference between laterite and ferricrete. The use of the term ferricrete is not very common outside Southern Africa, although it is used to a limited degree in Australia where ironpan is the more commonly used term. The term 'laterite' should be referred to a generally reddish coloured material formed by the relative accumulation of iron and aluminium oxides formed under tropical conditions by the weathering and leaching out of more of the more soluble constituents including silica. The term 'ferricrete' should be restricted to iron-rich materials formed by the absolute accumulation of iron oxides during the cementation and/or replacement of a pre-existing soil by iron oxide deposited by soil water or ground water (63). In the ferricretes the ferric compounds predominate,

whereas in the tropics a proportion of iron compounds is leached out, leaving a predominance of alumina compounds to form laterites.

2.2.3 Laterite Soil Profile

Laterite profiles may be a few centimetres to tens of meters thick (54). Topography and drainage conditions exert considerable influence on the nature of laterite soil profiles (36). In-situ weathering under tropical conditions usually results in the development of a weathering profile which is characterised by five distinct horizons (50):

1. Topsoil (A)
2. A sesquioxide rich laterite horizon, which may be a weakly cemented gravely layer and/or hardened in-situ crust (B1)
3. A mottled zone with evidence of sesquioxide enrichment (B2)
4. A pallid or leached zone overlying the parent material (C)
5. Sound parent rock (D)

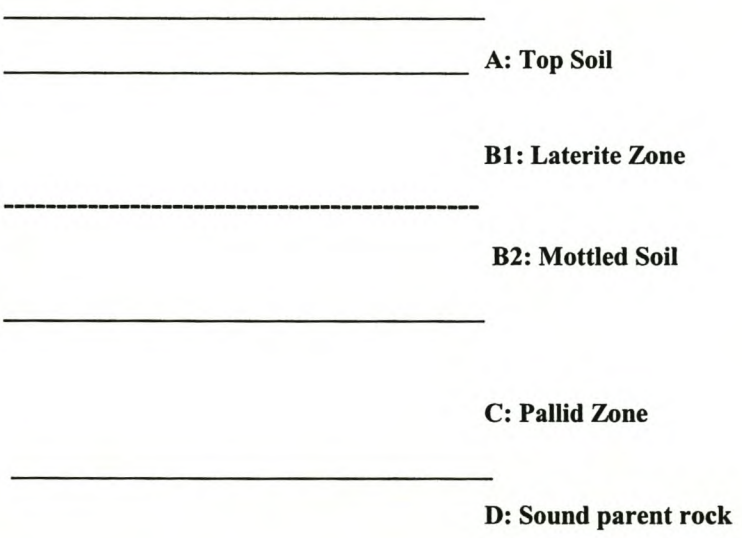

Figure 2.1 Schematic representation of a lateritic soil profile (after (50)).

The belief in such a profile appears to stem from the popularity of the upward enrichment hypothesis of laterite formation which requires the pallid zone, mottled zone and laterite be complementary and synchronous developments. It must be emphasised that the above description of three major horizons, laterite zone, mottled zone and pallid zone, is highly simplified because up to six major horizons have been recognised by some authors (51, 54). The situation is further complicated by the fact that the structure of the profile is a function of age, climate, position in the landscape and nature of the parent material (6). Laterites may overly many kinds of materials such as gneisses , schists, sandstones , shales, unconsolidated clays, sands, etc.

2.2.4 Chemistry and Mineralogy of Laterite Soils

The higher proportion of sesquioxides of iron (Fe_2O_3) and aluminium (Al_2O_3) relative to other chemical components is a feature characteristic of all grades of laterite soils. Bases are almost completely absent. Combined silica is generally believed to be low, but some soils may have significant amounts in the form of kaoline. Quartz may be absent or present in only limited amounts, but in rocks rich in quartz it is a significant or major component as in granite. Drainage is a key environmental factor affecting residual soils mineralogy. Kaolinitic clays predominate in well-drained areas, while montmorillonitic clays are found in more poorly drained regions (84). In most lateritic soils kaolin is the predominant clay mineral being the final stage of chemical weathering. The kaolinites are very stable clays and when wet are only moderately plastic than the other clay minerals. Laterites formed over basic rocks and volcanic ash or in regions of continuously wet climate (rainfall of more than 60 in. per year) are characterised by high natural water content, high liquid limits, and high contents of gibbsite, halloysite, and allophane types of minerals that undergo irreversible changes on drying.

2.3 Classification

2.3.1 Engineering Soil Classification Systems

Because of the uncontrolled conditions under which they form, there are an infinite variety of natural soils, each with slightly different physical properties. It is thus apparent that a method of identifying soils and grouping them into classes, each displaying similar physical properties and similar general behaviour characteristics is necessary. Numerous systems have been developed for classifying soils for engineering purposes, most based mainly on the particle size distribution and the plasticity chart. The most important of these are:

- Unified Soil Classification System, and
- AASHTO (HRB, Revised PRA, shown in Table 2.5).

Table 2.5 AASHTO classification system.

General classification	Granular materials (35% or less passing 0.075 mm sieve)							Silt-clay materials (> 35% passing 0.075 mm sieve)			
Group classification	A-1		A-3	A-2				A-4	A-5	A-6	A-7
	A-1-a	A-1-b		A-2-4	A-2-5	A-2-6	A-2-7				A-7-5 A-7-6
Sieve analysis, % passing											
2.00 mm sieve	50max										
0.425 mmsieve	30max	50max	51min								
0.075 mm sieve	15max	25max	10max	35max	35max	35max	35max	36min	36min	36min	36min
Characteristics of fraction passing 0.425 mm sieve											
Liquid limit			Non	40max	41min	40max	41min	40max	41min	40max	41min
Plasticity index	6 max.		plastic	10max	10max	11min	11min	10max	10max	11min	11min
Usual types of significant constituent materials	Stone frags. Gravel & sand		Fine sand	Silty or clayey gravel and sand				Silty soils		Clayey soils	
General rating as subgrade	Excellent to good							Fair to poor			

The critical condition on which the validity of these classification systems depends is that both the particle-size distribution and plasticity test results should be reproducible using the standard laboratory procedures. This condition is met by most laterite soils (88). The major difficulty in trying to develop satisfactory procedures for the identification and classification of laterite soils for engineering purposes revolves around the so-called "problem" laterites which may not give reproducible results

using standard classification test procedures. Plasticity and grading test results may be influenced by the pre-test preparation and testing procedures so that the correlation found between tests using different methods and operators may be misleading.

2.3.2 Pedological Soil Classification Systems

For studying the formation and physical properties of lateritic soils and gravels in a generalised way, the pedological grouping, developed mainly for use in agriculture, is of considerable value. The pedological soil classification system groups soils according to the description of the entire soil profile and according to the influence of factors of climate, vegetation, type of underlying parent material, topography, drainage conditions, etc. (37). The major limitation of the pedological classification is that a material in this classification system may have a wide range of engineering properties (37). The relationship between what we consider as lateritic soils with pedological groups is very complex in detail, so that it is not easy to use the pedologic information. Pedologically laterites belong to the following groups, according to the particular classification system (66):

(a) Old North American system: lateritic or latosols and yellow-red podzolic.
(b) Soil Taxonomy system: oxisols and part of ultisols and entisols.
(c) UNESCO-FAO system: ferralsols, ferralic arenosols, ferric luvisols, and part of nitosols and acrisols.

d'Hoore (26) in his pedologic map of Africa divided lateritic soils into ferruginous, ferrallitic, and ferrisol soils and showed a generalised distribution of those soils depending on climatic conditions alone.

2.4 Engineering Properties

The depth below the surface, their environment and the weathering condition among other factors generally influences the engineering properties of lateritic soils and gravels. With increasing depth below the surface, the clay content increases and the material becomes softer. The parent material influences the properties, e.g. laterites formed in clayey soils differ from those formed in sandy soils. The bedrock also influences the properties, e.g. basic igneous rocks are overlain by laterites containing more clay. The degree of laterization exerts great influence on most physical-mechanical properties of laterite gravels. The above factors clearly indicate that lateritic soils may have very variable physical properties.

Particle size distribution:

Considerable difficulty has been reported in trying to obtain consistent particle size distribution for some fine-grained lateritic soils due to the strong aggregation of clay size particles. Test results are affected by pre-test preparation and testing procedures. According to the intensity of the dispersing effort and the use of different dispersing agents, the clay size may vary considerably. The degree of drying and time of mixing of the sample prior to testing have also been found to influence the particle size analysis results. Figure 2.2 illustrates this behaviour.

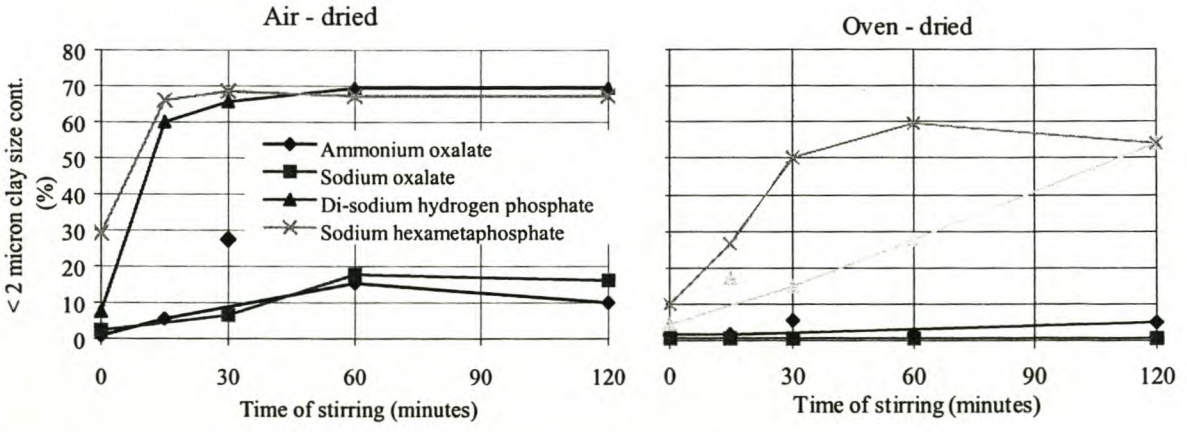

Figure 2.2 Effect of degree of drying on the clay-size content of Ghanaian laterite clay (after (37).

Figure 2.3 shows typical particle size distribution envelopes for laterite gravels and quartzitic gravels identified in West Africa. Quartzitic gravels are generally well graded with barely a 20% content of silt and clay size fraction, while the laterite gravels can have a high content of fines (between 35 and 40%).

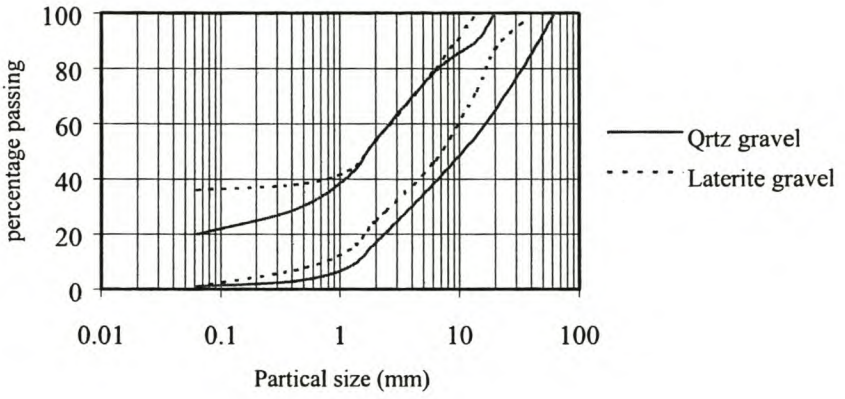

Figure 2.3 Gradation envelopes typical of lateritic and quartzitic gravels identified in West Africa (after Ackroyd (1959)).

Van der Merwe et al. (89) reported that most laterites exhibit an irregularity or gap in their particle size distribution, which is sometimes referred to as a "sand hunch". There is a lack of material usually between the 4.75 mm and 600 μm sizes and this is due to the formation of concretions leaving a size gap between the smallest concretions and the largest sand grains. However, this is not typical of all laterite soils as some varieties depending on parent rock and degree of laterization are well graded.

Atterberg limits:

As with particle size analysis, standard Atterberg limit tests do not yield reproducible results with some laterite materials because the test results are influenced by the methods of pre-test preparation and testing procedures. Studies have revealed significant variations between the undried, air-dried and oven-dried samples, Figure 2.4.

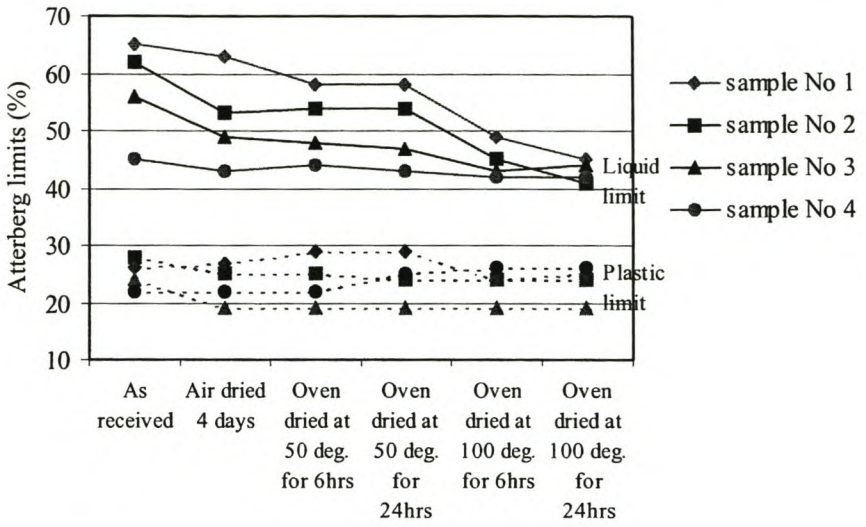

Figure 2.4 Effect of drying on Atterberg limits of four Ghanaian laterite soils (after (95)).

Another source of difficulty in obtaining reproducible plasticity tests results for some laterite soils is the tendency of some laterite soils to increase plasticity with the degree of mixing or remoulding of the soil sample prior to testing, Figure 2.5.

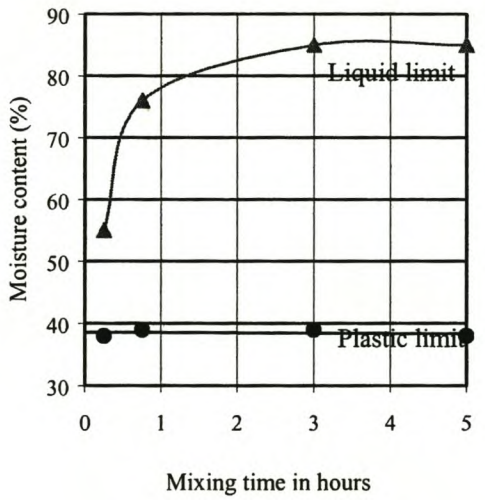

Figure 2.5 Effect of time of mixing on the liquid and plastic limits of a volcanic laterite clay (after (55)).

This does not, however, imply that all laterite soils present difficulty when their plasticity characteristics are evaluated using standard laboratory procedures. Laboratory investigations backed by field experience (e.g., Nixon et al., (65); USAID, (49); Gidigasu, (35)) have, in fact, shown that the plasticity characteristics of most laterite soils may be readily evaluated on the basis of standard laboratory procedures. Those that present difficulty are referred to as 'problem laterites'. Problem laterites have been generally observed to occur in regions of recent volcanic activity and/or continuously wet climate with an average annual rainfall generally above 1500 mm. They are characterised by high natural water contents and high liquid limits (Millard, (55)). The soils are known to contain hydrated iron and aluminium oxides, some of which change irreversibly to dehydrated forms on drying and desiccation. The soils could also contain the clay-mineral halloysite, sensitive to drying and relative humidity of the environment (37). De Graft-Johnson (24) has stated that the main laterite problem is to distinguish potential problem laterites from non-problem ones.

CBR:

One of the outstanding properties of lateritic soils and gravels is their high value of CBR when compacted at optimum moisture content and maximum dry density. The values predicted are usually much higher than those predicted from the consideration of grain size and Atterberg limits (66). For typical laterite gravel, maximum CBR values of between 100 and 200 are obtainable for Mod. AASHTO compaction and about 50 for British Standard (light) compaction (37). However, the strength may decrease abruptly on absorption of water as shown in Figure 2.6.

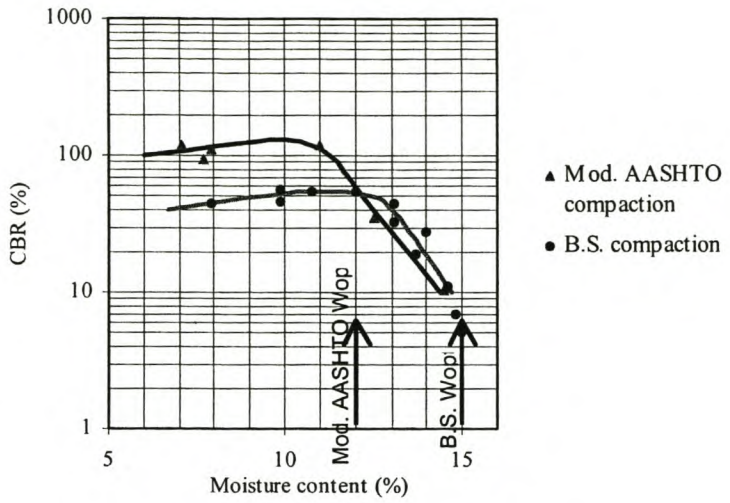

Figure 2.6 Relation between moulding moisture content and CBR of typical laterite gravel (after Evans(33)).

Durability:

Unlike the usual hardrock aggregate, some varieties of laterite gravels are highly susceptible to mechanical degradation during construction and in-service and to chemical and mineralogical changes under adverse drainage and/or chemical conditions. The hardness of laterite aggregate varies quite considerably from a hard aggregate, suitable for road construction to a friable, soft material, easily crumbled in the fingers. The absence of well-established laterite aggregate quality-control tests and specifications may result in improper utilisation of the aggregates, causing poor service performance (6). Results of several studies (4,11, 23, 51, 88) have shown that the mechanical strength and durability of laterite gravels depend primarily on their mineralogy, geochemistry and physical properties. The durability of lateritic gravels is reflected by their (75):

- aggregate impact value (AIV)
- aggregate crushing value (ACV)
- Los Angeles Abrasion (LAA)
- 10% FACT

Other aggregate specifications like water absorption and specific gravity cannot be similarly applied to determine the quality of laterite gravels without modifications, because of the highly porous nature and peculiar mineralogy of these materials (Akpokodje, (7)). Weinert (93) has reported that the strength of dry ferricrete in the 10% FACT is usually between 25 and 80 kN. Van der Merwe and Bate (89) also reports that the aggregate strength varies from 30 to 90 kN for 10% FACT tests carried out on several deposits used in road construction in Zimbabwe.

Classification:

In the AASHTO classifications (Table 2.4), most lateritic gravels fall broadly in group A-1 and A-2. However, even these two groups cannot be used effectively in the preliminary selection of gravels for pavements. A wide range of values for Atterberg limits, outside acceptable specification limits, are possible in group A-2.

Typical physical properties

Van der Merwe and Bate (89) have provided a summary of the properties of 130 different laterite deposits from various parts of Zimbabwe as shown in Table 2.6. The deposits have been sub-divided into plastic and non-plastic groups.

Table 2.6 Typical physical properties of 130 Zimbabwean laterites (after (89)).

No of deposits	PI		Dry density (km/m^3)		Opt. moisture content		Texas triaxial class		% passing 19 mm sieve		% passing 2.36 mm sieve		% passing 75 μm sieve	
	Mean	Std. Dev.	Mean	Std. Dev.	Mean	Std. Dev.	Mean	Std. Dev.	Mean	Range	Mean	Range	Mean	Range
50	Non plastic		2100	70	7.2	0.8	2.81	0.40	92	80-100	53	40-60	12	10-15
80	8.1	4.6	2150	75	7.4	1.0	2.85	0.43	85	75-95	56	40-65	15	10-15

Note: Texas triaxial and CBR tests were carried out on 9 samples from a laterite deposit and it was found that a mean triaxial class of 3.0 was equivalent to a mean CBR of 68.

2.5 Performance of laterite as a road building material

Laterite soils and gravels generally make good materials for sub-base and base construction for light and medium trafficked roads, being easy to win and manipulate on the road surface and having naturally stable gradings with a suitable proportion of clayey materials to act as a binder (55). De Graft-Johnson et al. (25) stated on the basis of their works in Ghana, that lateritic soils are extremely variable in physical and chemical characteristics and they naturally exhibit widely differing behaviour in pavements. Queiroz, C., et al. (70) obtained information from several countries on the behaviour and performance of bituminous surfaced road pavements with a base built from as dug laterite. Most of these roads carrying a wide range of traffic from the lower end of low volume roads to about 2,400 veh/day/lane, have performed well for 10 or more years; in many cases their useful life can be extended by simple resealings. The conclusion is that laterite bases can perform as well as crushed stone or stabilized laterites under a wide range of circumstances, at a cost of about 20 to 30% of these more expensive materials. The key factors in the performance of laterite bases appear to be a high degree of compaction, well-drained subgrade, and rigorous material selection in the borrow pits for application in the road. However some cases of unsatisfactory behaviour have also been observed (21).

Henry Grace (40) reports on full-scale trial sections in Kenya 1974/5 and in Malawi 1984/5 of bituminous-surfaced low volume roads constructed using as-dug laterite in place of stone or stabilised material as a base. The laterite did not conform to any accepted specifications but performed equally well when compared with adjoining sections of road using stone or stabilised material as a base. The significant features of the roads are listed in Table 2.7 and 2.8.

Table 2.7 Significant features of the Gatura-Matarra road in Kenya and test results of 1985 investigation (40).

Trial lengths
Laterite base, 6.2 km
Stone base, 5.7 km
Carriageway width, 5 m

Base
Thickness of laterite base, 150mm
Subgrade
A red residual clay

Construction period
Base, 1973-4
Bituminous seal, mid 1975 and resealed 1985

Traffic, study undertaken in 1983
Average daily traffic (ADT) (12hrs) 190
Medium and heavy lorries (% of ADT) 19

Raifall (mean yearly), 1980 mm
Mean monthly temperature, 15 - 20°
Depth to water table, over 10 m

Summary of significant tests results from 1985 investigation
Laboratory soaked CBR AT 95% of MDD British Heavy Compaction test, 54 average, 21 - 96 range
In situ CBR at surface of base beneath bituminous surfacing, 89 average, 47-209 range
In situ relative dry density (% MDD BS Heavy Compaction), 100 average, 92 - 105 range
In situ moisture content relative to OMC BS Heavy Compaction, 0.98 average, 0.78 - 1.18 range
Plasticity index, average 17.6, 7 - 21 range
Percentage passing 63 μm sieve, 28 average, 15 - 37 range

Comparison of defects in stone and laterite bases

	Stone base		Laterite base	
	1982	1985	1982	1985
Number of potholes per km	11.26	32.63	11.6	69.24
Area of potholes (% total area)	0.18	1.04	0.06	0.68
Area of cracking (% total area)	0.54	5.62	None	0.39
Total areas of potholes and cracking (% total area)	0.72	6.66	0.06	0.39
Area of edge failures (% total area)	0.57	1.92	0.17	1.09

Table 2.8 Significant features of the Luwawa-Champhoyo road trial section in Malawi and test results of 1985 investigation (40).

Trial lengths Laterite base, 1 km Stone base, at either end of remainder of road Carriageway width, 6.7 m
Base Thickness of laterite/stone base, 150mm Thickness of laterite subbase, 100mm **Subgrade** Residual sand clay
Construction period Base, Nov/Dec 1984 Bituminous seal, some sections Jan 1985, other sections Aug 1985
Traffic, study undertaken in 1983 Average daily traffic (ADT) (12hrs) 200 Medium and heavy lorries (% of ADT) 25
Raifall (mean yearly), 1300 mm, rainy season Nov to April Mean monthly temperature, 16 - 18° Depth to water table, over 10 m
Summary of significant tests results from 1985 investigation Laboratory soaked CBR AT 95% of MDD British Heavy Compaction test, 31.7 average, 12 - 45 range In situ CBR at surface of base beneath bituminous surfacing, 87 average, 58-120 range In situ relative dry density (% MDD BS Heavy Compaction), 95.4 average, 90.1 - 95.4 range In situ moisture content relative to OMC BS Heavy Compaction, 0.93 average, 0.7 - 1.14 range Plasticity index, average 16.3, 14 - 18 range Percentage passing 63 μm sieve, 37.6 average, 26 - 49 range

There is usually a big difference between the performance of roads with laterite bases that have an impermeable covering and those that doe not a guarantee of this, or of drainage (34). The main types of failure observed form studies in West Africa on laterite roads are the cracking of the pavement, stripping off of surface and waviness of the pavement surface sometimes only a few years after construction, Lundgren (48). These failures may result from poor materials selection, inadequate pavement design, poor subgrade condition and it appears that water plays a major role by entering the pavement structure (9).

Laterites are widely believed to exhibit a natural increase in strength in a pavement layer, not caused by traffic compaction or the addition of stabilising agents, a phenomenon known as self-stabilisation. Although hard evidence of self-stabilisation is not well documented, a test for potentially self-stabilizing laterites (i.e. petrification or self-cementing properties) was developed by Nascimento (61). However, Van der

Merwe and Bate (89) found no significant self-cementing properties after petrification tests carried out on some Zimbabwean laterites.

2.6 Stabilization of Laterite Soils

Although there are some laterites which do not require treatment to give them sufficient load bearing capacity, most laterites require some sort of stabilisation for their use in road construction (84). Lateritic soils respond to cement stabilisation and in some cases lime stabilisation. For the laterites, bitumen has been less widely investigated and is less used. Foam bitumen stabilization of a lateritic gravel material is part of the investigations in this research.

Lime stabilization

Mechanisms of lime-soil stabilization and the significant factors influencing the lime-soil reactions have been extensively researched in the past and have been well reviewed by the Transport and Road Research Board U.S.A (96). The changes that take place when lime is added to a soil are broadly divided into:

1. Cation exchange and flocculation-agglomeration reactions which take place rapidly and produce immediate changes in the soil plasticity, workability, and the immediate uncured strength and load deformation properties, and
2. Depending on the characteristics of the soil being stabilized, a soil-lime pozzolanic reaction may occur. These are reactions between lime, water and various sources of soil silica and alumina to form cementing agents which develop strength and durability. Pozzolanic reactions are time dependent and strength development can be gradual and continuous for long periods of time amounting to several years in some instances.

Practically all fine grained soils display improved soil properties through a reduction in plasticity, an increase in workability, an increase in CBR and an increase in the modulus of deformation of the compacted soil when treated with small quantities of

lime (3 - 7%). In some cases a marked increase in strength through the pozzolanic reaction occurs. Lime is most effective when there is sufficient amount of clay in the soil to react with lime. In South Africa THR 13 (29) proposes that lime be used for treating materials with a Plasticity Index higher than 10, to reduce he PI and increase the strength. H.S.Cartmell et al (19) report on a laboratory investigation in Zambia by the Public Works Department in which two typical laterite samples stabilized with various percentages of lime caused a marked improvement in soil properties, Figure 2.7.

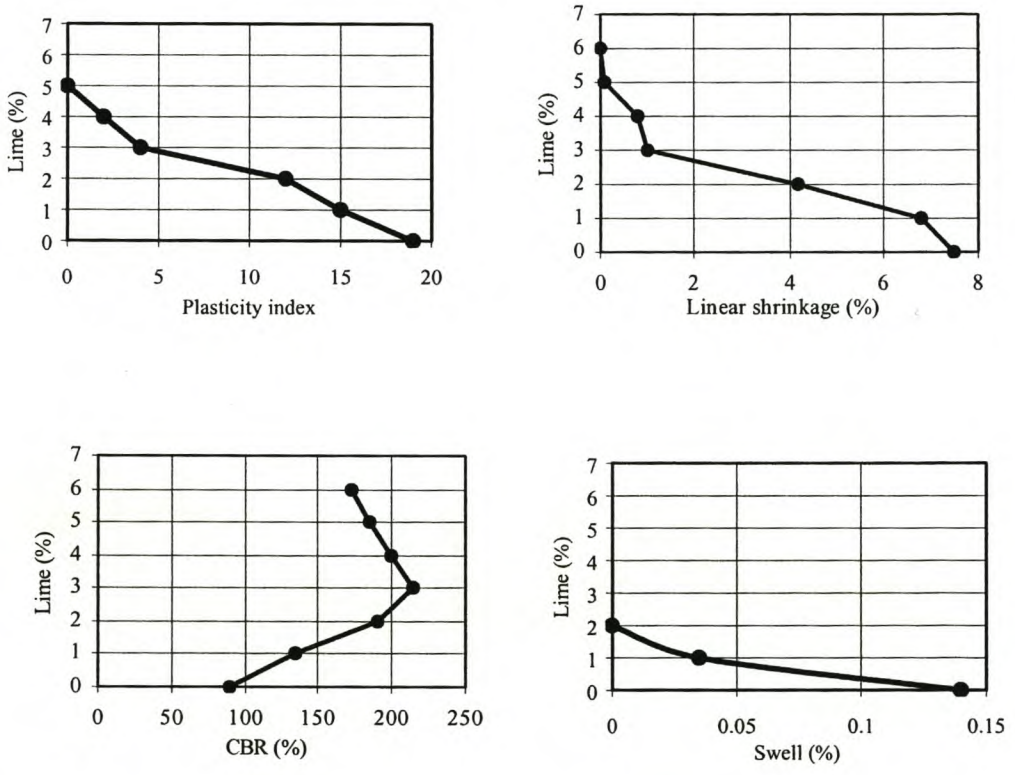

Figure 2.7 Effect of addition of different quantities of lime on the properties of a lateritic soil (after (19)).

One of the problems when dealing with red tropical soils (including laterites) is related to the nature of the components of the soil which are responsible for its pozzolanic properties. Harty et al (41) and Cabrera, J.G. (97) have done investigations concerning the pozzolanic properties and the significant factors influencing the lime-soil reaction of various red tropical soils, including laterites.

Cement stabilization

Cement-stabilized gravel, also referred to as cement-treated gravel or soil-cement, is essentially a low cost pavement material and is a shade better in quality than a naturally occurring suitable soil material for pavements designed to carry light to medium traffic. It is usually recommended for pavements that are designed to carry a cumulative standard axle not exceeding 1,500,000 over the design life. There are, however, soils that can not be stabilized with Portland cement, based on the Highway Research Board ("Use of soil-cement", (86)) suitability limits of:

- 50% passing 0.075 mm sieve
- 40% liquid limit, and
- 18% plasticity index

And also on the product of the plasticity index and percentage passing a 425 μm sieve not exceeding 1000 (Millard and O'Reilly, (56)). Such soils are difficult to work with and also require uneconomical proportions of cement. Morin and Todor (27) have recommended that cement be restricted to soils having plasticity index of 15 or less and a percentage passing the 0.075 mm sieve of not more than 25%. Lime is more practical for higher plasticity soils.

Evaluation criteria

The criteria used for determining the suitability of a particular stabilized soil for any purpose vary depending on the stabilization objective. The term 'modification' is used when the major stabilization objective is to improve the properties of the soil through PI reduction, improved workability and increased CBR. When there is significant strength development the term 'cementation' is used. A cemented material is usually accepted on the basis of meeting strength and durability requirements. Strength is assessed from unconfined compressive strength (UCS) or California bearing ratio (CBR) test results. The durability of a cemented material is assessed using the Portland Cement Association (PCA) wetting and drying test. The PCA specifies 7% as the maximum allowable weight loss. The usual value for seven days UCS is 1.7

N/mm^2 for the strength criterion. South African criteria for cemented materials are given in TRH14 (30). Typical design strengths for four classes of cemented materials consisting of crushed stone, crushed gravel or natural gravel are shown in Table 2.9.

Table 2.9 South African design strength criteria for cemented materials.

	C1 Cemented crushed stone or gravel		C2 Cemented crushed stone or gravel		C3 Cemented natural gravel		C4 Cemented natural gravel	
	min	max	min	max	min	max	min	Max
Lab. design UCS at 7 days, 100% Mod. AASHTO density (N/mm^2)	6	12	3	5	1.5	3.0	0.75	1.5
Lab. design UCS at 7 days, 100% Mod. AASHTO density (N/mm^2)	4	8	2	4	1	2	0.5	1

South African criteria for ITS have not yet been determined, but investigations carried out in Natal suggest the following:

Cemented material	Minimum ITS (kPa) (Test Method A16T())
C3	200
C4	120

2.7 Specifications for Laterite Soils and Gravels

Paving material specifications in use in most tropical countries have generally been adapted from those developed in temperate zone areas sometimes without due consideration for the traffic, climatic and soil conditions unique to the environments under which such specifications were developed (38). The main requirements of the generally accepted specifications for road bases are:

- CBR at mod. ASSHTO compaction not less than 80
- Plasticity index not more than 10
- % passing 75 μm, 5 - 25%

In the case of the Zambian specifications (78), the following is recommended for natural gravel base course materials (gradings given in **Appendix C**):

Table 2.10 Zambian specification for natural gravel pavement materials (78).

	Base	Sub-base
California Bearing Ratio (CBR)	>90% at 98% Mod. AASHTO	>25% at 96% Mod. AASHTO

	Base		Sub-base	
Material class*	A	B	C	D
Los Angeles Abrasion, Max. %	40	45	45	50
Plasticity Index, Max. %	6	6	8	10

*Four nominal gradings have been distinguished designated as material classes A - D.

These requirements exclude the use of all but the most rarely naturally occurring laterite deposits. The use of more conventional crushed stone or stabilized base course materials result in higher construction and rehabilitation costs. Based on experience of satisfactory performance of naturally occurring gravel materials, as for instance outlined in Section 2.5 of this report, modifications are necessary in order to make use of locally available materials. However, this relaxation should be well documented and be based on local research and experience. In their study of laterites in road construction, for instance, Morin and Tudor (57) suggested such an adaptation of the AASHTO specifications to tropical conditions. They proposed broader limits for grading and Atterberg limits than those given in the temperate zone AASHTO specifications. Some agencies in the tropical countries have in the past tried to disseminate more realistic material specifications for these regions as in the case of the Brazilian National Highway Department (DNER) (32) and Portuguese specifications (98). In many of the former UK-colonies use has been made of specifications outlined in British Road Note 31 (74) which were specially developed for tropical countries. These and other specifications are given in **Appendix C**.

2.8 Pavement Design

2.8.1 Introduction

Historically, the pavement design procedures used in tropical countries have been adopted from those developed in the temperate climates. Most of these procedures are based on empirical knowledge. This means that they were developed based on the experience of observed pavement performance on test tracks and other pavements and they take into account the traffic, climatic conditions and material characteristics in the locations where such designs were developed. For example, the AASHO Road Test (1958 -1960) represents one of the largest experimental projects ever undertaken to develop criteria for highways. In the tropics local conditions are very different from those found at the site of the AASHO Road Test. Yet most design methods in the tropics still follow the AASHTO design concepts as set forth in the "AASHTO Guide for Design of Pavement Structures", 1972-1993. In Zambian, the design guide as outlined in "Recommendations on Road Design Standards, Pavement Design Guide", 1994, follows concepts set forth in the AASHTO design guide for designs in the medium to heavy traffic range whereas for light traffic the British TRRL design stated in Road Note 31 (74) is taken into account. The main limitation of empirical methods is that they cannot be extrapolated with confidence beyond those conditions on which they were based. Nonetheless some basic concepts developed during the AASHO Road Test can still be applied in the development of any design procedure.

The principle behind any structural design procedure for pavements is that the pavement layers be of sufficient thickness and strength to prevent excessive deformation of the subgrade and at the same time have sufficient strength to resist damage to the pavement layers themselves under expected traffic loading and environmental conditions. Apart from depending on empirical knowledge gained at specific locations there must be a way of being able to make rational pavement designs in any region using information of traffic, climate and material characteristics in that region. Mechanistic or analytical design procedures are now in increased use. In general such procedures consist of the analysis of stresses and strains in the pavement structure and the determination of the allowable stresses and strains that can

be taken by the pavement materials. Such procedures involve careful material characterization, proper stress-strain analyses taking into account the complex stress-strain relationships of the materials, as well as translation of the mathematical functions into performance predictions. In such a way materials can be used to their fullest potential. Often, these mechanistic pavement design procedures need validation with long-term performance data from in-service pavements.

2.8.2 Pavement Design Procedures

A wide variety of pavement design procedures have been developed in time. One of the earliest empirical design procedure is the CBR-method. Other well known empirical design procedures are the AASHTO guide (1,2), the TRL's Road Note 29 (99) and Road Note 31 (74) which is especially developed for design of roads in tropical developing counties. The most well known of mechanistic design guides are the Shell Pavement Design Manual (100) and the Asphalt Institute method (101). These design guides are mainly focussing on the asphalt and the subgrade while it is a well known fact that proper attention should be paid to the performance of the unbound or bound base. The South African mechanistic design procedure is probably the best validated of all mechanistic design procedures and it also caters for the unbound granular base by limiting the magnitude of shear stresses in the unbound base. In this section, a description will be given of several design procedures used today. The methods described are the CBR method, AASHTO method, Road Note 13, and the South Africa method. The Zambian pavement design guide is also described.

The CBR-method

The CBR method is one of the oldest empirical design methods. The California Division of Highways through its investigations on in service pavements in the 1930's developed relationships between the CBR value of the subgrade and the required pavement thickness. The design curves are based on limiting the shear stresses at the top of the subgrade to a level well below failure, which in turn limits the permanent deformation of the subgrade. The CBR design chart is shown in Figure 2.8. From the CBR of the subbase the required thickness over the subbase is determined and the thickness of the subbase is the difference from total required thickness.

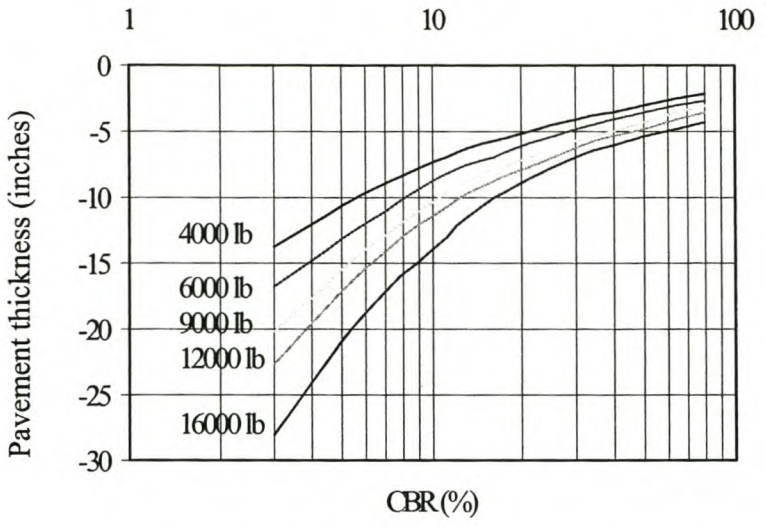

Figure 2.8 CBR design curves for highways (from Corps of Engineers).

The Road Note 31 - Method

Road note 31 "A guide to the structural design of bitumen-surfaced roads in tropical and sub-tropical countries" (74) was first published by the Transport and Road Research laboratory 1962, and later revised in 1966 and 1977. It is appropriate for roads that are required to carry up to an average of 1,500 heavy vehicles per day, thereby incorporating most non-urban roads in the tropical areas. Road note 31 gives a detailed procedure to estimate the moisture content at which the bearing capacity of the subgrade should be determined and it allows for stage construction approach, so that uncertainties in estimating the number of standard axle loads to be carried can be dealt with better.

The Road Note 31 procedure itself contains the following steps:

1. The bearing capacity of the subgrade is determined using the CBR-test, to be carried out on the soil in the wettest condition likely to occur.
2. The bituminous surfacing is fixed in Road Note 31. It is either a surface dressing (non-structural spray and chip treatment) or for heavier trafficked roads a 50 mm layer of pre-mixed bituminous material.

3. The thickness of the unbound granular base is also fixed. Depending on the number of standard axles to be carried, either a 150 mm or 200 mm base layer is prescribed.
4. The only real design variable is the thickness of the subbase, which can be read directly from a design chart having the CBR of the subgrade and the number of standard axles as input.

The design chart incorporated in Road Note 31 is shown in Figure 2.9.

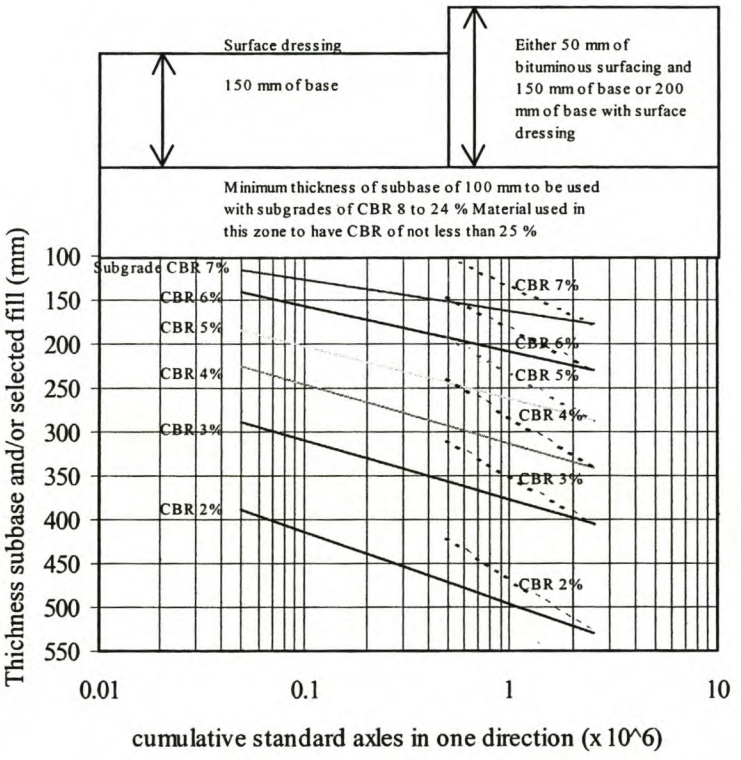

Figure 2.9 Road Note 31 pavement design chart.

The AASHTO - method

The American Association of State Highway and Transportation Officials in 1986 published the final version of "ASSHTO guide for the design of pavement structures" which was again revised in 1993 (2). The ASHTO Interim Guide of 1972 and its

revision of 1981 precede the final version. All these documents are based on the findings of the AASHO Road Test but in the final version new considerations were added in their interpretation, such as the concept of reliability and the use of resilient modulus to characterize soil support.

The design involves the following steps:

1. For input to the design, the soil support is characterized by the resilient modulus of the subgrade. It should be determined through the cyclic load triaxial testing according to ASSHTO T 274 "Resilient modulus of subgrade soils'. If no equipment for this test is available, the resilient modulus can be estimated from the results of the simpler laboratory tests, namely the California Bearing Ratio CBR and the Resistance R-value determined with the Hveem Stabilometer.
2. From the required reliability of the design, the soil support and the expected amount of traffic, a design "Structural number SN' is obtained from a nomograph in the guide.
3. The require design structural number is then met by selecting a combination of surfacing, base and subbase according to,

$$SN = \sum a_i D_i$$

where SN = structural number
a_i = layer coefficients
D_i = layer thicknesss

4. The layer coefficient a_i expresses the empirical relationship between the structural number SN of a layer and its thickness. It is a measure of the relative ability of a material to function as a structural component of the pavement. The layer coefficient a_i can be read from a number of charts incorporated in the guide, depending on the type of material. For granular material:

   - Granular base layer: the structural coefficient a_2 of this layer can be read from a chart having the resilient modulus E_{BS} of the granular material as input. E_{BS}

should be determined in cyclic load triaxial tests according to ASSHTO T 274 "Resilient Modulus of Subgrade Soils". If no equipment for this test is available, the structural coefficient can be obtained from other laboratory test data such as CBR or R-value.

- Granular subbase layer: the structural coefficient a can be read from a chart similar to that for the coefficient a_2 of the base layer, having resilient modulus E_{SB}, CBR or R-value as input.

The South African Mechanistic Design Method

The South African Mechanistic Design Method (82) was first developed in the early seventies and has since been updated over the years. The method has been extensively tested and validated mainly through accelerated testing of pavements with a fleet of Heavy Vehicle Simulators (HVS's) in South Africa.

The design procedure itself consists of the following step:

1. The road to be designed is classified into one of three categories depending on its importance, required service level and traffic intensity. The cumulative equivalent traffic, expressed in 80 kN standard axle loads, is classified into one of five categories.
2. The elastic properties (E-modulus) of the subgrade are estimated from its soaked CBR value, using a factor of proportionality dependent on the soil type.
3. For the granular base, recommended values of resilient modulus to be in the design calculation are given in the design procedure dependent on the quality of the material. Also allowable values of shear stresses are given, including a Safety factor dependent on the road category and the moisture regime.
4. For the asphalt, stiffness is given as a function of type of asphalt, temperature, speed of loading and depth below surface.
5. With the material parameters obtained, a structural analysis calculating strains caused by a standard dual wheel load is performed. At present linear elastic theory is used for the calculations. The calculated values of strains are subsequently compared to allowable values of strains (horizontal tensile strain at the bottom of the asphalt layer and vertical compressive strain at the top of the subgrade). For

these strains, allowable values are given in the guide, dependent on the number of load applications and the road category.

6. To circumvent the necessity for making computer calculations by the designer, standard designs are given in the guidelines for each combination of the road and traffic category. These standard designs have been verified using extensive in-situ monitoring under normal and accelerated trafficking.

The Zambian design guide

The Zambian guide (71) gives a brief description of the relevant pavement design parameters:

- design traffic
- climatic conditions
- subgrade bearing capacity
- material possibilities for the pavement layers and details to how these may be combined

The design involves the following steps:

1. The pavement strength required for a given combination of subgrade bearing capacity, traffic load, service level and climate is expressed by means of the structural number.
2. The AASHTO design equation has been used for the medium to heavy traffic range (0.5 to 20 million ESA), whereas for light traffic (less than 0.5 million ESA) the required structural number has been derived from TRRL Road Note 31 (43). The climatic condition is taken into account by calculating a weighted structural number (SDN) from the "wet" and "dry" structural numbers (SN_W and SN_D) based on the number of wet and dry months.
3. The soil support value has been derived from the logarithmic relationship between CBR and soil support developed by Utah State Department of Highways. The relationship assumes the form:

$$S = 1.3 + 3.75 \log CBR$$

where S is the Soil Support Value.

4. Layer coefficients for different material types, according to the position in the structure, are given. Criteria for adjustment of the layer coefficients to local prevailing conditions are included.

The design standard includes a catalogue of standard designs which has been included in **Appendix D.**

2.8.3 Analysis of stresses and strains

BISAR and ELSYM 5 are the most widely used computer programs to compute the magnitude of stresses and strains at any point in a multi-layer pavement structure from any given surface loading. For the stress-strain analysis the pavement-wheel load interaction is schematized as shown in Figure 2.10. Wheel loading is represented by uniformly distributed pressure over a circular area.

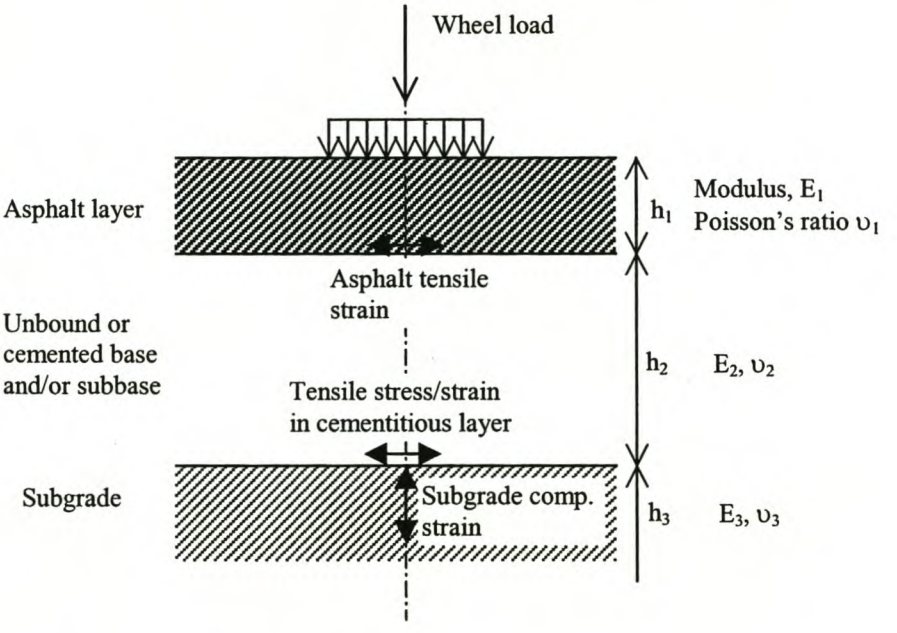

Figure 2.10 Schematic of pavement structure for stress-strain analysis.

BISAR and ELSYM 5 use linear elastic theory to calculate stresses and strains in pavement structures. This means a constant value of Young's modulus E and Poisson's ratio υ is assigned to each layer. This is a simplification that allows the use of relatively simple computer programs, though in reality these values vary throughout the pavement layers depending on the loading conditions and type of material. Asphaltic materials have properties that are sensitive to loading rate and temperature. Granular materials have non-linear stress-strain relationship, which are influenced by a range of variables. However, under a single load application, most pavements will respond in a resilient manner. Any irrecoverable deformations will be small relative to the resilient component. Conventionally, each layer is characterized by a value of Young's modulus and Poisson's ratio, but in view of the differences between real and idealized behaviour of pavement materials, the parameter 'resilient modulus' was introduced in California in the 1950s. Under conditions of moving traffic and normal temperatures, the response of an asphaltic material to a load pulse will be essentially resilient. Therefore when a thick asphalt layer forms the main structural layer of the pavement, linear elastic theory can be used with reasonable confidence. But for thinly surfaced pavements over a thick granular base, linear elastic theory is inappropriate unless approximate account is taken of non-linear behaviour. Several equations or models to characterize the non-linear stress-strain characteristics of granular materials have been proposed. Sophisticated testing procedures like cyclic load triaxial testing are used to establish parameters used in these models. Chapter 3 of this report has been devoted to describe the modelling of the non-linear stress-strain characteristics of granular materials. Cyclic load triaxial testing of a lateritic gravel material formed the major focus of this research and the procedure is described in later chapters of this report.

2.9 Construction

The performance of a laterite as a base course material is not just a function of properties such as particle size distribution, Liquid limit, Plasticity index or CBR. The construction technique used to win, place and compact the material is also important and should be carefully defined and closely controlled and supervised (21). This

control is particularly critical in quarry definition and winning. Lateritic materials being natural materials are more variable than crushed rock products. In particular there is a change in properties with depth in the borrow pit. During ripping, stockpiling and compaction a considerable amount of degradation takes place and this can result in a marked loss in strength in the case of clayey or silty laterite deposits (89). Also, surface ponding must be avoided by ensuring a well-drained surface profile. A period of about six weeks should be allowed after compacting the base and before surfacing during which time the base will be exposed to the weather and construction traffic. This will close up any cracks developing from the drying up of the base by the kneading action of traffic and allow for further compaction in areas were compaction has been incomplete (7). The bituminous surfacing should be applied when the laterite has dried out to approximately half Optimum Moisture Content (7). A marked increase in the moisture content along the edges of the laterite base is likely. The surfacing should therefore if possible be extended about 1.5-2m beyond the edge of the carriageway.

2.10 Summary

1. Most studies in the past on laterites have concentrated on standard tests to characterize the material properties. This means most of the knowledge of the engineering properties or performance of these materials in road construction is limited to the conditions under which such experience was gained.
2. Specifications for the use of granular materials in pavements are, for the most part, empirical. In general they are based on a definition of grading and a low level of plastic fines, attributing the best performance to high quality crushed rock. The specifications usually exclude the use of locally available lower quality materials which have proved to perform adequately in pavements.
3. Some laterites do not yield reproducible results for Atterberg limits and particle size analysis because the tests are influenced by methods of pre-test preparation and testing procedures. However, not all laterite soils present difficulty. In fact, most laterite soils may be readily evaluated on the basis of standard laboratory procedures.

4. Being a natural material, lateritic materials do exhibit a wide range of properties. However, most deposits generally make good materials for subbase and base construction with naturally stable gradings and high vales of CBR. Most lateritic gravels fall broadly in group A-1 and A-2 according to the AASHTO classification.
5. Pavement design procedures in use in most tropical countries are empirical in nature. With an increase in the use of analytical design methods, there is need to obtain more information on the fundamental stress-strain and permanent deformation characteristic of lateritic materials.

3 MECHANICAL PROPERTIES OF GRANULAR MATERIALS

3.1 Introduction

For many years road pavement design methods and specifications have been based upon relatively simple tests and empirical methods. Nowadays, there is an increasing application of the theory of elasticity to calculate stresses and strains in a layered pavement system. Central to this approach is the need for sound models to describe the materials fundamental behaviour. In traditional elasticity theories, the elastic properties of a material are defined by the modulus of elasticity (E) and Poisson's ratio (υ) which are material constants. With granular materials, the modulus of elasticity is replaced with the 'resilient modulus' (M_r) to indicate the non-linear behaviour. Study of the resilient and permanent deformation behaviour of granular materials is normally conducted in a laboratory, often using cyclic load triaxial tests. This behaviour can be described by models which are easily implemented in analytical pavement design procedures. In this chapter, the literature on the mechanical behaviour of granular materials under repeated loading and the models available to describe this behaviour are reviewed.

3.2 Mechanical Behaviour of Unbound Granular Materials

Under cycling loading with stress levels well below failure, granular materials present resilient strains, which are recovered after each cycle, and permanent strains, which accumulate with the number of cycles as shown in Figure 3.1.

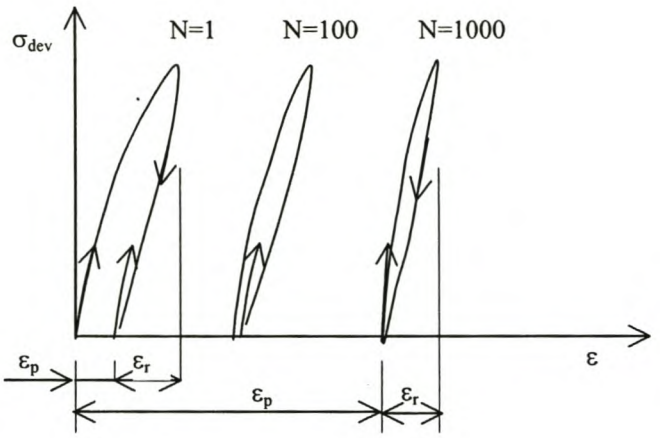

Figure 3.1 Stress-strain behaviour of granular materials

The resilient modulus is defined as,

$$M_r = \frac{\sigma_{dev}}{\varepsilon_r}$$

where σ_{dev} = deviator stress and ε_r = resilient strain.

However, this resilient behaviour is non-linear, with the resilient modulus increasing with increasing stress. The approach normally used in studying the behaviour of granular materials under cyclic loading is done is two stages:

- study of the resilient behaviour, which dictates the value of the resilient modulus used to carry out stress-strain analysis of pavements,
- study of the development of permanent strains with the number of load applications, which characterises the resistance of the material to rutting.

This behaviour can be described by models that can easily be implemented in analytical pavement design procedures. Studies in the literature show that the resilient modulus of granular materials is affected, with varying degrees of importance, by stress level, density, moisture content, grading, load frequency, and stress history.

3.3 Laboratory Testing of Unbound Granular Materials

International practice over the past decade has seen a move to the testing of pavement materials using cyclic triaxial testing. Due to its complexity, however, the test is still almost exclusively used for research purposes. A major step towards implementation of cyclic load triaxial test has been the standardization of the test by the American Association of State Highway and Transportation Officials. ASSHTO T 274-92 (3) gives a detailed description of equipment, specimen preparation and testing procedures. The latest AASHTO Guide for Design of Pavement Structures (1993) has now incorporated resilient modulus as the standard material quality measure. Australia has also made progress with the adoption of cyclic load triaxial test as a standard routine test. In 1995, Standards Australia issued Australian Standard AS 1289.6.8.1, "Determination of the Resilient Modulus and Permanent Deformation of Granular Unbound Materials" (10) based on work done by the Australian Pavement Reference Group (APRG). The APRG has since made substantial modifications to this standard which have been summarized by Vuong (92). Elsewhere in Europe research is underway to harmonize equipment and test procedures.

Cyclic triaxial testing in the laboratory aims to simulate the environmental and loading conditions to which the material is to be subjected both during and after construction. Though the simulation of road loading conditions in the laboratory is complex, the triaxial apparatus closely simulates the true loading situation. The various features of the cyclic load triaxial apparatus used in the test programme of this research are described in Chapter 5, where also the suitability and limitations of this testing approach are discussed.

3.4 Modelling of resilient behaviour

An approach widely used over the years for computational modelling of resilient behaviour of granular materials and subgrade soils is to characterize the stress-strain relationship using a stress-dependent resilient modulus and a constant Poisson's ratio, mostly $\upsilon = 0.35$. Figure 3.2 shows the idealised relationship between resilient

modulus and deviator stress for fine-grained soils obtained from laboratory cyclic triaxial tests.

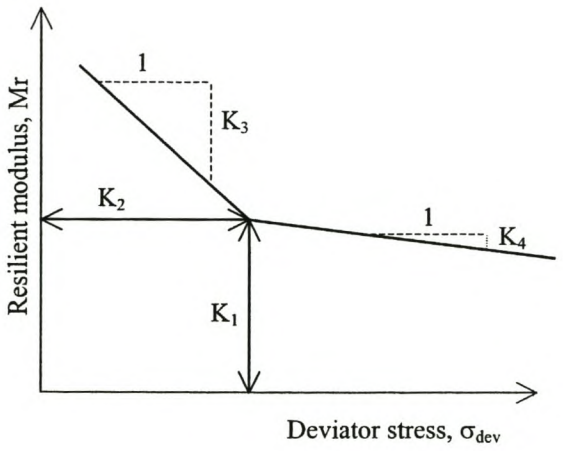

Figure 3.2 Generalised relationship between resilient modulus and deviator stress for fine-grained soils.

This bilinear behaviour can be expressed as,

$$E = K_1 + K_3(K_2 - \sigma_{dev}) \qquad \text{where } \sigma_{dev} < K_2$$

$$E = K_1 + K_4(\sigma_{dev} - K_2) \qquad \text{where } \sigma_{dev} > K_2$$

in which K_1, K_2, K_3 and K_4 are material constants and deviator stress $\sigma_{dev} = \sigma_1 - \sigma_3$.

For granular materials, several mathematical models have been suggested using different stress components. In the past the most well known model to predict the resilient modulus is the M_r-Θ model which expresses resilient modulus as a function of bulk stress (Θ), equal to the sum of the principal stresses ($\sigma_1 + \sigma_2 + \sigma_3$) acting on the specimen,

$$Mr = k_1\left(\frac{\Theta}{P_0}\right)^{k_2}$$

where Mr = resilient modulus

k_1 and k_2 = material parameters

$\Theta = (\sigma_1 + \sigma_2 + \sigma_3)$ = sum of principal stresses

P_0 = reference stress, 1 kPa - for dimensional purposes

The experimentally determined relationship between M_r and Θ is a straight line on a log-log plot, Figure 3.3. Therefore, the constants k_1 and k_2 used in the M_r-Θ model can be readily obtained using a linear regression analysis of the log M_r - log Θ data.

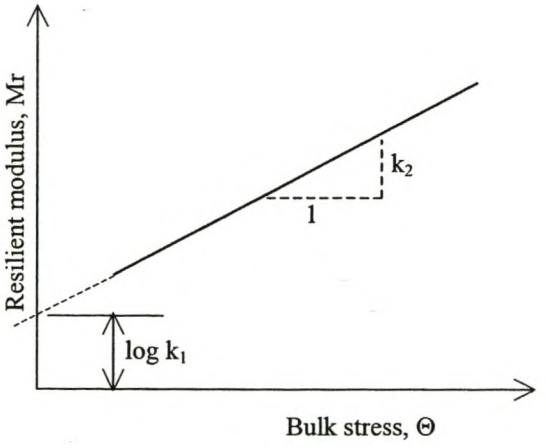

Figure 3.3 Generalised relationship between resilient modulus and bulk stress for granular materials.

This model does not take into account the confining stress σ_3 which clearly influences the resilient modulus. Theoretically, it also allows high Mr values to be obtained at high vertical stresses without lateral confinement.

Uzan (104) developed a model that takes into account the effect of bulk stress Θ and deviator stress $(\sigma_1 - \sigma_3)$ which is,

$$M_r = k_1 \left(\frac{\Theta}{P_0}\right)^{k_2} \left(\frac{\tau_{oct}}{P_0}\right)^{k_3}$$

where, τ_{oct} = octahedral shear stress = $\sigma d^* \sqrt{2}/3$

σ_d = deviator stress (σ_1 - σ_3)

Huurman et al. (63) reported a decrease in resilient stress with an increase in deviator stress or sum of the principle stresses and developed a model capable of describing this behaviour. It should be noted that Huurman et al. developed their model for a large number of sands which are typically used for subbases in the Netherlands.

Advanced models

Research by others has shown that not only the resilient modulus but also the Poisson's ratio is stress dependent. Van Niekerk et al (64), Figure 3.4, illustrated the stress dependency of the Poisson's ratio.

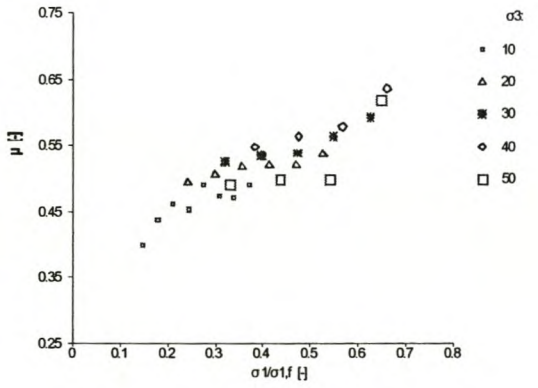

Figure 3.4 μ plotted against the $\theta_1/\theta_{1,f}$(64)

Poisson's ratios larger than 0.5 mean dilation taking place in the granular material. Uzan et.al. (87) also reported dilation in the granular material and developed a constitutive model for the Poisson's ratio.

In more advanced models the stress-strain relationship is characterized by decomposing both stresses and strains into volumetric and shear components. Instead

of resilient modulus and Poisson's ratio, the resilient response of the material is then defined by the bulk and shear moduli. Although some researchers favour this approach, the models of this kind are usually more complex in nature and the parametric values are more difficult to determine from collected test data.

Boyce (12) developed a non-linear three parameter model given by the following equations for volumetric and shear strain,

$$\varepsilon_V = (1/K_1)p^n(1-\beta(q^2/p^2))$$

$$\varepsilon_S = (1/3G_1)p^{n-1}q$$

and $\beta = K_1(1-n)/6G_1$

where, $\varepsilon_v = \varepsilon_1 + 2\varepsilon_3$ = volumetric strain

$\varepsilon_q = 2/3\ (\varepsilon_1 - \varepsilon_3)$ = shear strain

$p = (\sigma_{1r} + 2\sigma_{3r})/3$ = mean normal stress

$q = \sigma_{1r} - \sigma_{3r}$ = deviator stress

K_1, G1, n = constants

3.5 Estimating resilient modulus from standard tests

Resilient modulus obtained from repeated load triaxial testing usually requires sophisticated equipment not suitable for routine testing in most laboratories. An alternative is to calculate resilient modulus values from generalised empirical relationships.

Estimating resilient modulus for subgrade materials

Probably the commonest approach to calculate resilient modulus for subgrade materials is from CBR values. Heukelom and Klomp (42) proposed the relationship between the subgrade resilient modulus and the CBR value, developed on clays and sandy soils, as follows:

$E = 10\ CBR$

where E = Youngs modulus, CBR = California Bearing Ratio (%)

Figure 3.5 shows that the value of the constant can have tremendous variation if such a relation is used. It is clearly not advisable to use the CBR for estimating the resilient modulus. Moreover, the relationship does not take into account the stress dependency of the resilient modulus.

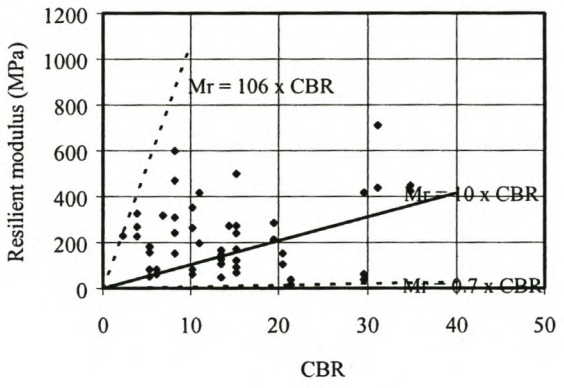

Figure 3.5 Comparison of CBR and resilient modulus (91)

Estimating resilient modulus for granular base course materials

The British Transport and Road Research Laboratory developed the following relationship, valid only for 2% < CBR < 12% (69),

$E = 17.6\ (CBR)^{0.64}$

where E = Young's modulus, CBR = California Bearing Ratio (%)

Another approach is to assume relationships between the modulus of the granular base and that of the subgrade. Shell researchers (20) proposed the following:

$E_b = k\ E_s$

Where, E_b = modulus of the base

E_s = modulus of the subgrade

$k = 0.2\ h_b^{0.45}$, $2 \leq k \leq 4$

h_b = thickness of base in mm

This relationship, however, should be treated with caution. Work by Brown and Pappin (15) using non-linear finite element analysis suggested a winder range of the ratio from $1.5 \leq E_b/E_s \leq 7.4$. In fact they found the equivalent stiffness of the granular base E_b to be constant for a given quality of base and not to depend on the subgrade stiffness E_s. Furthermore, since granular materials show stress dependency behaviour, the concept of a single E-value for any granular material is unsuitable.

3.6 Modelling of Permanent Deformation

One of the main aspects of the design philosophy of flexible pavements is limiting the development of rutting at the pavement surface. In comparison to resilient behaviour, less research has been devoted to plastic response and permanent deformation development in granular materials. One of the reasons is perhaps due to the fact that monitoring the build up of permanent deformation in these materials is a very time consuming process. Nevertheless, it has been shown that the stress level is one of the most important factors affecting the development of permanent deformation in granular materials. Other factors that affect the development of permanent deformation in granular materials are the reorientation of principal stresses under a rolling wheel, number of load applications, moisture content, stress-history, and degree of compaction.

The modelling of the permanent deformation comprises two aspects:

- the variation of the permanent strain with the number of cycles,
- the relations between the permanent strain and the stress.

Results of permanent strain tests are generally interpreted using relationships of the form,

$\varepsilon_{1p} = f(\sigma,N)$

where, ε_{1p} = plastic axial strain
N = number of load cycles
σ = stress tensor

These relationships are valid only for stress states well below failure. Such models are developed using data from laboratory cyclic triaxial testing. A well known relationship for the development of permanent strains with the number of load cycles is that proposed by Barksdale (106),

$$\varepsilon_{1p} = a + b\log N$$

The plastic axial strain ε_{1p} plots against the logarithm of the number of load applications N, for different ratios $(\sigma_1 - \sigma_3)/\sigma_3$ as shown in Figure 3.6. This values of the constants a and b in the above relation therefore depend on the ratio $(\sigma_1 - \sigma_3)/\sigma_3$.

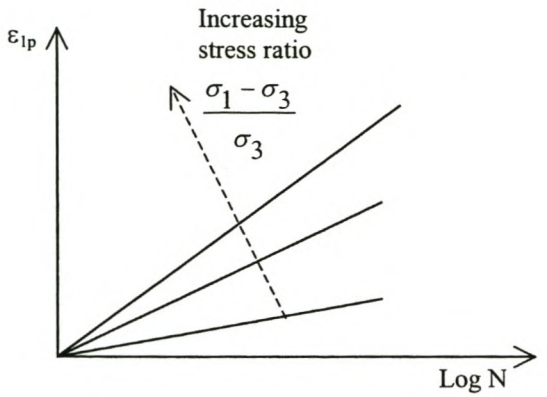

Figure 3.6 Plastic strain ε_{1p} vs log N.

Sweere (81) performed permanent strain tests up to 10^6 cycles for which he did not get good results with Barksdale's relationship, but he obtained a good fit with a relationship of the form,

$$\log \varepsilon_{1p} = a + b \log N$$

Paute et al. (68) based on research done in France obtained a relationship between the strain rate $\delta\varepsilon_{1p}/\delta N$ and number of load cycles which they expressed as,

$$\ln\left(\delta\varepsilon_{1p}/\delta N\right) = a + b \ln N$$

For plastic strain developed after 100 load cycles ε_{1p}*, this becomes,

$$\varepsilon_{1p}^{*} = A\left[1 - (N/100)^{-B}\right]$$

where B is positive. The parameter A was shown to relate to applied stress level as follows,

$$A = \frac{\eta}{c + d\eta}$$

where, c,d = positive constants

η = applied stress ratio

Wolff and Visser (105) based on data from full scale HVS testing (Heavy Vehicle Simulator) on various pavement types developed a design method for limiting rutting in granular layers. They developed the following relationship between permanent strain and number of load repetitions,

$$\varepsilon_p = (mN + a)(1 - e^{-bN})$$

where a, b and m are constants, ε_p = permanent strain and N = number of load repetitions.

3.7 Summary

1. Under repeated loading, the response of unbound granular materials is essentially resilient.
2. The resilient and permanent strain deformation characteristics of granular materials are non-linear with respect to applied stress level and this fact should be taken into account to obtain a reasonable distribution of stresses in the pavement layer system in the process of analytical design.
3. The repeated load triaxial test provides a realistic means of determining the resilient and permanent strain properties of unbound granular materials.
4. The resilient and permanent deformation behaviour of granular materials as determined in the repeated load triaxial apparatus may be represented by practical and usable models which are suitable for implementation in computer-based analyses of pavement structures.

4 ZAMBIAN ROAD DESIGN RELATED INFORMATION

4.1 Introduction

A four weeks visit to Zambia was made during which information on road design and that pertaining to the road delivery network was collected. This was undertaken as part of the research programme in order to make the study relate to pavement design and construction in Zambia, where lateritic gravel remains an important road building material. It was originally intended to conduct tests on lateritic gravel from Zambia, but attempts to transport large quantities of gravel required for triaxial testing from Zambia to South Africa proved difficult and very costly. As a result testing was done on a lateritic gravel from a nearby borrow pit at Maaitjies Kuil in CapeTown which was considered a suitable substitute. Despite this difficulty, the relevance to the Zambian situation was not lost. Due to lack of proper documentation at the Roads Department in Lusaka most of the information encountered was not comprehensive. In particular, information on the occurrence, nature and distribution of lateritic gravels and other road building materials is very scanty. This chapter presents general information collected from the relevant government departments, contractors and consulting engineers, and other agencies. Extra information is given in **Appendix D**.

4.2 General Information, Climate and Geology

Zambia, with an area of 752,600 km^2, is approximately two thirds the size of South Africa and 1.4 times the size of France. It has a population of around 10 million people. Plateaus at altitudes between 650m and 1200m occupy the larger part of the

country. These elevations, in conjunction with Zambia's position between latitudes 8° and 18°, contribute to its excellent (and sunny) climate.

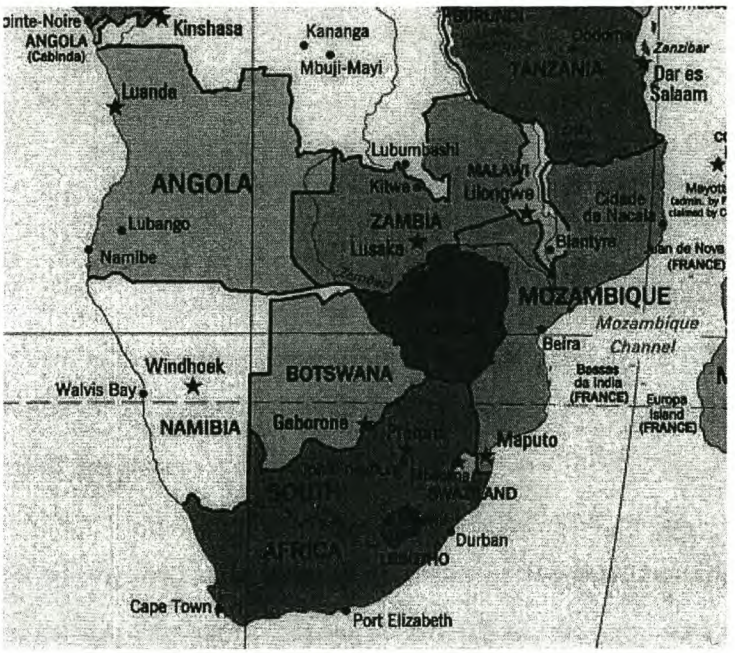

Figure 4.1 Zambia - General location map.

Rainfall

A map of annual rainfall, Figure 4.2, illustrates an approximate north-west to south-east decreasing rainfall gradient of about 1400mm in the north to about 700mm in the south. The rain season lasts about six months from mid-October to the end of April.

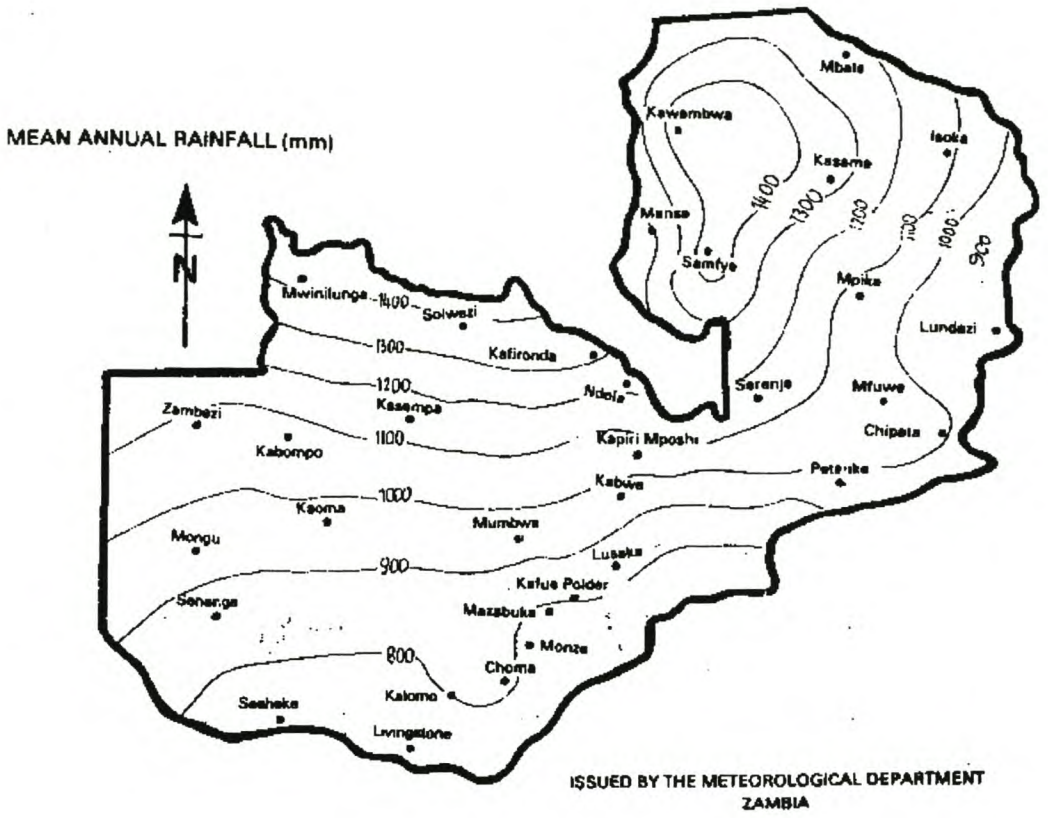

Figure 4.2 Zambian mean annual rainfall map.

Temperature

Compared to other areas at similar latitudes, two factors contribute to the generally lower temperatures in Zambia. One is the elevation of the land surface, most of Zambia lying above 1000 metres. The other is due to the cooling effect of showers and clouds during the potentially hottest time of the year. July is the coldest month and has the lowest minimum temperatures. October is the hottest month with mean daily maximums reaching 30°C almost everywhere. There is generally increasing gradient from the north to south, with variation due more to altitude than any other cause. Climatic data on various climatic elements is available in a computerised database from the Meteorological Department in Lusaka for an extended period of time for the 36 main weather stations distributed around the country. Figures 4.3 to 4.5 illustrate the annual mean temperature, minimum and maximum temperatures.

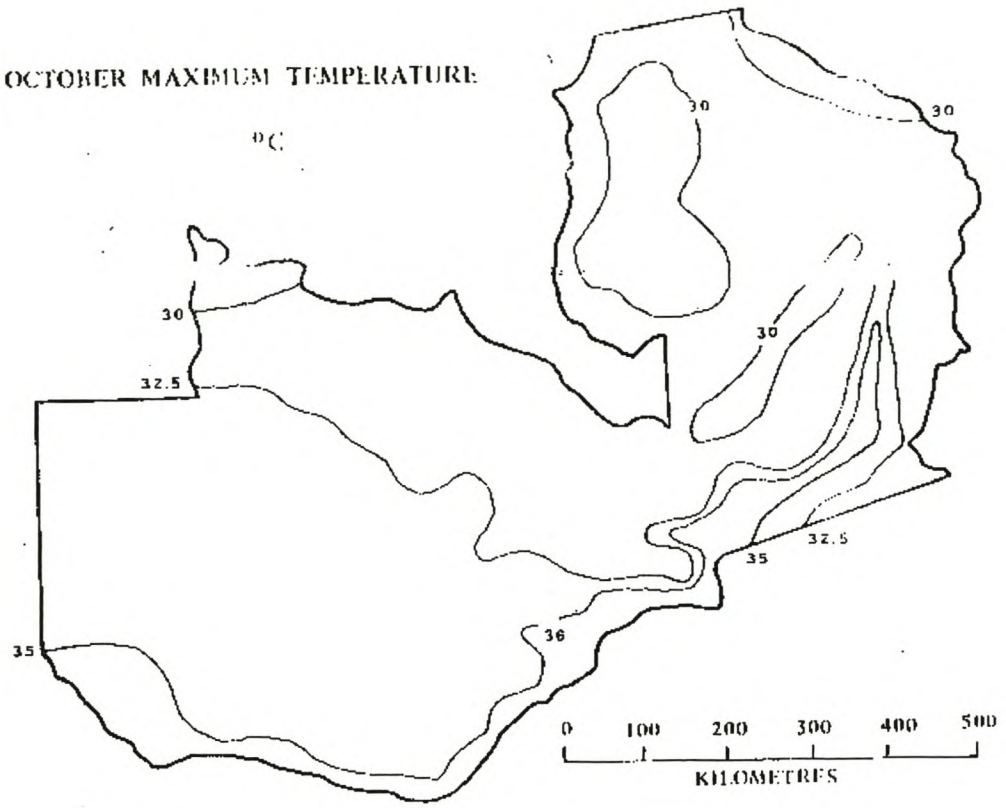

Figure 4.3 October maximum temperature for Zambia.

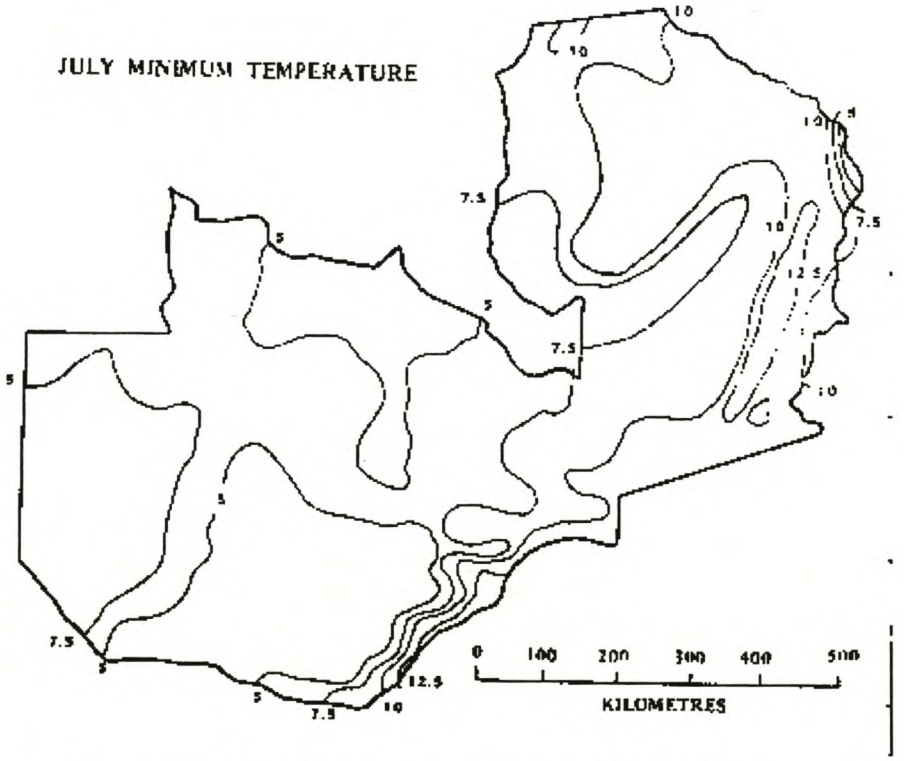

Figure 4.4 July minimum temperature for Zambia

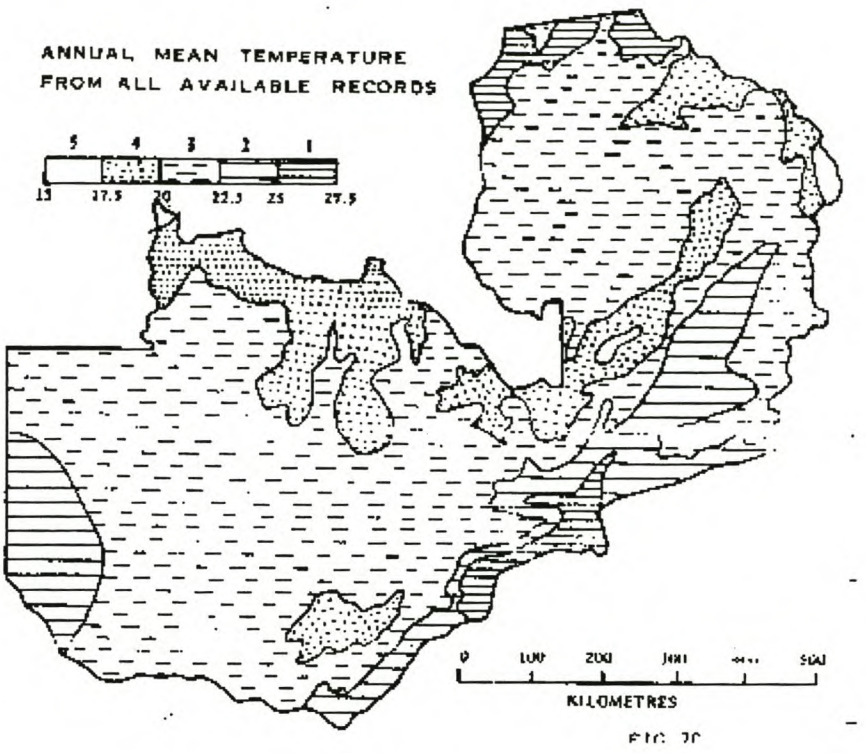

Figure 4.5 Annual mean temperature for Zambia.

4.3 Zambian Road Delivery Network (39)

Background

Zambia has 37,000 km of gazetted roads. Approximately 21,000 km, which comprise trunk, main and district roads are under the jurisdiction of the Roads Department in the Ministry of Works and Supply. The balance, which includes feeder, urban and rural roads fall under the jurisdiction of city, municipal and district councils in the Ministry of Local Government and Housing and under the Department of National Parks and Wildlife in the Ministry of Tourism.

Historical perspective

Since independence in 1964, emphasis of both Government and donor funded road projects was on opening new areas for communication and economic development through construction of new roads. Few mechanisms were put in place for maintenance of the newly constructed roads so much so that by the end of the seventies, although the road network was valued at US $ 2.3 billion, only about 40-50% was in good condition. Funding of roads during the eighties and early nineties averaged only 10-20% of budgeted amounts and this had an adverse effect on the condition of the roads. Owing to lack of maintenance the value of Zambia's road network has shrunk to about US $ 1.5 billion by the start of the nineties. Road agency capital expenditures concentrated on capital projects aimed at rehabilitating failed sections of roads. Little or no maintenance was done. Currently, of the 37,000 km road network, only 20% is in good condition, 40% is classified as fair and the rest is poor.

Road sector reforms in Zambia: 1993 to date

In 1993 the Zambian Government joined the World Bank sponsored Road Maintenance Initiative (RMI) under the auspices of the Sub-Saharan African Transport Programme (SSATP). Under the RMI reform programme, the biggest realisation made was that problems faced by road management institutions included serious human resource constraints, inadequate financing arrangements, lack of clarity in responsibilities amongst road agencies, inefficient structures and weak management systems. Government established a Road Fund comprising a levy on fuel and subsequently, Statutory Instrument No. 42 of 1994 established the National Roads Board (NRB) for the purpose of managing and financing the Road Fund. Zambia has since embarked on an ambitious reform programme in the roads sector known as Road Sector Investment Programme (ROADSIP).

Maintenance Management

In 1995, a Highway Management System (HMS) was established within the Roads Department with financial assistance from the World Bank to serve as an effective

planning tool to assess the rehabilitation and maintenance needs for the road network under the jurisdiction of the Roads Department. A total of 12,674 km selected paved and unpaved roads have been surveyed and data input to the system out of a total expected road network of 21,000 km.

4.4 Common Pavement Structures in Zambia (90)

Most of the main roads in Zambia constructed before 1990 were constructed using a cement treated natural gravel base (usually 150mm) on a natural gravel sub-base and surfaced with double surface dressing. New construction and rehabilitation work in the 1990's, has seen the increased use of more expensive graded crushed stone base. A new material has been tried on two new projects were a foam bitumen stabilized gravel base was used. In 1998 a road project was completed on the Mazabuka-Monze road (a section of the T2) where the base was constructed using a 150 mm foamed bitumen stabilized natural gravel over a natural gravel base with a double surface dressing surfacing. The residual bitumen content was 4.7%. A similar method has been used in the current (1999) reconstruction of the Luanshya-Mpongwe road (a 64km district road).

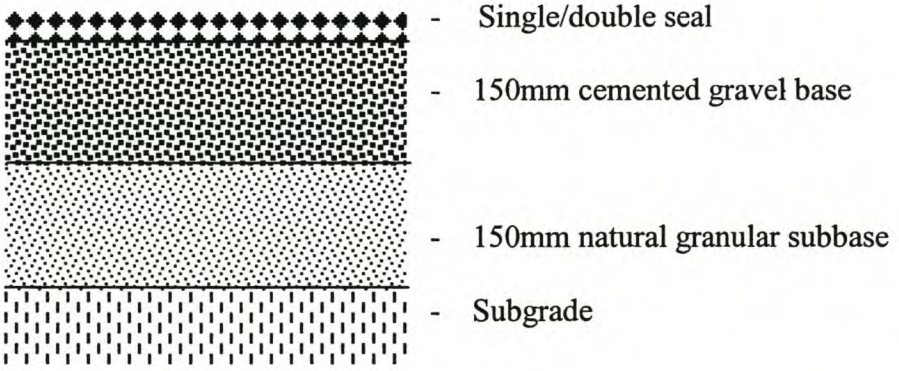

Figure 4.6 Typical pavement structure in Zambia before 1990.

The cement treated bases, used to construct most roads in Zambia in the past, have generally performed well but are less preferred now because of the problem of cracking. A comparison of the performance of cement treated gravel bases with the more expensive crushed stone base or foam bitumen treated base which are newer methods of construction in Zambia would require a more detailed study.

4.5 Road Building Materials in Zambia

The following soils occurring in Zambia are of particular interest for road construction (the terminology and description is according to available Zambian engineering literature (19)):

Quartz gravels. These are found in Southern Province and in limited quantities elsewhere. Their group classification is A1 (AASHTO classification).

Decomposed rocks. Decomposed igneous and sedimentary rocks including quartzites, dolomites, granites, limestones, sandstones and basalts are widely distributed. They fall normally within sub-group A-2-4 and A-2-6.

Laterite. It is a residual deposit resulting from extensive decomposition of rock, in Zambia mainly from basic rocks. It consists mainly of oxides of iron and aluminium. Deposits are widely distributed in Zambia, sometimes in association with quartz pebbles or quartzitic and schisty nodules. The sub-group classification is usually A-2-4 or A-2-6.

"*Kalahari sands*". They occur over the greater part of western Zambia and in the vicinity of Livingstone in the south. These soils can usually be classified as A-4. They are uniform sands that present a difficult problem due to their lack of cohesion.

"*Dambo clays*". Low lying marshy areas known as "dambos" occur in most parts of the country. They are formed of material which is similar to the "black cotton soil" found in many other parts of the world. The soil has little bearing value and is subject

to exceptional swell and shrinkage between the wet and dry seasons. The soil is usually A-6 and sometimes A-7.

Quartzitic and lateritic gravels are used as bases under thin bituminous surfacings. They are usually stabilized with cement or by the incorporation of small quantities of hydrated lime. Cement is the most commonly used of the two. While some of these materials are suitable as bases in their natural state, in most places the best materials have to be hauled for considerable distances. The choice of stabilisation is therefore a problem of economics in that the cost of such treatment has to be compared with the savings in haulage costs.

There is a striking lack of documented information in the engineering literature on the occurrence, nature and distribution of road building soils and gravels. The only source of information available is pedogenic soil maps whose intended use is in agriculture. With an understanding of the basis of classification used pedogenic information can provide valuable information on the availability of suitable road building materials and can also provide a first approximation of expected behaviour in road construction. Pedological soil maps are produced by and available at the Soil Survey Unit at Mount Makulu in Lusaka.

4.6 Traffic surveys information and axle loads data

The Highway Maintenance System (HMS) of the Roads Department in Lusaka maintains comprehensive information from traffic surveys including axle loads data in its database that is part of its highway management system. The database is designed to be updated every two years when new information is collected. The latest information available is for 1996. Traffic count data from surveys conducted in 1995 for the six trunk (T) roads extracted from the data base is presented in **Appendix D**.

Weigh bridges:

A total of eight permanent weigh bridge stations are strategically located countrywide. Twelve other temporary investigation points usually supplement these. The Roads Department maintains all the weigh bridges. Manual mechanical servo balance weigh scales with a maximum capacity of 30 tonne are used at the eight permanent stations while portable electronic weigh scales are used at the temporary stations.

4.7 Design Standards, Maintenance and Construction Specifications

The revised Southern Africa Transport and Communication Commission (SATTC) design standards and construction specifications (1994) have been adopted in Zambia. These can be ordered from SATTC in Mozambique. These are:

1) Recommendations on Road Design Standards (71,72).
   - Volume 1. Pavement design guide.
   - Volume 2. Geometric design of rural roads.
2) Standard Specifications for Roads and Bridges (78).

The design method follows the design concept as set forth in the "AASHTO Interim Guide for the Design of Pavement Structures", 1972-1986, published by the American Association of State Highway and Transportation Officials. The interim guide was replaced by its final version published in 1986, which was again revised in 1993. A brief description of the AASHTO method and the Zambian pavement design guide are given in Section 2.8.2. The Zambian pavement design guide includes a catalogue of standard designs which has been included in **Appendix D.**

Other design guides are in use of which the most often used in the past has been TRRL design stated in Road Note 31 (74). A brief description of the method has been given in Section 2.8.2.

Zambian specifications for gravel base and subbase materials are given in **Appendix C.**

5 DESCRIPTION OF TEST PROGRAMME

5.1 Introduction

In Zambia, lateritic gravels are widely used as base and subbase layers of light to medium trafficked roads. Because they are often used under thin bituminous surfacings, they perform a very important structural role taking up most of the traffic loading. Empirically based pavement design procedures and material characterization criteria are used. The full contribution of granular layers to a successful pavement structure is never fully realised because of lack of a rational approach to pavement design and material characterization. The aim of this research, therefore, is to conduct a laboratory study into the properties of a natural lateritic gravel suitable for use in the layers of a pavement structure as base or subbase, stabilized or unstabilized. A successful granular layer must exhibit high resilient moduli in order to spread load adequately and must also resist internal deformation which might contribute to surface rutting. Triaxial testing in the laboratory, which offers the best opportunity to study the mechanical behaviour of granular materials under repeated loading, formed the main focus of the test programme. This chapter gives a description of the test programme. The results of all tests are presented in Chapter 6.

5.2 Materials Used in the Test Programme

It was originally intended to perform testing on a laterite gravel sourced from Zambia but this was made difficult by the very high cost of transporting large quantities of gravel required for use in triaxial testing to South Africa. An alternative nearby source of lateritic gravel was found at a borrow pit at Maaitjies Kuil near Cape Town belonging to Malans Transport which at the time was the only active pit in the area.

Municipalities in the area at the time used this source of gravel in their township services. However, gravel from this place is not consistent as varieties from outlying areas are also stockpiled at this place. Gravel taken from only one stockpile was used in the entire test programme. Results for standard tests done on the gravel are given in Chapter 6.

In Zambia lateritic gravel in highway pavements finds use in a number of ways:

- Most roads in the past were constructed using a cement treated gravel base over a natural gravel subbase. Apart from the problem of cracking and problems in the construction process, these roads have performed satisfactorily over the years.
- Lime treated base is often applied like the cement treated base, but works well when the plasticity of the materials is greater than 10. Lime has been less used compared to cement.
- Untreated gravel base has given satisfactory performance in many instances. Field studies (40) in the recent past have shown that roads build using untreated lateritic gravel bases, have performed very well sometimes even better than those built with crushed rock.
- Bitumen emulsion has been less widely used and investigated. Two recent road projects in Zambia where foamed-bitumen stabilized gravels base was used have generated local interest into the potential of the use of this material as an alternative to cement stabilized gravel and expensive crushed rock.

The choice of material used in any specific case depends on a number of factors such as availability of suitable quality materials within favourable distances, cost of additives and problems during the construction process. Based on the above possibilities, testing was undertaken on the following categories of materials:

1. Unstabilized gravel
2. Cement stabilized gravel, with cement contents of 2% to 6%.
3. Foamed-bitumen treated gravel, with residual bitumen contents from 2% to 5%.

Because the material studied had a low plasticity (slightly plastic, SP), lime treatment was not considered.

5.3 Test Programme

The test programme comprised:

1. Standard tests, for material characterization and,
2. Triaxial testing, to study the resilient and permanent deformation behaviour of the materials

Triaxial testing formed the main part of the test programme. In addition a chemical analysis was performed on the lateritic gravel at the geology department of the University of Stellenbosch using X-Ray Fluorescence. The following standard tests were conducted on the lateritic gravel:

- Gradation
- Atterberg limits
- compaction tests
- specific gravity
- durability
- CBR.

Standard test procedures given in TMH1 (83) were followed for all standard tests. The 10% Fines Aggregate Crushing Test (10% FACT) as described in SABS Method 842 was used for assessing durability of the aggregate. As mentioned in the literature review (Chapter 2), some types of lateritic soils do not give reproducible standard tests results when tested using varying pre-test preparation and testing procedures. Extra standard tests were therefore performed to investigate the effects of varying the mixing-time and method of drying (oven or air-dried) on the index properties and gradation of the lateritic gravel used in this test programme. Test results and chemical analysis results are presented in Chapter 6.

Triaxial testing was conducted in the MTS machine (described in Section 5.4.2). Three types of triaxial tests were conducted:

- Static test, to determine the shear strength parameters, c and ϕ.
- Cyclic load test, for determining the resilient modulus, Mr.
- Cyclic load test with up to 100,000 load repetitions, for determining the permanent deformation behaviour.

Triaxial specimens where prepared at different conditions of compaction and moisture. Results from the above tests describe the resilient and permanent deformation properties and provide inputs to mechanistic design methods. The following additional tests were conducted on the treated gravel:

- California Bearing Ratio (CBR)
- Unconfined Compression Strength (UCS)
- Indirect Tensile Strength (ITS)

A summary of the test programme is given schematically in Figure 5.1.

	Tests	Material	Tests Objective
Standard tests	Gradation Atterberg limits Compaction tests Specific gravity Durability CBR	Untreated gravel	Material characterization and classification
Chemical analysis	X-ray fluorescence	Untreated gravel	Laterization degree
Triaxial tests	Static triaxial testing Cyclic triaxial testing	Untreated/treated gravel	Mechanical characteristics for input to analytical design procedures.
Standard tests on treated materials	CBR, UCS, ITS	Treated gravel	Mechanical characteristics

Figure 5.1 Schematic summary of test programme

For foamed-bitumen, distinction was made between two types of treatment using an approach similar to that in South Africa's TRH 13 (29) and GEMS manual (103),

- *modification*. Low binder contents 2% - 3%. Here the material is treated as a granular material.
- *stabilization*. Higher binder contents more than 3%. Here the material is treated as if it were an asphaltic mix.

Detailed information on the characteristics of the tested specimens, i.e. binder/cement content, density, test moisture has been presented with the results in Chapter 6.

The use of the model accelerated testing machine to investigate performance aspects was also planned but due to time constraints this could not be done. Model APT testing in the laboratory can be used as a cheaper alternative to long term testing in the field to evaluate performance of pavement materials.

5.4 Description of the Triaxial Test

5.4.1 General

Figure 5.2 illustrates the forces applied on the triaxial specimen:

- the confining pressure via the air or water pressure inside the load cell and,
- the axial deviator stress (σ_{dev}) applied via a hydraulic actuator.

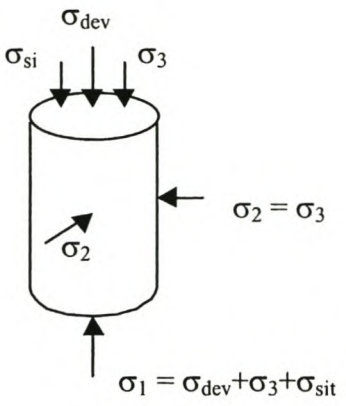

Figure 5.2 Schematic of triaxial specimen.

As shown in Figure 5.2, the first principal stress (σ_1) consists of three components, i.e. the deviator stress (σ_{dev}), the confining stress σ_3, and a static sitting load (σ_{sit}). A small static sitting load, σ_{sit} = 20 kPa is applied in order to ensure continuos contact between the top platen and the loading ram. The second and third principle stresses are equal to each other (σ_2=σ_3).

World wide, triaxial equipment for testing of granular materials exists to various levels of sophistication. Figure 5.3 shows that in a real pavement structure the principle stresses at any point rotate through a phase of 180° and there is a shear stress reversal under a moving wheel load. Therefore to simulate better the field loading conditions, some equipment has been build which is able to apply a variable confining pressure. However, research has shown that even equipment which apply only a constant confining pressure give reasonable results.

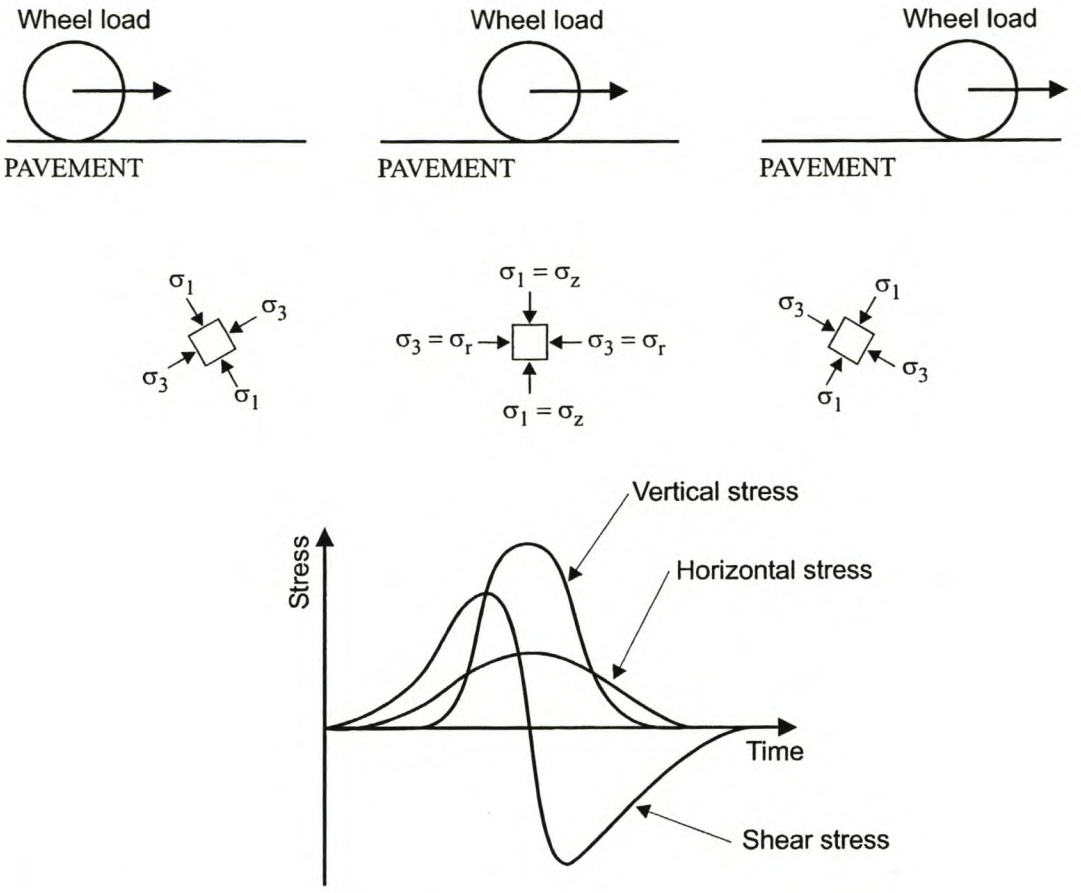

Figure 5.3 Stresses beneath a rolling wheel load (after (47)).

5.4.2 MTS machine

Triaxial testing was conducted in the MTS machine (Materials Testing System) of the Civil Engineering Department at the University of Stellenbosch. This is a servo-hydraulic testing apparatus capable of a wide range of test configurations. The triaxial test configuration, Figure 5.4, includes a triaxial cell, servo-hydraulic system, and a control and data acquisition system. The cell can be filled with air or water and only a constant pressure can be applied. A cell pressure up to 1000 kPa is possible. The cell can sit a specimen of size 150 mm diameter and 300 mm high. The axial loading system has a loading capacity of 10 ton. The configuration includes the following transducers which capture data onto a logged on computer:

- A 10 ton load cell, measures the axial load
- 2 displacement transducers (LVDT's) measure the axial strain.

The test configuration does not include transducers for radial deformation measurement. This means the Poisson's ratio cannot be computed. A constant value of 0.35 is assumed during analysis.

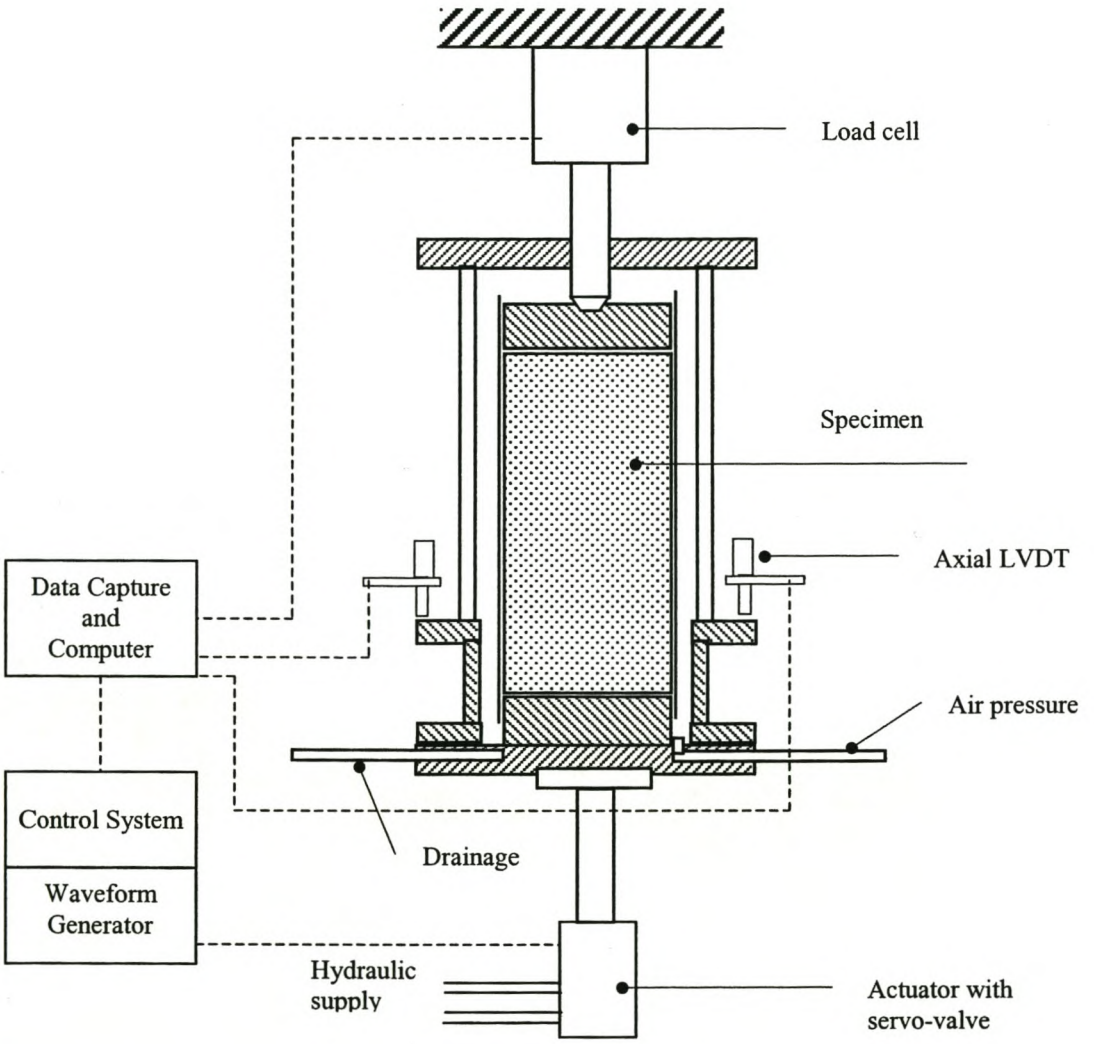

Figure 5.4 Schematic of triaxial configuration.

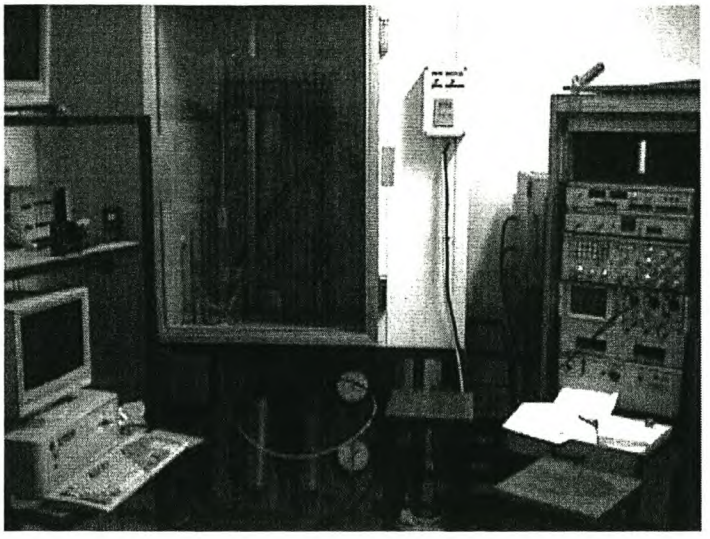

Figure 5.5 MTS Machine.

5.4.3 Triaxial specimen

The minimum specimen diameter is determined by the maximum aggregate size. A minimum ratio of 4 is commonly accepted. The lateritic gravel tested had a maximum aggregate size of 26.5 mm, implying a diameter of at least 100mm. A specimens diameter of 150 mm was chosen for these tests. It can be shown using the Möhr-Coulomb diagram that the failure plane in a triaxial test specimen makes an angle of $(45° + \phi/2)$ with the horizontal as shown in Figure 5.6. A trial test was done with a special made 400 mm high specimen. The result gave a failure plane angle of 74° measured on the failed specimen. This suggests even a higher specimen height of at least 520 mm in order to obtain a fully developed failure plane Such a height would present practical difficulty in the manufacture and handling of the specimens. A specimen height of 300mm was used.

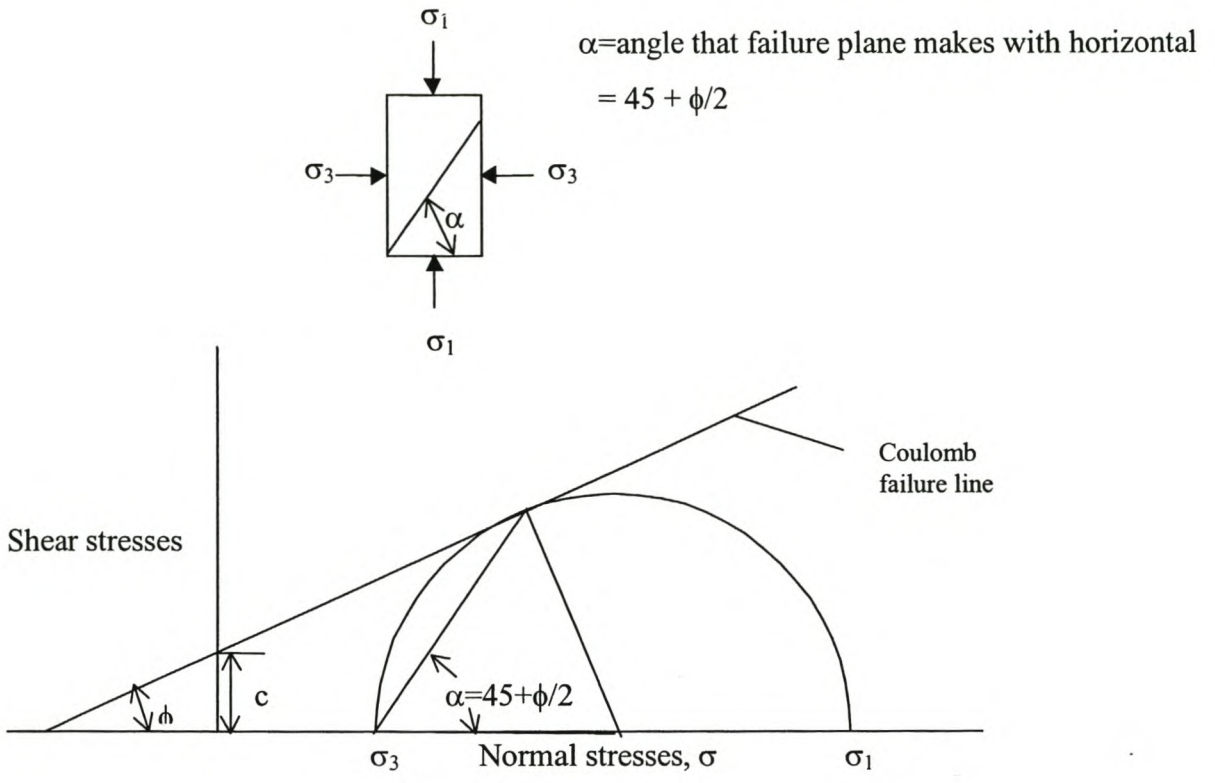

Figure 5.6 The angle that the failure plane makes with the σ_3 direction.

5.5 Test Procedure

5.5.1 Static load testing

The objective was to compute the shear strength parameters of the material, c and ϕ. The procedure involves gradual axial loading of the specimen at constant strain until failure. For any condition of moisture and compaction, at least three tests at different confining stresses are required to be able to compute the shear strength parameters. The deformation rate for the static test was 1.25 mm/min or approximately 0.4 % strain/min. This test rate is much lower than that used by Maree (52) of 3.8 mm/min. It was observed during trial tests that the specimen failed at a strain of about 0.5%. The chosen rate thus allows for at least a minute to failure of the specimen. The

confining stress levels used were 50 kPa, 150 kPa and 300 kPa. Because the static test is a destructive test, a new sample is used for every confining stress level. During the test, deformation (internal MTS LVDT) and load data are captured on a logged on computer. Sample output from the static test is shown in a stress-strain plot in Figure 5.7.

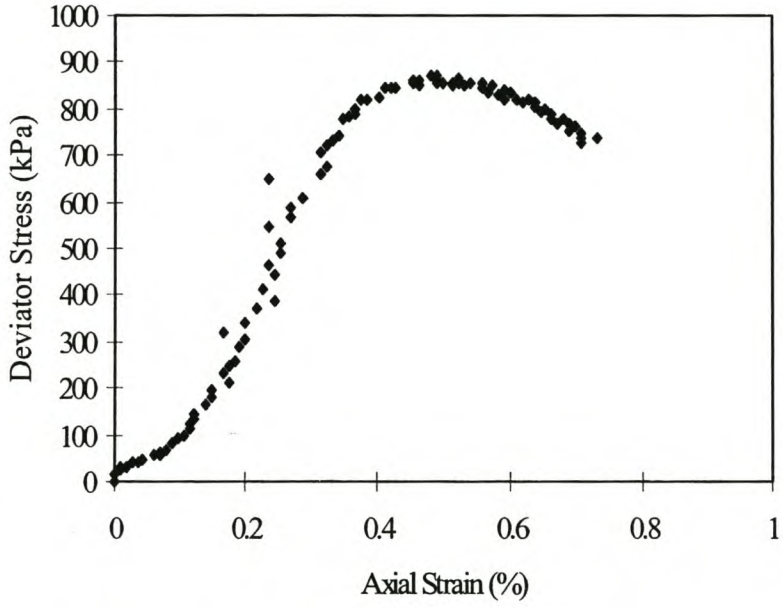

Figure 5.7 Sample output from static test

5.5.2 Cyclic loading for resilient testing

The objective was to analyse the resilient behaviour of the material. The test procedure adopted is similar to that described by Maree (52). Testing for resilient modulus was conducted at different conditions of moisture and compaction. A loading rate of 2 Hz which approximates an average wheel speed of 10 km/h (52) was used. Stress levels as shown in Table 5.1 were applied. Stress levels were chosen to represent a range of those that occur in a pavement structure as obtained from an elastic analysis programme. Three confining stress levels of 50 kPa, 150 kPa and 300 kPa were used. At each confining stress level up to five deviator stress levels where used.

Table 5.1 Stress levels used in cyclic triaxial test programme.

Confining stress (kPa)	Deviator stress (kPa)				
50	50	100	200	300	400
150	150	250	350	450	550
300	300	350	400	450	500

The following procedure was followed:

- a static sitting load of 20 kPa was applied on setting up
- confining stress was set on the first level
- deviator stress was applied to the first level
- 1200 conditioning cycles were then applied at end of which the first stress-strain data was recorded
- at that confining stress level, recordings were made on subsequent application of 120 conditioning cycles on every increase in deviator stress
- the confining stress was set to the next level, 1200 cycles again applied, and the procedure repeated.

The initial conditioning cycles were to allow for the large permanent strains during the first hundreds of cycles to stabilize. For at least one sample testing was also done at varied loading frequencies, between 0.5 Hz to 4 Hz to investigate the effect of the loading frequency on the resilient modulus. The specimen response (stress and strain data) was captured on a logged on computer within a five seconds period at each recording. In that period ten load cycles were picked up as shown in Figure 5.8. This data was used to calculate the resilient modulus.

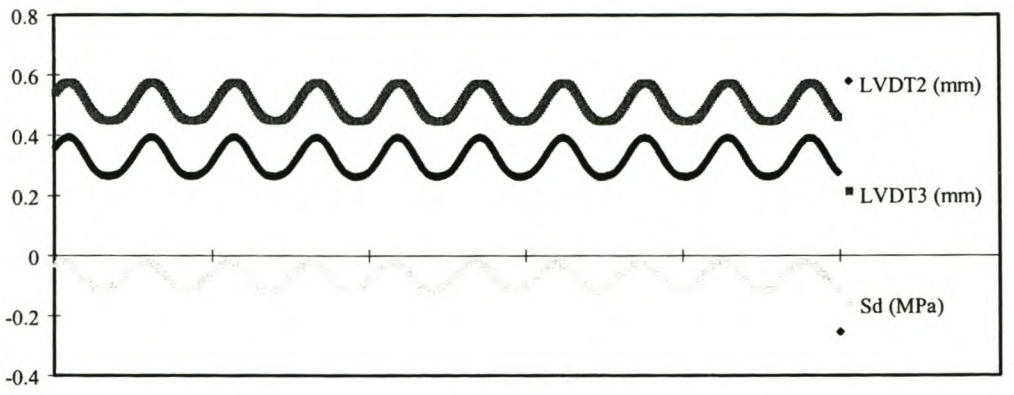

Figure 5.8 Sample output from cyclic load test.

5.5.3 Cyclic loading for permanent deformation testing

The objective was to analyse the development of permanent strains with the number of cycles of loading for different stress levels. The study comprised four tests at different stress levels. Each test consisted of applying up to 100 000 cycles of loading. All specimens were at optimum moisture (6.3 %) and almost the same degree of compaction (94 - 95 %). Only a confining stress level of 50 kPa was used because of the lengthy test, while the deviator stress was varied at ratios of $\sigma_1/\sigma_{1,f}$ = 0.4,0.5,0.7,0.8 for the four specimens. The stresses applied are given in Table 5.2.

Table 5.2 Stress levels used in cyclic loading for resilient testing.

	Confining stress (kPa)	Deviator stress (kPa)	$\sigma_1/\sigma_{1,f}$
1	50	200	0.4
2	50	300	0.5
3	50	400	0.7
4	50	500	0.8

The following testing regime was followed:

- a static sitting load of 20 kPa was applied on setting up
- confining stress was set at 50 kPa
- 100 000 cycles were applied at a loading rate of 2 Hz
- The stresses and strains were recorded at load cycles, N = 100, 500, 1000, 2000, 3000, 5000, 10 000, 20 000, 30 000, 50 000, 75 000, 100 000.

No data was recorded before the first 100 cycles as this was regarded as an initial settling in phase. The stress and strain data was recorded in the same manner as for the 'cyclic loading for resilient testing' which thus also allows for the calculation of resilient modulus. In this way the change in resilient modulus with number of load cycles can also be monitored.

5.6 Preparation of triaxial specimens

The natural gradation from the stockpile was used. The material was air dried after which the hygroscopic moisture was determined. A riffler was used to divide the material into the required amounts. Compaction moisture was then mixed in and compaction carried out for each type of material as described below and summarised in Table 5.3.

Table 5.3 Modes of compaction used for the different materials.

	Untreated gravel	Foamed-bitumen treated	Cement treated
Compaction mode	Vibrating table	Gyratory compactor	Gyratory compactor
Specimen size	150 x 300 mm high	150 x 100 mm high	150 x 100 mm high
Additives	-	Foamed-bitumen +/– 1.5% cement	Cement

5.6.1 Untreated gravel

Compaction

The procedure adopted was similar to that suggested by Maree (52). Compaction was done on a vibrating table in a 150 mm diameter by 300 mm high split mould. Compaction was done in five layers, each layer vibrated for 2 minutes under a 50 kg surcharge load. This method of compaction is less severe as regards degradation of the aggregate as compared to the falling hammer method in Modified AASHTO. The sides of the mould were smeared with oil to facilitate easy removal of the sample from the mould.

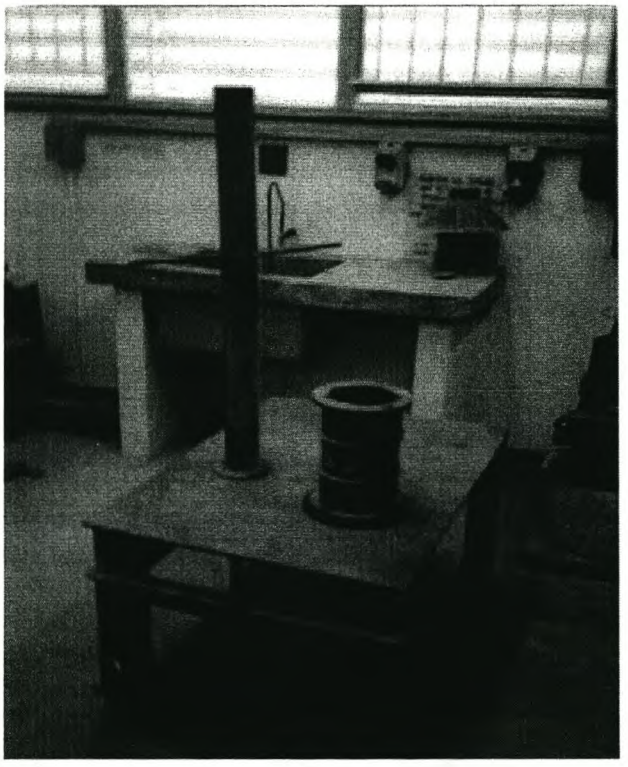

Figure 5.9 Vibrating table, compaction mould and surcharge weight.

Compaction was done at Mod. AASHTO Optimum Moisture Content of 6.3 % established earlier from the standard tests programme. The compactive effort (i.e. amplitude and time of vibration) was also chosen so as to achieve Mod. AASHTO level of compaction. This was determined after a series of trials with the material at optimum moisture content compacted at different times of vibration (amplitude of vibration remained the same). The results are as shown in Figure 5.10. It is evident that after a period two minutes of vibration time, little further compaction seems to take place. Therefore, the vibration time was set at two minutes per layer. Levels of compaction up to 97% Mod. AASHTO were achievable with this compactive effort.

Vibration time (sec)	45	60	120	180
% Compaction	94	93	97	97

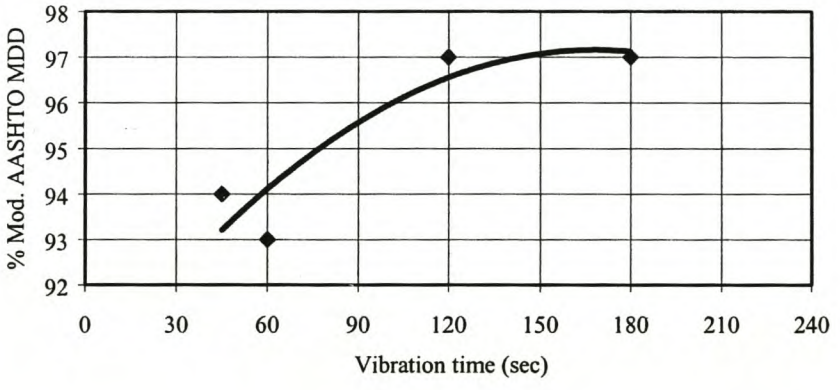

Figure 5.10 Density vs. compactive effort for vibration table.

Curing of samples:

Specimens were kept under a polythene covering to preserve the moisture content until the time of testing. Testing was done at least 24 hours after compaction.

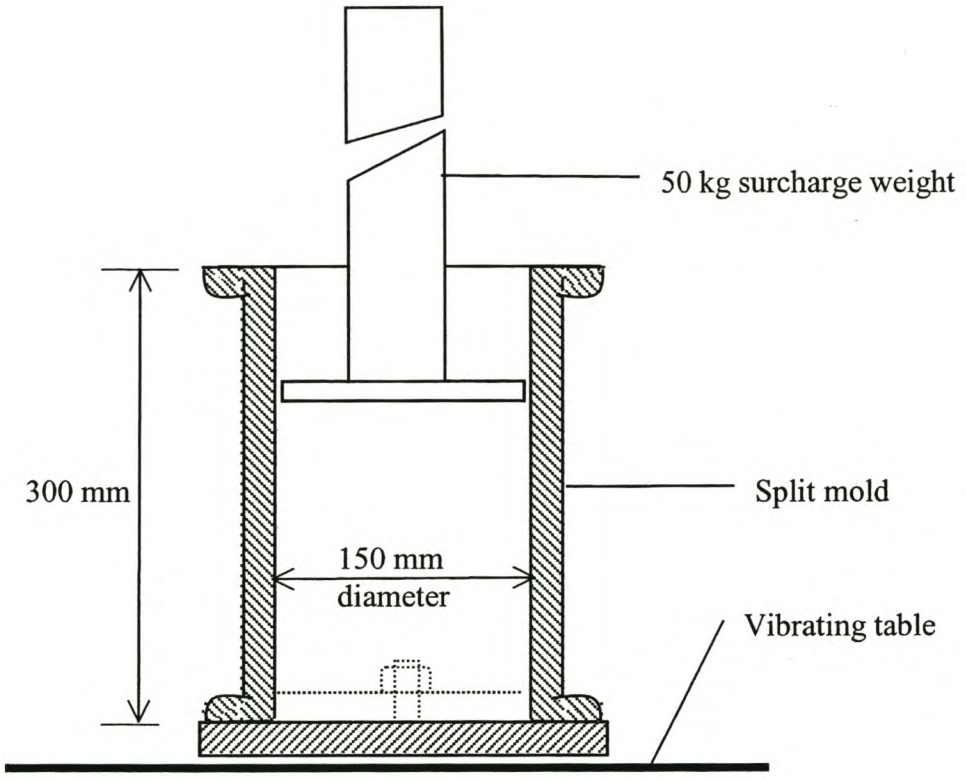

Figure 5.11 Schematic of compaction mould.

5.6.2 Foamed-bitumen treated gravel

Foamed bitumen is produced by injecting a small quantity of water into hot bitumen, causing it to expand several times its volume. The low viscosity and high volume then allows thorough mixing with cold aggregate. A number of studies have been done into the properties of foamed bitumen mixes (22,45). However, not much work has been done on foamed-bitumen treatment of natural gravel materials. In this study foamed-bitumen treatment of a lateritic gravel was investigated.

A laboratory scale foam plant was used to prepare the mixes, Figure 5.12.

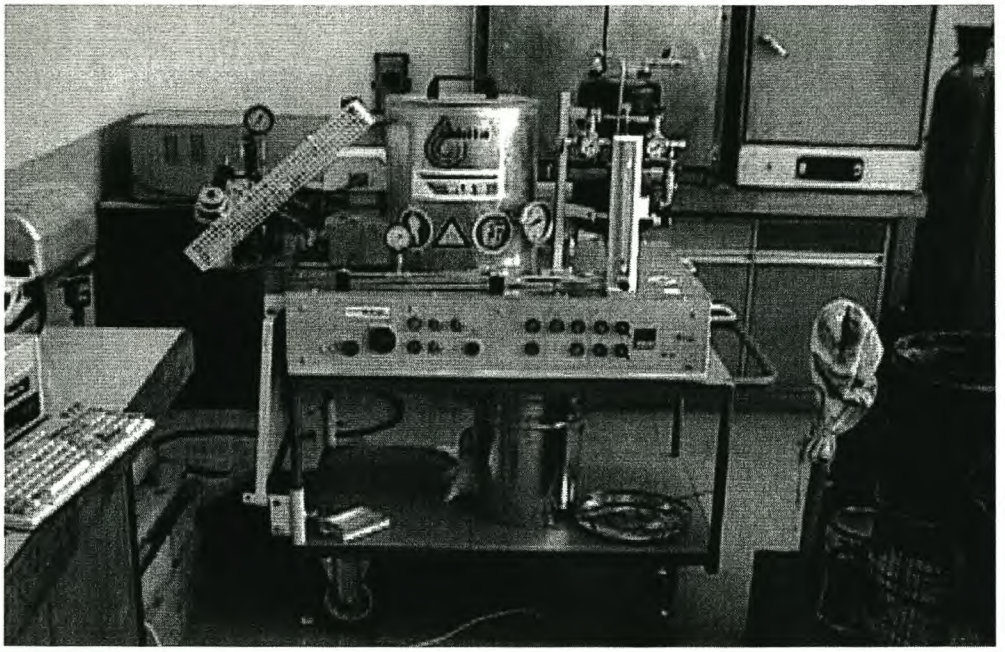

Figure 5.12 Laboratory scale foam plant.

Samples were prepared at the residual binder contents shown in Table 5.4.

Table 5.4 Binder contents for foamed-bitumen treated mixes.

	Binder content (%)		Additives
Modified mixes	2	3	With or without 1.5% cement
Stabilized mixes	4	5	-

Bitumen of penetration grade 80/100 was used. Some cement, 1.5%, was added to some modified mixes to investigate its effect on the properties. No other additives were added.

Compaction

Compaction of foamed-bitumen modified and stabilized mixes was done in the gyratory compactor. The size of the specimens was 150 mm diameter by 100mm high. Using a pressure of 600 kPa, 100 gyrations were applied at which number it was

found from trial compactions that a compaction level close to 100% Mod. AASHTO was achieved as shown in Figure 5.13.

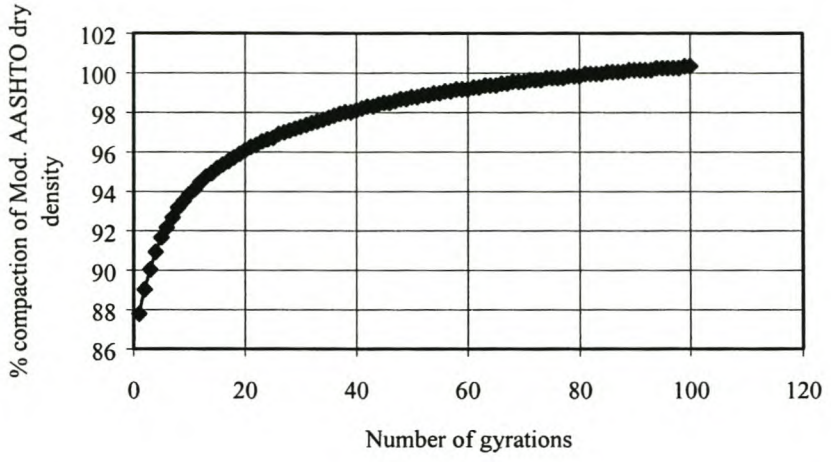

Figure 5.13 Gyratory compaction curve for foamed-bitumen treated gravel.

Mixing and compaction moisture

The definitions given apply to terms used in the following paragraph:

- Optimum moisture content (OMC) - refers to the water content (i.e. hygroscopic moisture and water added for compaction) that gives maximum density when the untreated material is compacted at the Modified AASHTO compaction effort.
- Fluid content - is the total quantity of fluid in the mix, i.e. hygroscopic moisture, water added for compaction, residual bitumen content, and water within the foamed bitumen. Therefore optimum fluid content is the fluid content that gives maximum density for the material when compacted at the Modified AASHTO compactive effort.

Trial compaction at different moisture contents revealed that the highest compaction was achieved with the water content in the mix close to optimum moisture content. Compaction was therefore done at optimum moisture content. Some procedures

elsewhere (76) dealing with higher quality aggregate use the concept of compacting at "optimum fluids" with the result that the amount of water in the mix could be much lower than the optimum moisture content. Results of trial compaction at different moisture contents are shown in Figure 5.14.

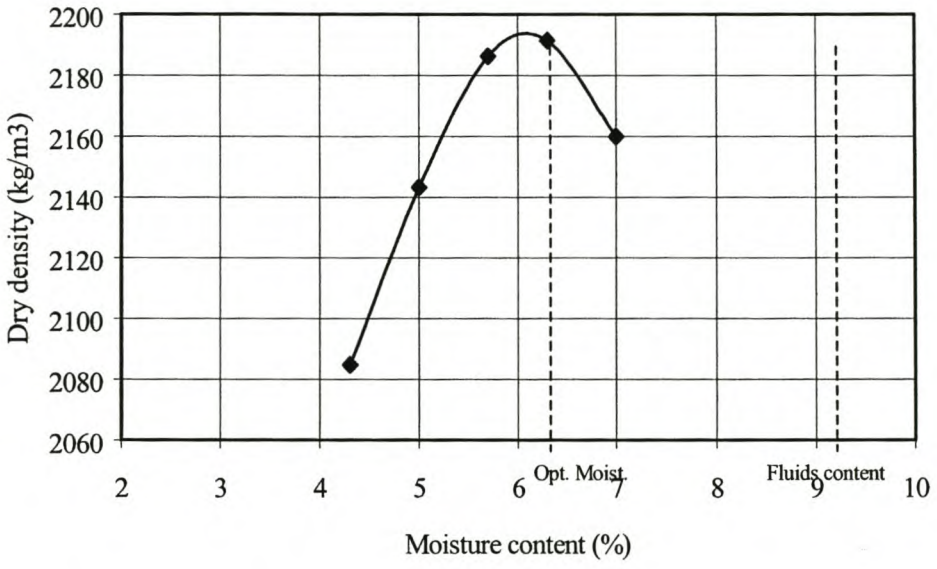

Figure 5.14 Density/moisture content curve for foamed-bitumen treated gravel, (bitumen content 3%).

Since the triaxial test specimens where to be approximately 300mm high, three of the 100mm high gyratory compactor specimens had to be placed on top of each other to form one 300mm high triaxial test specimen. The lack of full contact at the interfaces was assumed to have little effect on the results because failed specimens from static tests showed no slippage on the interface of adjacent specimens with the failure plane cutting continuously through the interface.

Curing of specimens

Specimens were cured for 24 hours in the mould and then a further 6 days outside the mould covered in polythene bag at room temperature (7 days total) after which testing was done. At this stage, the specimen had lost about 1 % from the optimum moisture

content. Some specimens were soaked at the end of seven days by immersing in water for at least 24 hours and then draining off for a few hours prior to testing.

5.6.3 Cement treated gravel

Specimens were prepared at three cement contents of 2%, 4% and 6%.

Mixing moisture and compaction

Compaction of cement stabilized specimens was done in the gyratory compactor. The size of the specimens was 150 mm diameter by 100mm high. Using a pressure of 600 kPa, 100 gyrations were applied at which level of compaction close to 100% Modified AASHTO was achieved. Compaction was done at Modified ASSHTO optimum moisture content. Here also three of the 100mm high specimens had to be placed on top of each other to form one 300mm high triaxial test specimen.

Curing of specimens

Specimens where cured for 24 hours in the mould and then a further 6 days outside the mould covered in polythene bag at room temperature (7 days total) after which testing was done. Some specimens were soaked at the end of seven days for at least 24 hours prior to testing.

6 RESULTS AND ANALYSIS

6.1 Introduction

In this chapter, results of the test programme are presented. Further analysis of the results is done in Chapter 7. The test programme covered a wide range of tests on the untreated and treated gravel, which have been divided into four groups:

- Standard tests
- Chemical analysis
- Static and cyclic load triaxial tests
- Standard tests on stabilized materials

Table 6.1 gives a breakdown of the tests under the various groupings and format for the results.

Table 6.1 Summary of test programme.

	Tests	**Material**	**Results**
Standard tests	gradation Atterberg limits compaction tests specific gravity durability CBR.	Untreated gravel	Section 6.2
Chemical analysis	X-Ray Fluorescence	Untreated gravel	6.3
Static/cyclic load triaxial tests	Static test Cyclic Triaxial Test, resilient testing Cyclic Triaxial Test, permanent deformation	Untreated/treated gravel	6.4
Standard tests on stabilized materials	California Bearing Ratio, CBR Unconfined Compressive Strength, UCS Indirect Tensile Strength, ITS	Treated gravel	6.5

6.2 Standard tests results

Standard tests were carried out on the original untreated gravel according to testing procedures in TMH1 (83). These included: Gradation, Atterberg limits, compaction tests, specific gravity, durability and CBR.

6.2.1 Gradation

Results of gradation analysis obtained using two different pre-test preparation procedures (oven dried and air dried) are given in Table 6.2 and graphically in Figure 6.1 for the air dried sample.

Table 6.2 Results of gradation analysis on Maaitjies Kuil gravel

Sieve aperture (mm)	Percentage passing	
	Maaitjies Kuil Gravel (Oven dried)	Maaitjies Kuil Gravel (Air dried)
26.5	100	100
19.0	91.4	85.1
13.2	88.0	79.0
4.75	73.5	66.2
2.0	52.3	47.2
0.425	25.5	24.4
0.075	11.9	14.6

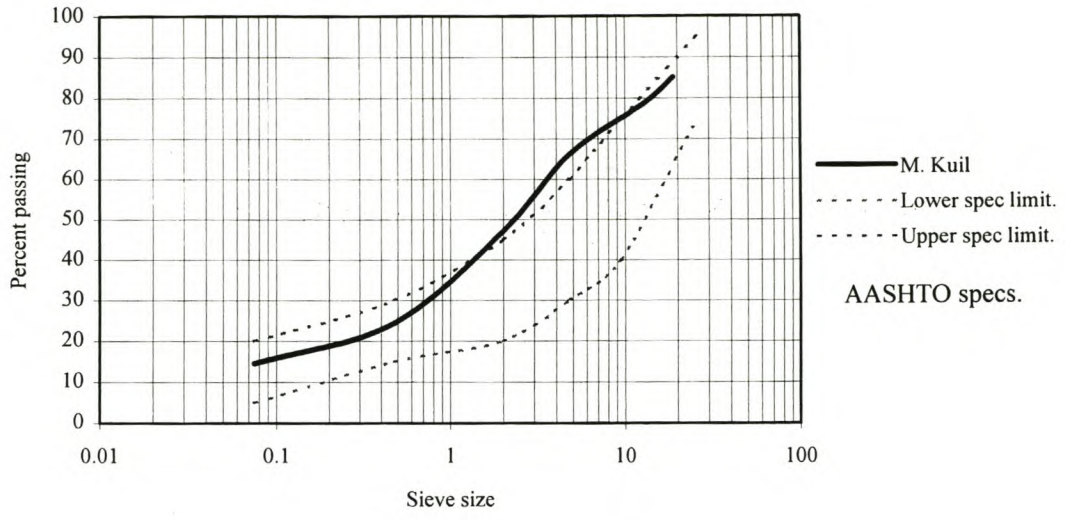

Figure 6.1 Gradation - Maaitjies Kuil Gravel (Air dried)

Figure 6.2 illustrates the difference in gradation for the two different pre-test preparation procedures. Even though oven dried shows a slightly finer gradation, this difference is more likely due to natural variability and the difficulty of controlling the gradation of the natural gravel rather than due to the different pre-test preparation procedures.

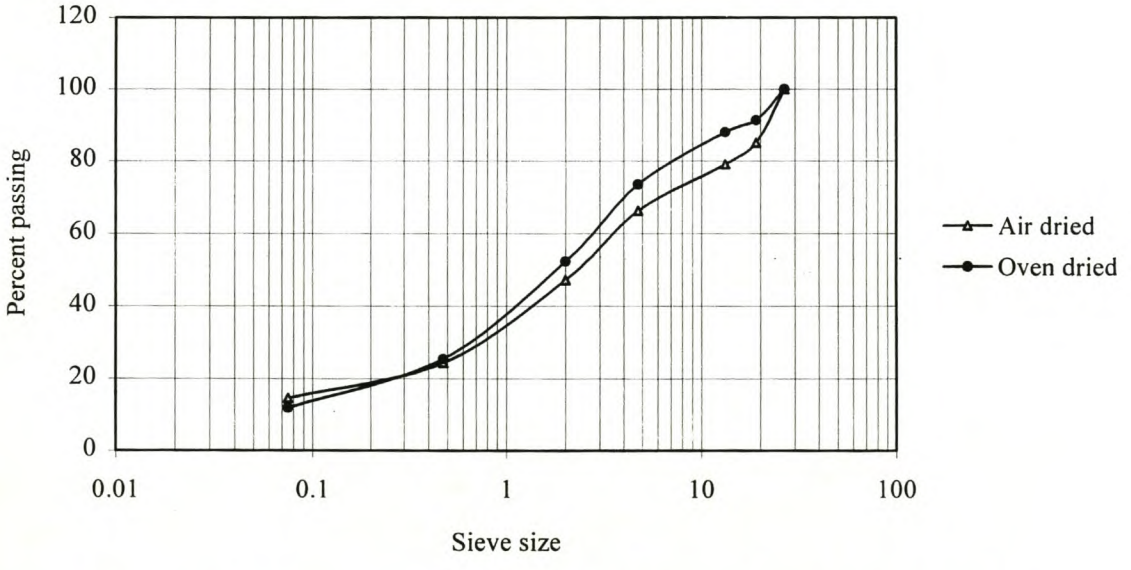

Figure 6.2 Effect of different pre-test preparation procedures on gradation.

6.2.2 Atterberg Limits

Atterberg limits testing was conducted at varied pre-test preparation and testing procedures as follows:

- oven and air-dried
- mixing times of 20 and 40 minutes

This was done to investigate the effect of pre-test preparation and testing procedures on the Atterberg limits of the soil. Results shown in Table 6.3, reveal that there was an increase in both the Liquid limit and Plastic limit but no change in Plasticity index when the sample is air-dried as compared to when it is oven-dried. When the mixing time was increased from 20 minutes to 40 minutes, there was an increase in Plasticity index largely caused by an increase in Liquid limit.

Table 6.3 Atterberg limits results.

Mixing time	Oven dried sample			Air dried sample		
	LL	PL	PI	LL	PL	PI
20 min	19	16	3	23	20	3
40 min	23	15	8	30	22	8

6.2.3 Maximum dry density and optimum moisture content

Results for compaction characteristics are presented in Table 6.4. Compaction was done using Modified AASHTO compaction effort. The density-moisture relationship is shown in Figure 6.3.

Table 6.4 Modified AASHTO results.

MDD (kg/m3)	2185
Optimum moisture content	6.3

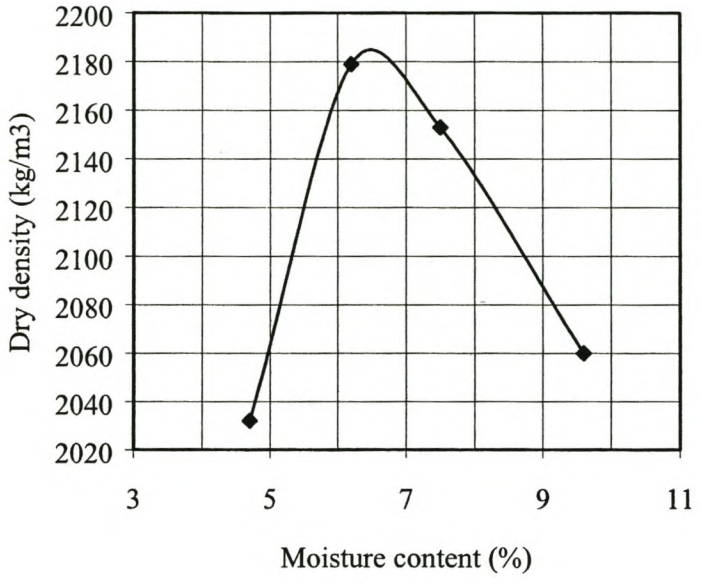

Figure 6.3 Density-moisture relationship (at Mod. AASHTO compaction).

6.2.4 CBR and Swell

CBR and swell were determined after four days of soaking at three compaction levels according to standard test procedure given TMH1 (83). Results are given in Table 6.5 and graphically in Figure 6.4.

Table 6.5 CBR results from load penetration curve taken at 2.54 mm

% Mod. ASSHTO compaction	99	97	91
CBR (%)	145	150	41
CBR swell (%)	0.02	0.06	0.05

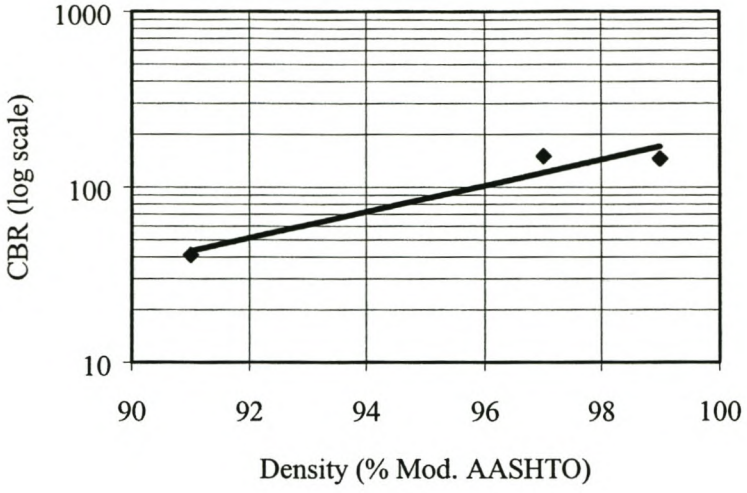

Figure 6.4 CBR-density relationship.

6.2.5 Durability of coarse aggregate and specific gravity

The 10% Fines Aggregate Crushing Test (10% FACT) as described in SABS Method 842 (77) was used to determine the durability or degradation strength of the aggregate. The dry 10% FACT was determined to be 48 kN from Figure 6.5.

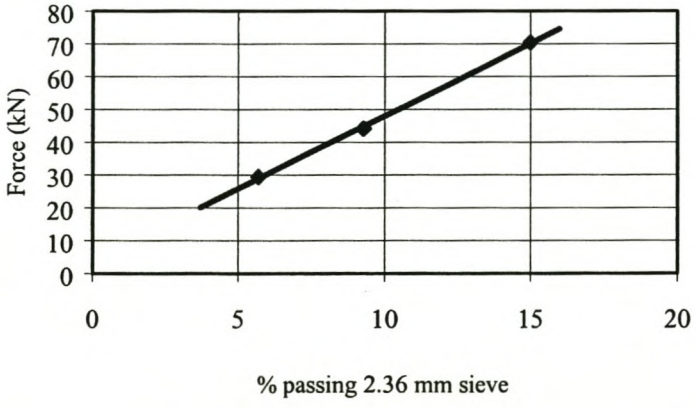

Figure 6.5 10% FACT results.

Specific gravity was determined using Method A12T of TMH1 (83). The test was performed on two particle-size fractions, that passing 0.425 mm sieve and that retained. Results are shown in Table 6.6.

Table 6.6 Specific gravity results.

Particle-size fraction	Specific gravity
passing 0.425 mm	2.60
retained on 0.425 mm	2.63

6.2.6 Summary of material characterization

1. The method of pre-test drying and the amount of manipulation during testing were found to affect the Atterberg limits of the lateritic gravel tested.
2. The gradation was relatively unaffected by the method of pre-test drying.
3. The lateritic gravel had quite a high CBR of 150 at 97 % Modified AASHTO and swell of 0.06 % after four days of soaking.
4. The gravel tested falls under the following classification:

    - According to the ASSHTO classification the gravel falls in the A-1-b group.
    - According to South African TRH14 (30), the gravel falls is group G4.

5. The strength of gravel tested was found to be 45 kN. Weinert (93) reports that the strength of dry ferricrete in the 10% FACT usually lies between 25 and 80 kN.

6.3 Chemical analysis results

Chemical analysis was performed at the Geology department of the University of Stellenbosch using X-Ray Fluorescence. The results are presented in Table 6.7.

Table 6.7 Major Element Analysis by XRF.

	SiO2	TiO2	Al2O3	Cr2O3	Fe2O3	MnO	NiO	MgO	CaO	Na2O	K2O	P205	H2O-	LOI	Total
Weight %	61.95	0.19	11.99	0.01	13.09	0.01	0.01	0.04	0.00	0.23	0.00	0.13	4.00	7.81	99.45

Silica/sesquioxide ratio is computed as follows,

$$S/R = \frac{\frac{SiO_2}{60}}{\frac{Al_2O_3}{102} + \frac{Fe_2O_3}{160}}$$

The results for S/R are given in Table 6.8. According to the literature reviewed, it is generally accepted that ratios less than 1.33 are indicative of true laterites, those between 1.33 and 2.00 of lateritic soils and those greater than 2.00 of non-lateritic (94). The S/R is higher probably because the lateritic gravel tested was formed in a soil whose parent material is sandstone. Confusion surrounding the true definition of a laterite has already been referred to in the literature review in Chapter 2.

Table 6.8 Summary: Silica / sesquioxide ratio

SiO_2	Al_2O_3	Fe_2O_3	S/R
61.95	11.99	13.09	5.18

6.4 Triaxial testing results

Triaxial testing was conducted in the MTS machine. Three types of triaxial tests were conducted on the untreated and treated gravel:

1. Static triaxial tests
2. Cyclic load triaxial testing (CLT) for resilient modulus
3. Cyclic load triaxial testing (CLT) for permanent deformation

Tests were conducted under different conditions of moisture content, compaction and stress levels as shown in Table 6.9. In this chapter, test results are presented in the simplest tabular and graphical form while further analysis is done in Chapter 7 where models for resilient modulus and permanent deformation are examined in more detail.

Table 6.9 Summary triaxial testing.

	Static Triaxial Test	**CLT for Resilient Modulus**	**CLT for Permanent Deformation**
Materials tested	Untreated gravel	Untreated gravel Foamed-bitumen treated and cement treated gravel	Untreated gravel
Test characteristics	- Same moisture and density - 3 confining pressures	- different conditions of moisture and density - 3 confining pressures - range of deviator stress levels	- Same moisture, density and confining pressure. - N = 100,000
Results	Section 6.4.1	Section 6.4.2	Section 6.4.3

6.4.1 Static Triaxial Test Results

The purpose of the static test was to determine the shear strength parameters, c and ϕ. At least three tests, each at a different confining pressure, are required to determine the shear strength parameters for any condition of moisture and compaction. Because the static test is a destructive test, a different specimen is used for each confining pressure. Testing was conducted on untreated gravel according to the schedule shown in Table 6.10.

Table 6.10 Schedule static triaxial testing.

Material	No. of tests	Characteristic	Value
Untreated gravel	2 sets	confining pressure, σ_3 (kPa)	50, 150, 300
		density	$\approx$ 97 % Mod AASHTO
		moisture content	optimum moisture content

The results of two sets of static tests are shown in Table 6.11.

Table 6.11 Static triaxial test results for untreated gravel.

confining pressure (kPa)	moisture content (%)	% Mod AASHTO MDD	At optimum moisture content	
			load at failure σ_{dev} (kPa)	strain at failure (%)
50	6.8	97	645	0.40
150	6.8	97	875	0.47
300	6.8	97	832	0.54

Figure 6.6 shows a plot of stress-strain curves for one set of results, while Figure 6.7 shows the Möhr-Coulomb diagram for the above results.

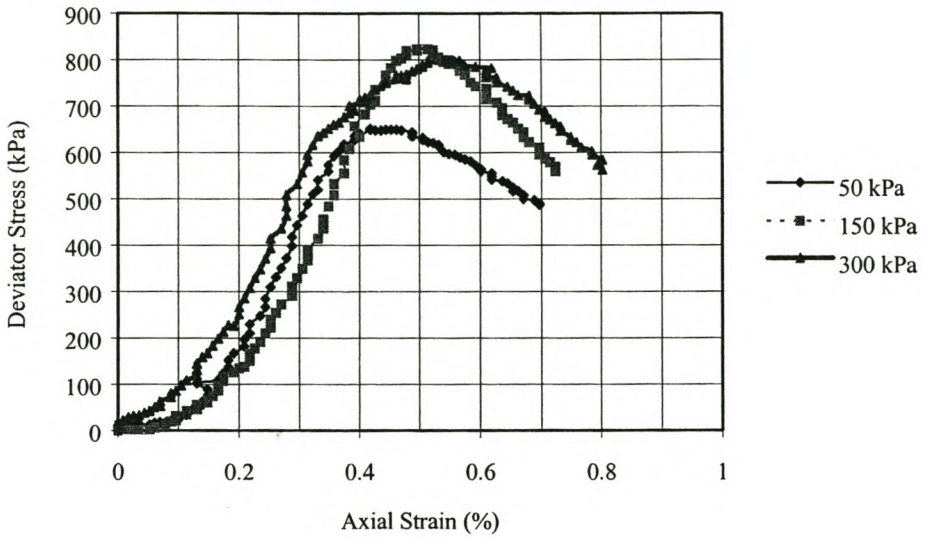

Figure 6.6 Static stress-strain curves for unstabilized gravel.

σ_3 (kPa)	$\sigma_{1,f}$ (kPa)
50	695
150	1025
300	1132
c (kPa)	146
ϕ	32

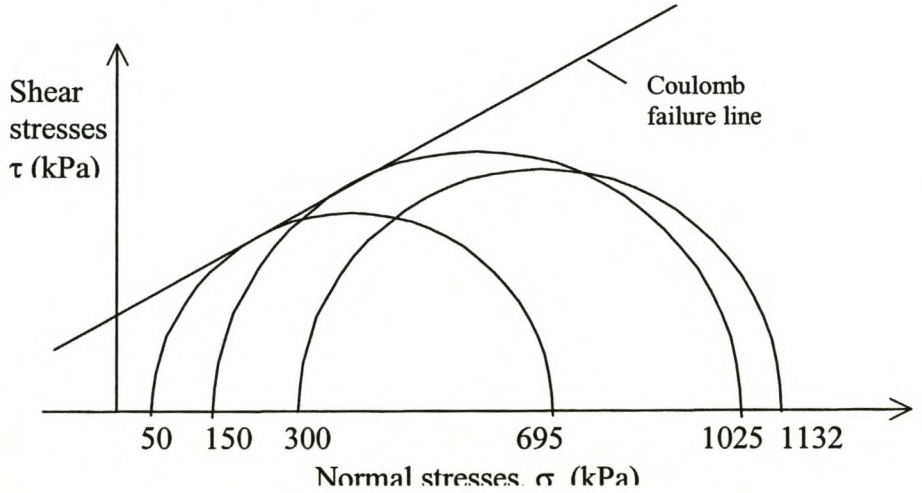

Figure 6.7 Möhr-Coulomb diagram for untreated gravel.

For $\sigma_3 < 150$ kPa, the shear parameters are c = 146 kPa and $\phi = 32°$. No tests were performed for $\sigma_3 < 50$ kPa, but the cohesion c could be lower in this range as illustrated by Figure 6.8. Maree (52) based on tests on different base course materials modelled the lower confining stress levels using a second line.

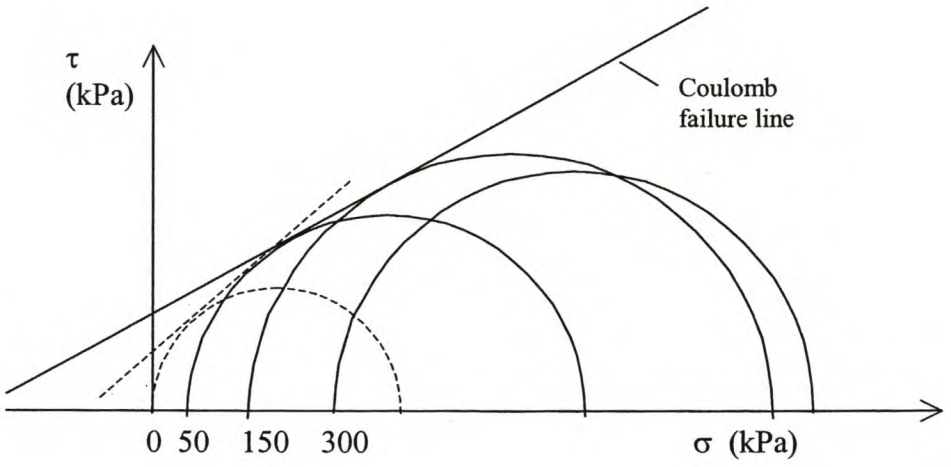

Figure 6.8 Möhr-Coulomb diagram illustrating second failure line at low confining stresses.

Figure 6.7, shows that at higher confining stress levels, the deviator stress at failure is lower than that expected according to the Möhr-Coulomb failure model. This could be because of the over stress at the particle contacts. This implies a failure model of the form shown in Figure 6.9 could be appropriate, though only limited test results are available for higher confining stress levels to establish this. Based on the available results a maximum deviator stress level of 850 kPa (= 2 x 425 kPa) could be applied to the material tested. This modified failure model was implemented in the design of a model pavement structure in Chapter 7.

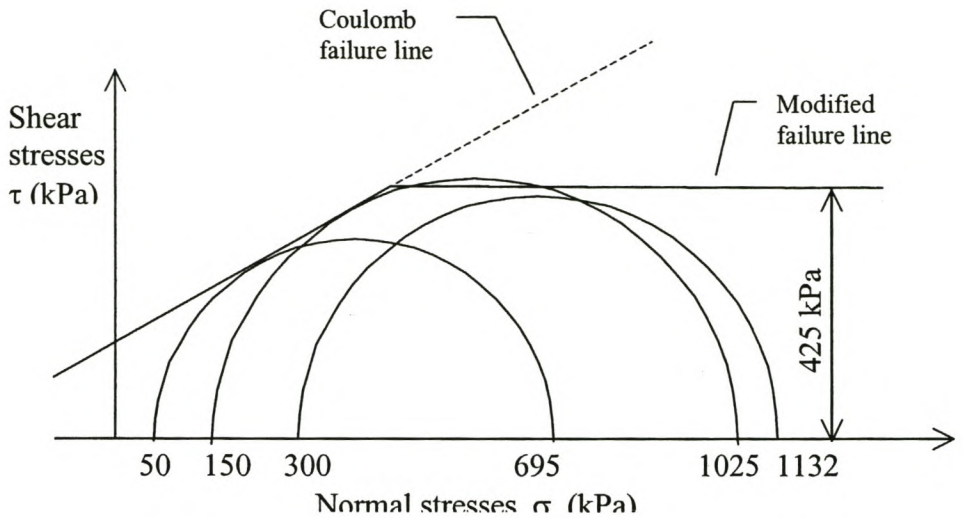

Figure 6.9 Modified Möhr-Coulomb diagram.

6.4.2 Cyclic load triaxial testing for resilient modulus - Test results

The purpose of the cyclic triaxial test is to determine the resilient modulus under various conditions of moisture, compaction and stress levels. The stresses applied in this test are well below the failure condition, making it possible to use one specimen for a range of stress levels. The test was conducted on untreated and treated gravel according to the schedule shown in Table 6.12.

Table 6.12 Test characteristics of CLT for resilient testing

Material	No. of tests	Characteristic	Value
Untreated gravel	1 set	confining pressure, σ_3 (kPa)	0, 50, 150, 300
		moisture content	three different moisture contents
		density	three different densities
		loading rate	2 Hz
Foamed-bitumen treated gravel	1 set	bitumen content	2, 3, 4, 5 %
		confining pressure, σ_3 (kPa)	150
		moisture content	same moisture content
		density	same density
		loading rate	2 Hz
Cement treated gravel	1 set	cement content	2, 4, 6
		confining pressure, σ_3 (kPa)	150
		moisture content	same moisture
		density	same density
		loading rate	2 Hz

A distinction was made between 'modified gravel' for residual bitumen contents of 2 - 3 % and 'stabilized gravel' for higher bitumen contents of 4 - 5 %. The results for resilient modulus are presented as plots on a log-log scale of resilient modulus M_r against the sum of the principal stresses $\Theta = \sigma_1 + \sigma_2 + \sigma_3$. This approach is according to the well-known K- Θ which has been used just to facilitate easy presentation of the test results. The suitability of this model and other more appropriate models are considered in detail in Chapter 7.

6.4.2.1 Resilient modulus of untreated gravel

The effects of stress level, moisture, compaction, loading frequency, and increasing number of load repetitions on the resilient modulus of untreated gravel are illustrated in Table 6.13 - 6.18 and the accompanying figures.

(a) Table 6.13 and Figure 6.10 show the relationship between bulk stress Θ, confining pressure σ_3, and resilient modulus M_r, for tests conducted at three confining pressures of 0, 50, 150 and 300 kPa.

Table 6.13 Effect of stress level on the resilient modulus of untreated gravel.

confin. press. (kPa)	moist. cont. (%)	% Mod ASSHTO MDD	Resilient modulus (MPa) /deviator stress (kPa)											
			50	70	100	150	200	250	300	350	400	450	500	550
0	6.3	94		165		200			268					
50	7	98	173		194		247		287		315		331	
150	7	97				235		267		292		313		328
300	7	97							281		307	321		

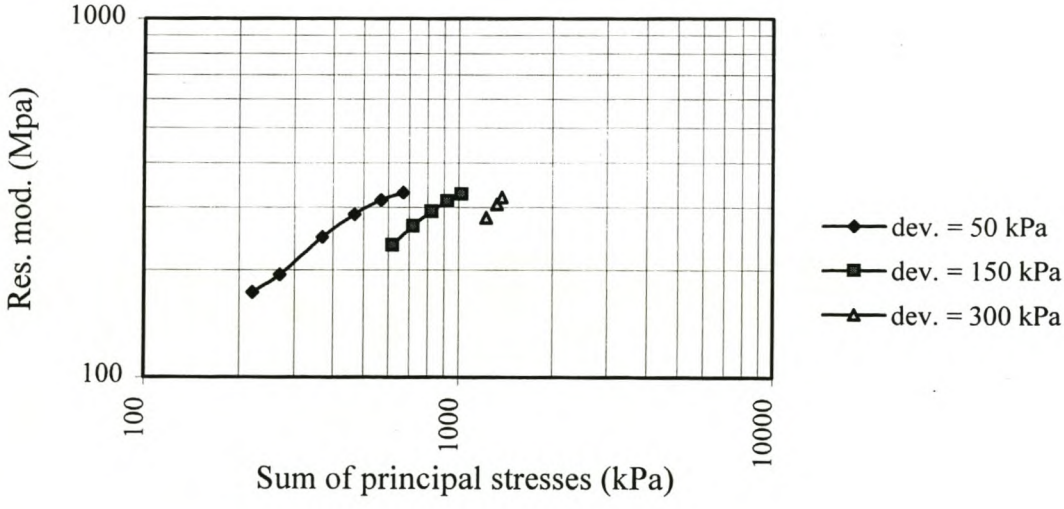

Figure 6.10 Effect of stress level on the resilient modulus (untreated gravel).

(b) Table 6.14 and Figure 6.11 show resilient modulus results for tests conducted at three moisture contents of 3.3%, 4.5% and 6.6%, all at the same confining stress of 150 kPa.

Table 6.14 Effect of moisture content on resilient modulus for untreated gravel.

confin. press. (kPa)	moist. cont. (%)	% Mod ASSHTO MDD	Resilient modulus (MPa) /deviator stress (kPa)											
			50	100	150	200	250	300	350	400	450	500	550	Av.
150	6.6	97			312		335		358		379		382	353
150	4.5	97			370		413		455		488		517	449
150	3.3	98			291		345		393		430		466	385

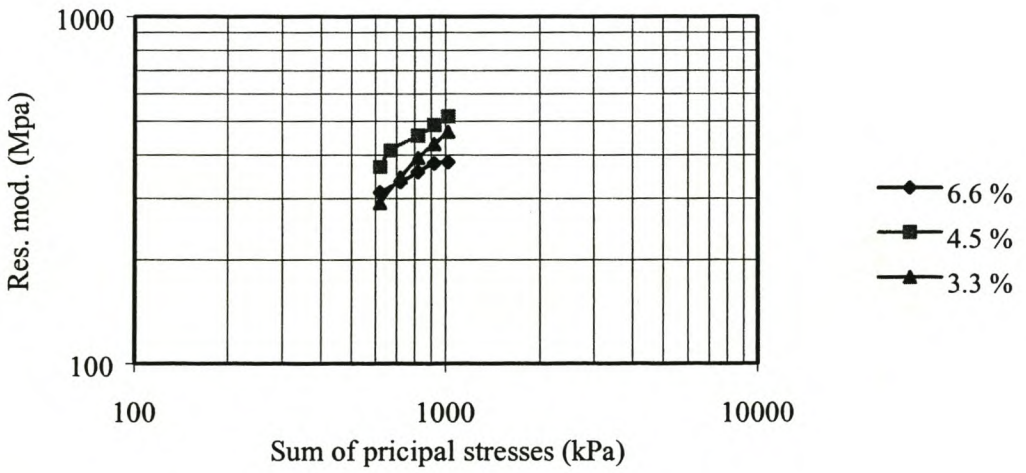

Figure 6.11 Effect of moisture content on resilient modulus (untreated gravel).

(c) Table 6.15 and Figure 6.12 show the resilient modulus results for untreated gravel for tests conducted at 92%, 93% and 97% compaction, all at a confining stress of 150 kPa.

Table 6.15 Effect of density on resilient modulus for untreated gravel.

confin. press. (kPa)	moist. cont. (%)	% Mod ASSHTO MDD	Resilient modulus (MPa) /deviator stress (kPa)											
			50	100	150	200	250	300	350	400	450	500	550	Av.
150	6.6	97			312		335		358		379		382	353
150	5.9	93			278		299		315		319			303
150	6.3	92			306		319							313

Figure 6.12 Effect of density on resilient modulus (untreated gravel).

(f) Table 6.16 and Figure 6.13 show the resilient modulus results for untreated gravel for tests performed at varied loading frequencies of 0.5, 1, 2 and 4Hz.

Table 6.16 Effect of loading frequency on resilient modulus (untreated gravel).

confin. press. (kPa)	dev. stress (kPa)	moist. cont. (%)	% Mod ASSHTO MDD	Loading rate (Hz)	Resilient modulus (MPa)
150	250	7	98	4	321
				2	312
				1	304
				0.5	299
150	350	7	98	4	354
				2	342
				1	329
				0.5	324

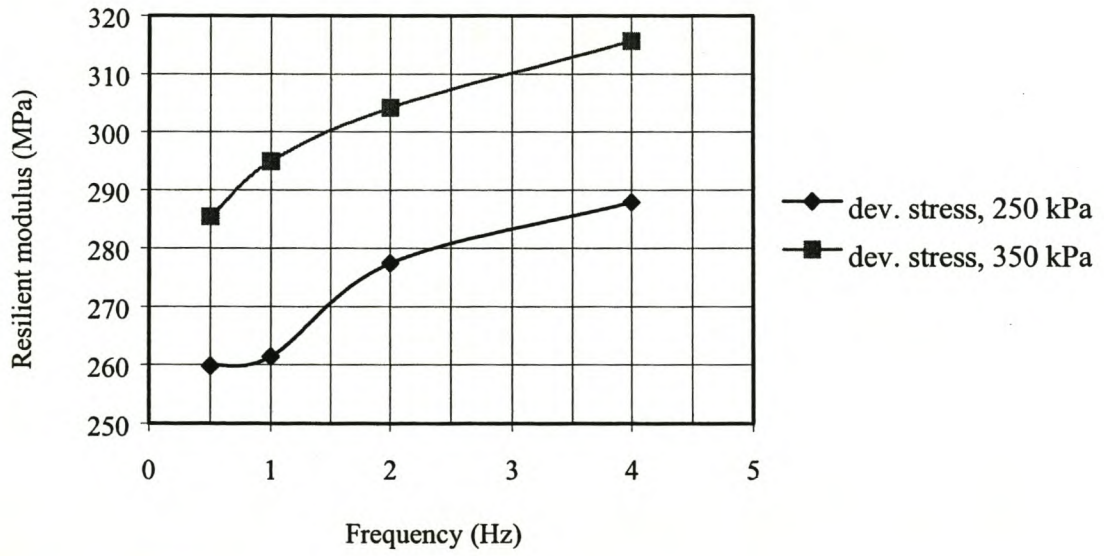

Figure 6.13 Effect of loading frequency on resilient modulus for confinement stress of 150 kPa, at 7% moisture (untreated gravel).

(g) During cyclic load testing for permanent deformation, data for resilient modulus was recorded at various intervals up to 100,000 load cycles. Table 6.17 and Figure 6.14 illustrate M_r with increasing number of load cycles.

Table 6.17 Resilient modulus with increasing number of load cycles at loading frequency of 2 Hz (untreated gravel).

confin. pressure (kPa)	% Mod. AASHTO MDD	dev. stress (kPa)	Moist. content (%)	Resilient modulus (MPa) /load repetitions											
				100	500	1000	2000	3000	5000	1.E+04	2.E+04	3.E+04	5.E+04	8.E+04	1.E+05
50	95	200	6	197	217	226	225	225	217	196	224	211	219	220	225

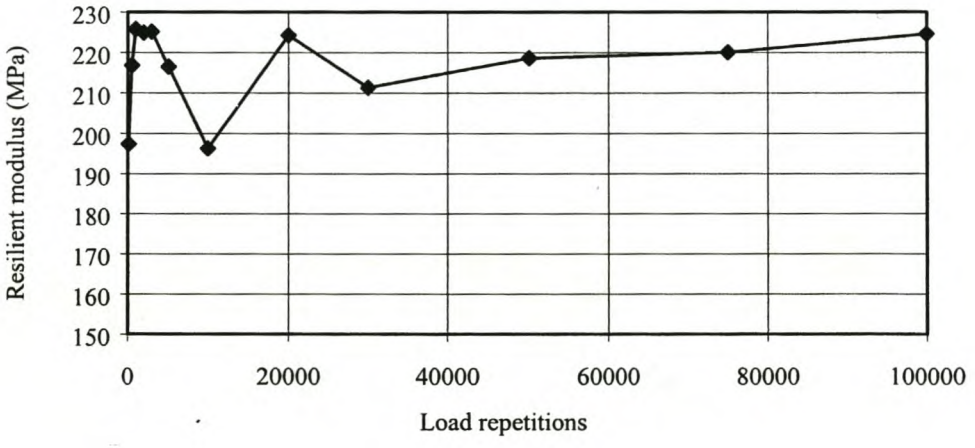

Figure 6.14 Resilient modulus with increasing number of load cycles at loading frequency of 2 Hz (untreated gravel).

The data of Figure 6.14 shows that the variation in the resilient modulus with increasing number of load repetitions appears to be random and remains stable with a standard deviation of 10 MPa. It can also be seen that the resilient modulus stabilizes just after a few load repetitions.

6.4.2.2 Resilient modulus of foamed-bitumen modified gravel

Table 6.18 and Figures 6.15 and 6.16 give the resilient modulus results for foamed-bitumen treated gravel. Residual bitumen contents are 2 % and 3 %, with or without addition of 1.5 % cement. All tests were at a confining pressure of 150kPa and a loading frequency of 2 Hz. Tests were conducted on soaked specimens and unsoaked specimens.

Table 6.18 Results of resilient moduli for foamed bitumen stabilized gravel at loading frequency of 2 Hz.

	confin. pressure (kPa)	% bitumen	% cement	Resilient modulus (MPa) /deviator stress (kPa)						
				150	250	350	450	550	650	Av.
Unsoaked (≈ opt. moisture content, 6.3%)	150	2	1.5							
	150	2	-	302	326	349				326
	150	3	1.5	356	373	394	418	425		393
	150	3	-	299	323	352	369	377		344
Soaked	150	2	1.5	310	338	369				339
	150	2	-	239	248					244
	150	3	1.5	292	333	370	430	448		375
	150	3	-	285	322	356	386	399		350

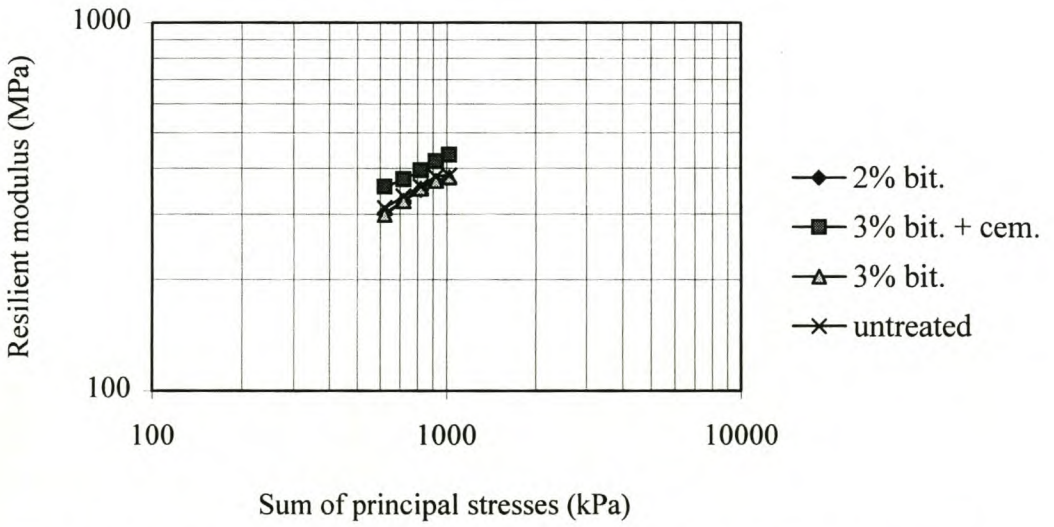

Figure 6.15 Resilient modulus of foamed-bitumen modified gravel (unsoaked).

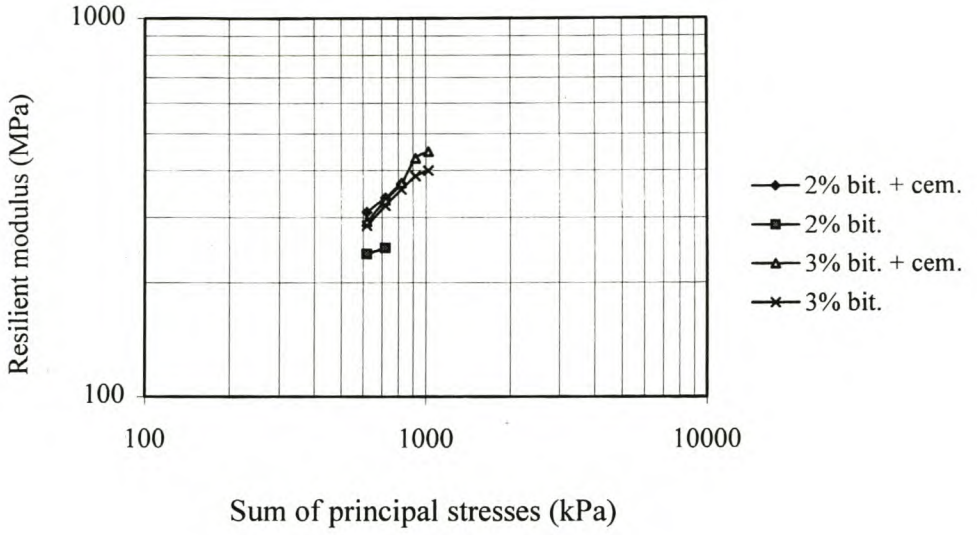

Figure 6.16, Resilient modulus of foamed-bitumen modified gravel (soaked).

6.4.2.3 Resilient modulus of foamed-bitumen stabilized gravel

Resilient modulus of foamed-bitumen stabilized gravel with residual bitumen contents of 4 % and 5 % was investigated using cyclic load triaxial testing. All tests were at a confining pressure of 150kPa. No testing was conducted on soaked specimens. Results for resilient modulus are given in Table 6.19 and Figure 6.17.

Table 6.19 Results of resilient modulus for foam bitumen stabilized gravel.

	conf. press. (kPa)	% bitu.	moisture content (%)	% comp	Resilient modulus (MPa) /deviator stress (kPa)						
					150	250	350	450	550		Av.
Unsoaked (≈ opt. moisture, 6.3%)	150	4	6	100	384	420	456	495	523		456
	150	5	6	97	434	483	528	563	584		518

Resilient modulus values of the foamed-bitumen stabilized gravel are lower than expected because of the test method used. In cyclic triaxial testing the specimen is loaded only in compression and the loading rate of 2 Hz is very low compared to the ITT test (Indirect Tensile Test) which would have been expected to give higher results. Unfortunately, no tests were done in the ITT mode.

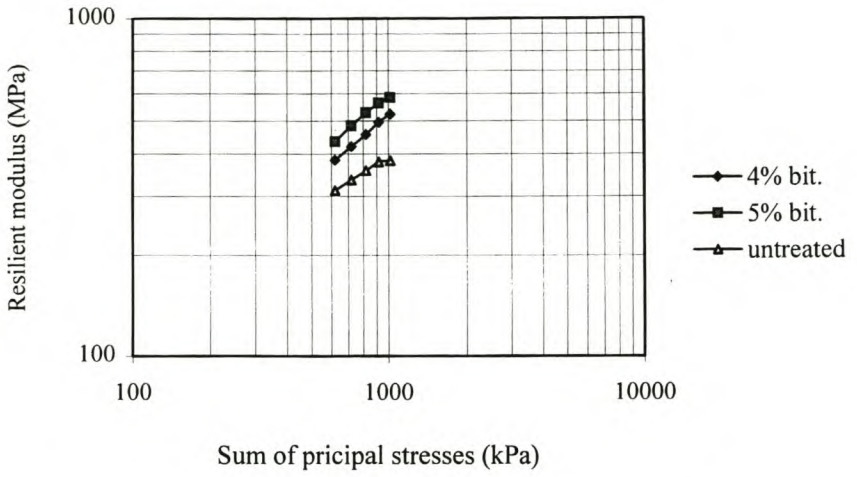

Figure 6.17, Resilient modulus of foamed-bitumen stabilized gravel (unsoaked).

6.4.2.4 Resilient modulus of cement treated gravel

Resilient modulus for cement treated gravel was investigated using cyclic load triaxial testing for cement contents of 2 %, 4 % and 6 %. All tests were at a confining pressure of 150kPa. Testing was conducted after curing for 7 days in a polythene bag. No soaking of specimens was done. Results are given in Table 6.20 and Figure 6.18.

Table 6.20 Results of resilient modulus for cement treated gravel.

confin. pressure (kPa)	% cement	moisture content (%)	% Mod ASSHTO MDD	Resilient modulus (MPa) /deviator stress (kPa)						
				150	250	350	450	550	650	Av.
150	2	5	96	247	265	300	356	397		313
150	4	5	96	390	438	478	523	558		477
150	6	5	96	349		420	480	520		442

Like the foamed-bitumen stabilized gravel, the resilient modulus values for the cement treated gravel are lower than expected because of the test method used. The ITT test is expected to have given higher results. However, no tests were done in the ITT mode.

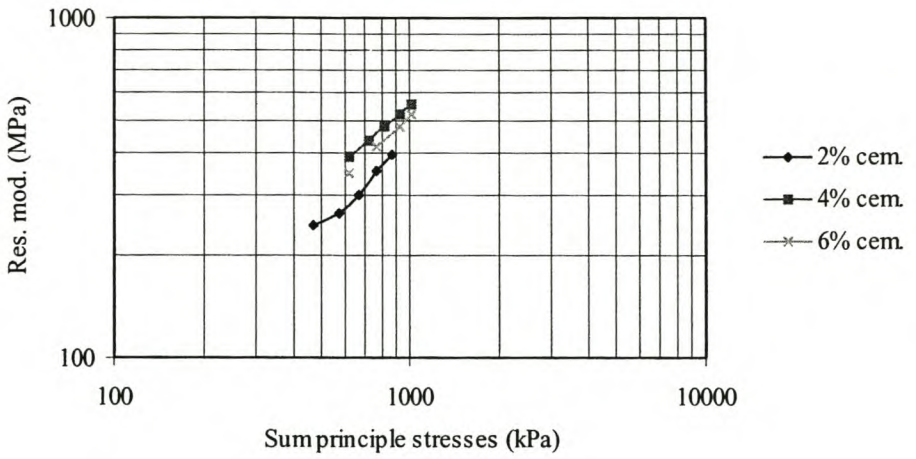

Figure 6.18, Resilient modulus for cement treated gravel.

6.4.2.5 Summary of resilient modulus results

The resilient modulus of the lateritic gravel tested was found to be affected by the stress level, moisture, density and rate of loading. The treated gravel, both foamed-bitumen and cement treated gravel, also displayed stress-dependent resilient modulus behaviour with a noted increase in resilient modulus with increase in deviator stress. Other models for modelling the resilient modulus, apart from the K-Θ, are examined in Chapter 7. However, the foamed-bitumen and cement treated gravel material gave lower values of resilient modulus than expected because of the test method used. The ITT test is expected to have given higher results. However, no tests were done in the ITT mode.

Table 6.21 gives a summary of resilient modulus values for untreated gravel, foamed-bitumen treated gravel and cement treated gravel. Average values at a confining stress of 150 kPa are used. It is clear that the treated gravel, both foamed-bitumen treated and cement treated gave higher values of resilient modulus compared to the untreated gravel.

Table 6.21 Comparison of resilient moduli for the different materials.

	Average resilient modulus at 150 kPa confining pressure (MPa)
Unstabilized gravel	
@ 97% Mod. AASHTO	287
Foam bit. modified gravel	
2% bitumen	381
3% bitumen	346
2% bitumen + 1.5% cement	
3% bitumen + 1.5% cement	414
Foam bit. stabilized gravel	
4% bitumen	456
5% bitumen	518
Cement stabilized gravel	
2% cement	313
4% cement	477
6% cement	422

6.4.2.6 Observed behaviour during failure

In instances where the specimen failed in the process of testing for resilient modulus, it was observed that the resilient behaviour could still be picked up as shear failure progressed as shown in Figure 6.19. The resilient modulus picked up in this manner was still close to that obtained before the specimen failed. This happened with the foamed-bitumen treated mixes. This implies that the resilient modulus in itself measured in this way (i.e. from cyclic triaxial testing), does not give a good indication of the condition of the material as regards shear failure.

deviator stress (kPa)	Mr (MPa)
100	211
200	238
300 (fail)	273
400 (fail)	269

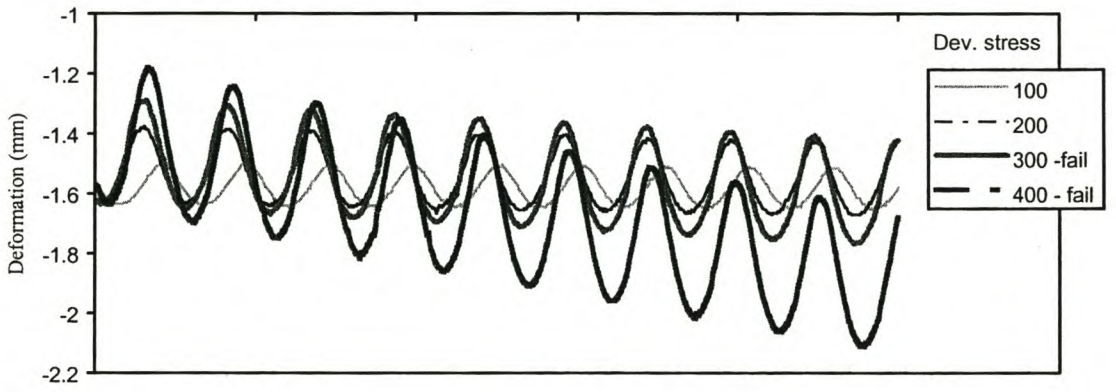

Figure 6.19 Observed behaviour during failure. MTS LVDT.

6.4.3 Cyclic loading for permanent deformation testing - Test results

The purpose of this test is to investigate the permanent deformation behaviour. Due to the length of the test, testing was conducted only on the untreated gravel and using only a confining stress of 50 kPa while the deviator stress was varied. The testing was done according to the characteristics shown in Table 6.22.

Table 6.22 CLT test characteristics for perm. deformation on untreated gravel.

Material	No. of tests	Characteristic	Value
untreated gravel	4	confining pressure, σ_3 (kPa)	50
		deviator stress, σ_{dev}	200, 300, 400, 400
		moisture content	Optimum moisture content ($\approx$ 6.3 %)
		density	Same density
		loading rate	2 Hz
		number of load cycles, N	up to 100,000

Results for permanent deformation testing are given in Table 6.23 and Figure 6.20.

Table 6.23 CLT test for permanent deformation, test results for confinement stress of 50 kPa.

moist. content (%)	% Mod ASSH-TO.	dev. stress (kPa)	Deformation (mm) /load repetitions											
			100	500	1000	2000	3000	5000	1.E+04	2.E+04	3.E+04	5.E+04	8.E+04	1.E+05
6.2	95	200	0.000	0.029	0.039	0.059	0.068	0.088	0.117	0.137	0.156	0.176	0.186	0.205
6.3	94	300	0.000	0.156	0.224	0.283	0.332	0.361	0.410	0.459	0.469	0.508	0.557	0.557
6.3	94	400	0.000	0.518										
6.3	95	500	0.000	Rapid deformation before 500 load cycles										

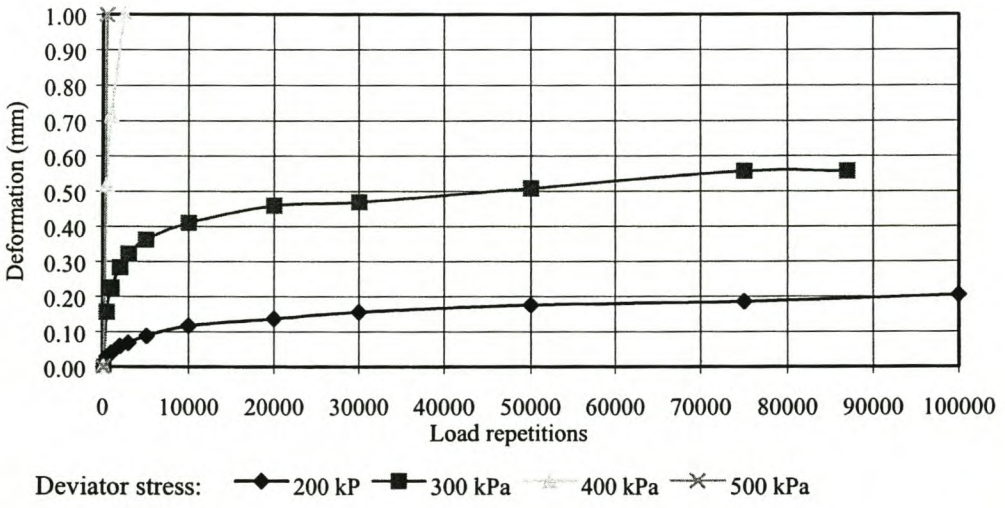

Figure 6.20 Deformation against number of load repetitions for confinement stress for σ_3=50kPa and degree of saturation 75 - 80%.

6.5 Results of UCS, ITS and CBR on treated gravel

The following standard tests are usually used to assess the quality of treated materials:

- Unconfined Compression Strength, UCS
- Indirect Tensile Strength, ITS
- California Bearing Ratio, CBR

These tests were conducted on the treated materials according to the test characteristics shown in Table 6.24. Testing was done on both unsoaked specimens and on specimens that were soaked in water for 24 hours.

Table 6.24 Test characteristics for UCS, ITS and CBR testing on treated materials.

Material	Tests	Characteristic	Value
Foamed-bitumen modified gravel	UCS CBR	bitumen content (%)	2 and 3 % (+/- 1.5 cement)
		moisture content (%)	Soaked/unsoaked
		density	≈ 100 % Mod. AASHTO
Foamed-bitumen stabilized gravel	ITS	bitumen content (%)	4 and 5 %
		moisture content (%)	Soaked
		density	≈ 100 % Mod. AASHTO
Cement treated gravel	UCS ITS	cement content (%)	2, 4 and 6 %
		moisture content (%)	Soaked
		density	≈ 100 % Mod. AASHTO

UCS and ITS testing were conducted in the MTS machine according to the test procedure described in TMH1, Method A14 and Method A16T. CBR testing was conducted according Method A9 of TMH1

6.5.1 Unconfined Compression Strength (UCS) test results

The Unconfined Compression Strength, UCS, for foamed-bitumen stabilized and cement treated gravel after curing and soaking at the end of seven days are given in Tables 6.25 and 6.26.

Table 6.25 UCS for foamed bitumen modified gravel.

% Bitumen	% Cement	Failure load (kPa)	
		Unsoaked	Soaked
2		1322	1281
2	1.5%	4623	2085
3			1114
3	1.5%	3738	2044

Table 6.26 UCS for cement stabilized gravel

% Cement	Failure load (kPa)
	Soaked
2	2162
4	4447
6	> 5473

According to South Africa's TRH 13 (29) which classifies cemented materials according to their UCS values, the gravel treated with 2 % cement would classify as C3 (1.5 to 3.0 MPa), while that with 4 % and 6 % gravel would classify as C2 (3 to 6 MPa). Criteria for foamed-bitumen stabilized materials are not available.

6.5.2 Indirect Tensile Strength (ITS) test results

The Indirect Tensile Strength, ITS, for foamed bitumen stabilized and cement treated gravel after curing and soaking at the end of seven days are given in Tables 6.27 and 6.28.

Table 6.27 ITS for foamed bitumen stabilized gravel (soaked).

% bitumen	Average ITS (kPa), soaked
4	290
5	460

Table 6.28 ITS for cement treated gravel (soaked).

% cement	Average ITS (kPa), soaked
2	370
4	400
6	660

The above ITS values for the cement treated gravel are above the minimum limit of 200 kPa suggested by South Africa's TRH 13 (29) for the class C3 of cemented materials. ITS criteria for foamed-bitumen stabilized materials are not available.

6.5.3 California Bearing Ratio (CBR) test results

The California Bearing Ratio, CBR, for foamed bitumen modified gravel cured for seven days and a further four days soaking are given in Table 6.29.

Table 6.29 CBR for foamed-bitumen modified gravel.

% Bitumen	% Cement	CBR (%), Soaked
2	-	45
3	-	52

The CBR values above are much lower than the 150 % obtained for the unstabilized gravel. The reasons for this are not clear but because the behaviour of bituminous material is dependent on the rate of loading, the slow rate of loading in the CBR test could be cause for the low CBR values.

6.6 Relating results to specifications for gravel materials

There has been a drive towards adopting resilient modulus values from cyclic triaxial testing in performance related specifications for granular materials (for example, in Australian (92)). However, results from this research show that the resilient modulus measured from cyclic triaxial testing is not a good indicator of shear strength and therefore performance of a granular material. Furthermore, the type of testing as in triaxial testing does not give any indication of other factors that might impact on performance like the durability of the coarse aggregate under traffic loading. Lateritic gravels are especially susceptible to mechanical break down under both construction traffic and during service. In addition, repeated load triaxial testing does not supply the kind of information given by the Atterberg limits on plasticity, the value of which affects performance. Therefore, resilient modulus cannot be used independently for predicting performance of granular materials but must be used in conjunction with experience already gained from standard tests. In addition, there is need to establish a link between results of resilient modulus from cyclic triaxial testing and results from tests like Unconfined Compression Strength (UCS) and Indirect Tensile Test (ITT).

7 MODELLING OF RESILIENT MODULUS, PERMANENT DEFORMATION AND MODEL PAVEMENT DESIGN

7.1 Introduction

Results of the test programme have been presented in Chapter 6. In this chapter, results from cyclic triaxial testing are fitted to different resilient modulus models for granular materials. A permanent deformation model for the material is also developed. Finally, the adopted models are used for analysing stresses and strains in the design of a light pavement structure.

7.2 Modelling of resilient modulus for untreated gravel

The resilient behaviour of granular materials is usually characterized using a stress-dependent resilient modulus M_r and a constant Poisson's ratio, mostly $\upsilon = 0.35$. Several mathematical models have been suggested using different stress components. Some of the common ones, discussed in Chapter 3, are given in Table 7.1.

Table 7.1 Models for resilient modulus.

Model	Expression	Equation
M_r-Θ	$Mr = k_1\left(\frac{\Theta}{P_0}\right)^{k_2}$	(1)
M_r-σ_3	$Mr = k_1\left(\frac{\sigma_3}{P_0}\right)^{k_2}$	(2)
Uzan	$M_r = k_1\left(\frac{\Theta}{P_0}\right)^{k_2}\left(\frac{\tau_{oct}}{P_0}\right)^{k_3}$	(3)

where, Mr = resilient modulus

σ_1, σ_2, σ_3 = principal stresses (in kPa)

σ_d = deviator stress ($\sigma_1 - \sigma_3$)

Θ = $\sigma_1 + \sigma_2 + \sigma_3$ = sum of principal stresses

τ_{oct} = octahedral shear stress = $\sigma_d \times \sqrt{2}/3$

P_0 = reference stress = 1 kPa

k_1, k_2, k_3 = material parameters

Regression analysis for the three models gave results summarized in Table 7.2. Full results of regression analysis are given in **Appendix A**.

Table 7.2 Regression results for the resilient modulus models.

Model	Model coefficients			r^2
	k_1 (MPa)	k_2	k_3	
M_r-Θ	60	0.272		0.69
M_r-σ_3	143	0.160		0.35
Uzan	61	0.064	0.225	0.86

Fitting of models to results is illustrated graphically in Figures 7.1 to 7.3

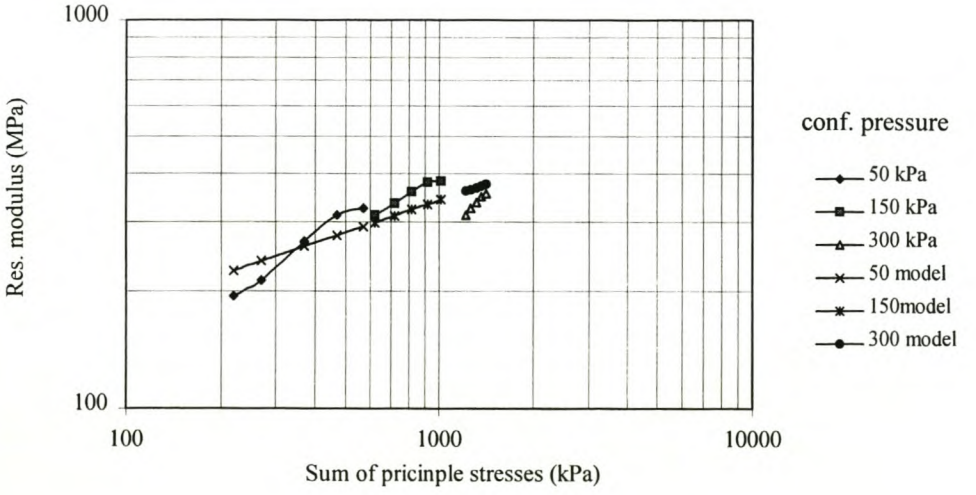

Figure 7.1 M_r-Θ model.

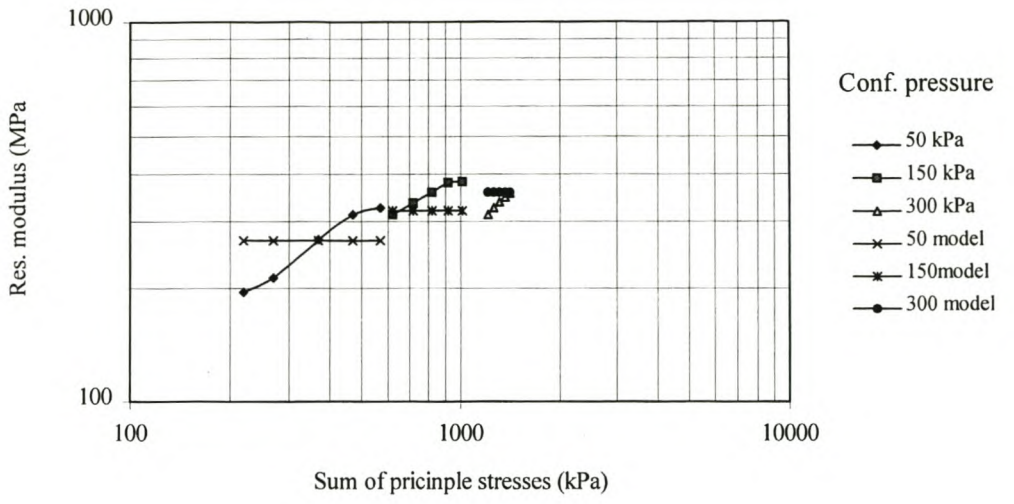

Figure 7.2 M_r-σ_3 model

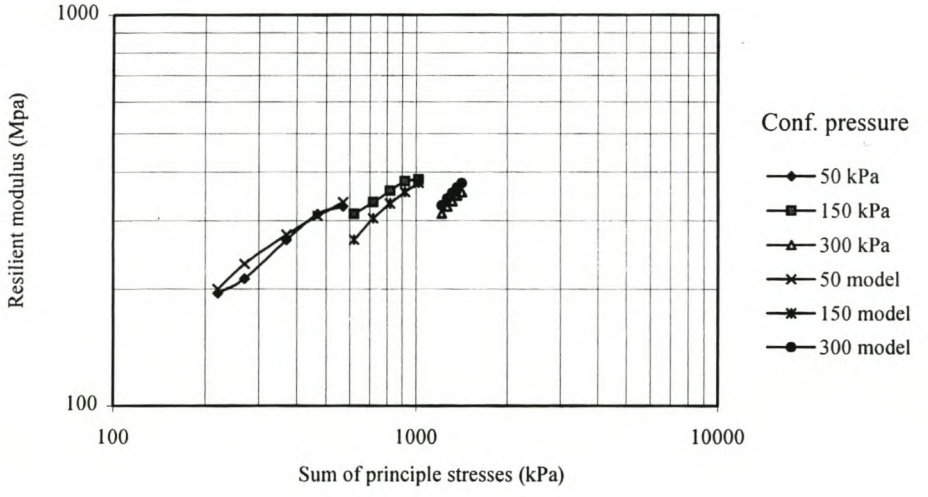

Figure 7.3 Uzan model

Uzan's model gives the best fit to the data with an r^2 value of 0.86. This model takes into account both the effects of deviator stress and confining pressure, which are independent variables. However, the model does not take into account the effect of high stress conditions close to failure where the resilient modulus is observed to decrease. It should be noted that this model applies to the material tested or similar materials. Other researchers have reported a decrease of resilient modulus with increase of deviator stress (63).

7.3 Models for treated gravel

Non-linear behaviour is also evident for both foamed-bitumen modified and stabilized gravel (i.e. higher and lower bitumen contents). Testing was done using the same procedure used for the untreated gravels with a loading rate of 2 Hz and a room temperature of approximately 25°C. Figure 7.4 shows an example of resilient modulus results modelled using Uzan's model for foamed-bitumen modified gravel (3% bitumen + 1.5% cement). Value for $r^2 = 0.84$.

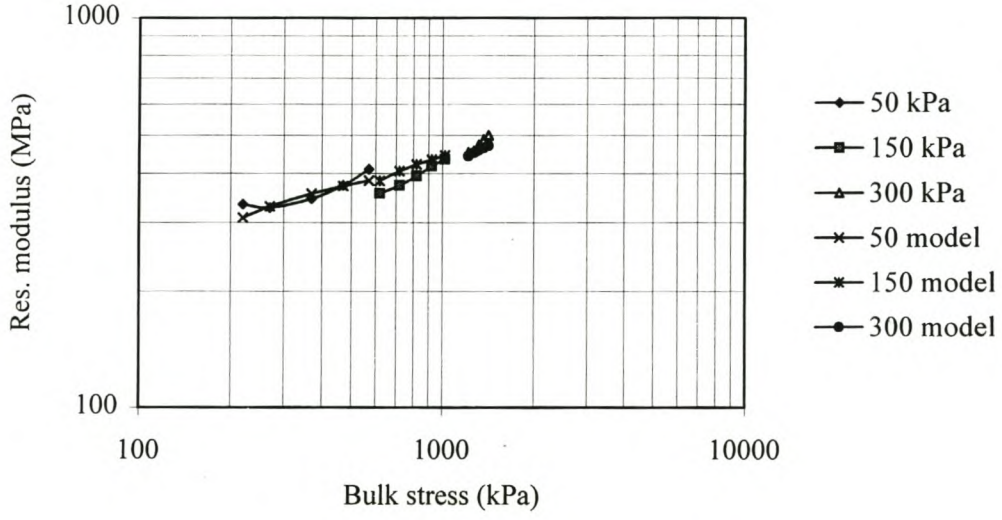

Figure 7.4 Uzan's model for foamed-bitumen modified gravel (3% bitumen + 1.5% cement).

7.4 Concept of failure factor

A measure of how close a given state of stress is to the failure condition can be made by use of the concept of failure factor (F), defined as,

$$F = \frac{\text{working shear stress}}{\text{maximum safe shear stress}} = \frac{\sigma_{1,w} - \sigma_{3,w}}{\sigma_{1,f} - \sigma_{3,w}}$$

where, $\sigma_{1,w}$ and $\sigma_{3,w}$ = working major and minor principal stresses

$\sigma_{1,w}$ = major priciple stress at failure

From the Mohr-Coulomb failure model, it is known that the failure stress can be calculated using,

$$\sigma_{1,f} = \sigma_{3,w}\left[\tan^2(45+\phi/2)\right] + 2c\tan(45+\phi/2)$$

where ϕ = angle of internal friction

c = cohesion

Therefore,

$$F = \frac{\sigma_{1,w} - \sigma_{3,w}}{\sigma_{3,w}\left[\tan^2(45+\phi/2) - 1\right] + 2c\tan(45+\phi/2)}$$

This concept of failure factor is used later to develop a permanent deformation model in a granular layer. The failure factor is defined reciprocal to the safety factor used in the South African Mechanistic Pavement Design Analysis Method (SAMPDAM) (82) for design of a granular base. The advantage of defining the failure factor as adopted in this report is that the safe state is conveniently represented by values between 0 and 1, which can easily be incorporated in analysis. Results from static triaxial testing presented in Chapter 6 have shown the need for a modified Mohr-Coulomb model indicated by Figure 7.5.

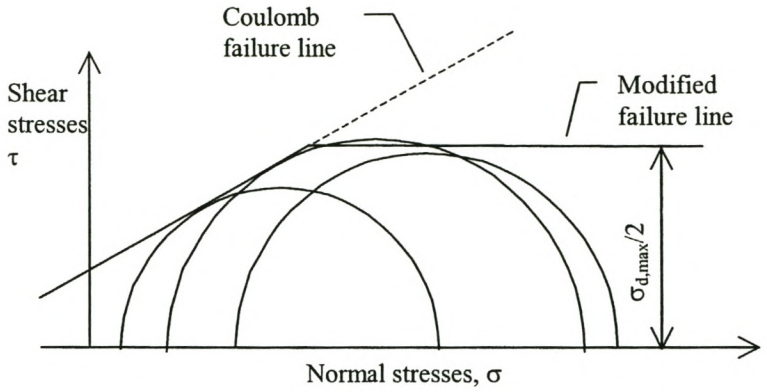

Figure 7.5 Modified Mohr-Coulomb model.

This means the failure factor has to be defined differently for the second part of the failure model. For this part,

$$\sigma_{1,f} = \sigma_{d,max} + \sigma_{3,w}$$

where $\sigma_{d,max}$ = maximum allowable deviator stress

Therefore,

$$F = \frac{\sigma_{1,w} - \sigma_{3,w}}{\sigma_{d,max}}$$

The second failure line applies when,

$$\sigma_{3,w} > \frac{\sigma_{d,max} - 2c\tan(45 + \phi/2)}{\tan^2(45 + \phi/2) - 1}$$

7.5 Permanent deformation model

Each load application has an elastic and plastic part. The elastic part accounts for the resilient behaviour of the material. The plastic part accounts for the permanent deformation behaviour of the material. A plot of test results for plastic strain ε_p versus log N shown in Figure 7.6 reveals a model of the form,

$$\varepsilon_p(N) = a + b\log N$$

where, ε_p = plastic strain

N = number of load repetitions

a,b = material parameters

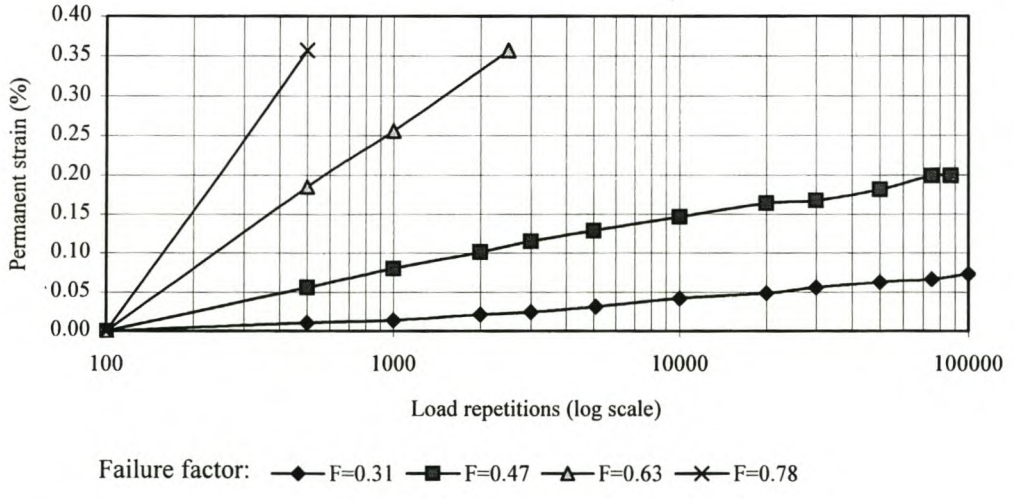

Figure 7.6 Deformation with increasing load repetitions for σ_3=50kPa and degree of saturation 75 - 80%.

Each curve represents a different value of failure factor (F) calculated according to the equation given in section 7.4. Since the value of the failure factor affects the slope of the deformation curve, it implies that the constants a and b in the model are functions of the failure factor (F). The model should then be,

$$\varepsilon_p(N) = a_i + b_i \log N$$

where, a_i, b_i = f {failure factor}

This relationship is similar to that proposed by Barksdale (106). Regression analysis was used to obtain values of a_i and b_i for the different levels of failure factor (F). A summary of regression results is given in Table 7.3.

Table 7.3 Summary of regression results for deformation model.

Curve	F	Regression coefficient		r^2
		a	b	
No 1	0.35	-0.0592	0.0255	0.971
No 2	0.47	-0.1174	0.0648	0.987
No 3	0.63	-0.4059	0.2061	0.999

Deformation is referenced to that after 100 load repetitions. The constant 'a' then takes on a value of zero. A linear relationship is apparent when log b_i is plotted against F as shown in Figure 7.7.

This relationship takes the form,

$b = c10^{d*F}$ where c,d = constants

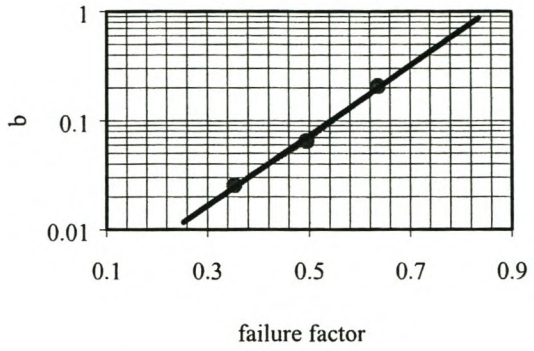

Figure 7.7 Safety Factor vs. Log b (σ_3=50kPa) .

Further regression analysis established the constants, c=0.0018 and d=3.21 with r^2=0.99.

Hence the relation, $b = 0.0018 * 10^{3.21F}$

Therefore the model for plastic deformation for this material is,

$$\varepsilon_p(N) = 0.0018 \times 10^{3.21F} \log N$$

where ε_p = plastic strain
N = number of load repetitions
F = failure factor

This model has been developed for the case σ_3 = 50 kPa and 75 - 80% saturation. Figure 7.8 makes a graphical comparison between the experimental results and the model results.

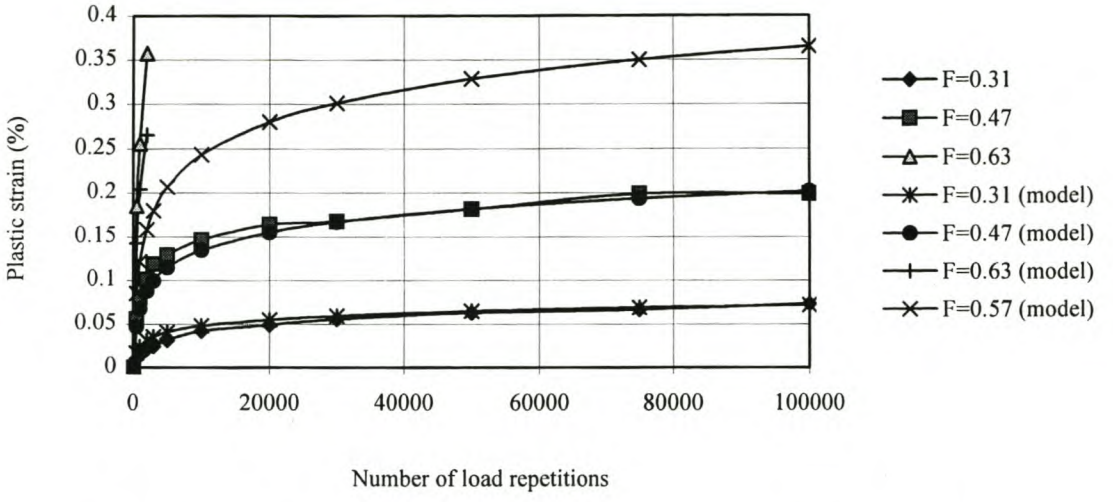

Figure 7.8 Deformation model fitted to laboratory results for σ_3=50kPa and degree of saturation 75 - 80%.

It is evident from the results that there is a certain value of failure factor (F) above which there is rapid shear deformation after a few load repetitions. For this material this is about 0.6. This agrees with research by others in the U.K. and South Africa. This means, to minimise permanent deformation within a granular layer in a pavement structure it is necessary that the failure factor is below the critical value. However, the South African Mechanistic Pavement Design and Analysis Method (SAMPDAM) (82) allows points to plot above the failure line of the Möhr-Coulomb failure line.

The permanent deformation model developed in this study does not take into account the influence of factors as moisture content, gradation, loading frequency, etc. Another limitation of such a deformation model developed from cyclic load triaxial testing is that it is valid only for stress states below failure (i.e. failure factor F < 0.6). Stress-strain analysis results in the next section, however, show that stress states with failure factor F above the critical 0.6 value do occur in granular layers under a thin pavement surfacing.

7.6 Model pavement design

7.6.1 General

Results from this study are used in analysing stresses and permanent strains in a simple pavement structure. Although the Uzan model was found to be the best model to describe the stress-dependent resilient modulus of the lateritic gravel tested, no computer program was found that could implement this model for non-linear stress-strain analysis. KENLAYER computer program (44), which employs the popular M_r-Θ model was used for non-linear analysis.

Pavement structure:

A light pavement structure applicable to light and medium trafficked roads employing a lateritic gravel as one of the structural layers is used. The pavement structure comprises a 150mm lateritic granular base over 150mm granular subbase and on a suitable subgrade as shown schematically in Figure 7.9.

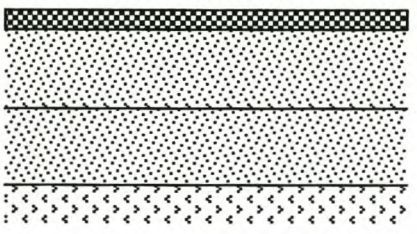

Figure 7.9 Pavement structure used for model pavement design.

Environment:

Assumption is that the water table is well below pavement foundation. Although the structure is under sealed surface, this does not inhibit the ingress of water, hence both saturated and partially saturated conditions can occur. The South African Mechanistic

Pavement Design Analysis Method (SAMPDAM) (82) accounts for various possible moisture conditions in the granular layer by way of a factor applied to the Safety Factor against shear failure. For this study, not enough results were obtained to enable various moisture conditions to be taken into account. This could rationally be done through applying adjustment factors to shear strength values (c and ϕ) for different moisture conditions expected in the pavement. For this analysis only one set of c and ϕ values obtained for 75 - 80% saturation are used.

Traffic load:

Initially a standard 40 kN dual wheel load with tyre pressure of 520 kPa is used in the analysis. Further analysis is conducted using a single wheel load and using varied axle loads, tyre pressures and other design parameters to evaluate their effect on pavement response.

Failure mechanism:

For pavements under a thin surfacing the main cause of failure will be permanent deformation in the granular layers and foundations leading to unevenness of the surface. Deformation is either caused by accumulation of plastic strains or shear failure. Deformation due to shear failure causes more extensive damage. The distribution of failure factor (F) in the pavement layers is the parameter that will influence plastic strain development. Values of failure factor (F) more than about 60% will lead to shear failure after a few load repetitions.

7.6.2 Stress-strain analysis

Under a single wheel load the pavement behaves in a resilient manner. However, plastic strains accumulate under repeated loading. This thus presents the opportunity to separate the theoretical analysis of pavements into two parts. The elastic response for which various programs are available for stress-strain analysis and the plastic response.

Most computer programs for stress-strain analysis of pavement structures are based on linear elastic analysis. The most common of these are BISAR (46) and ELSYM5 (31). In real pavements, granular layers have marked non-linear stress-strain behaviour influenced by a range of variables. Linear elastic analysis can be used with reasonable confidence for pavements with thick bituminous layers but is inappropriate for unsurfaced or thinly surfaced pavements. The use of linear elastic analysis also produces non-realistic stress fields; radial stresses in tension at the base of the layers, or stresses out of the failure plane. To accommodate non-linear behaviour in theoretical analysis, two general approaches are usually used:

1. An iterative procedure using linear elastic layered systems. The layers of granular materials are sub-divided into sub-layers to accommodate the variations in resilient modulus caused by the changes in stress which occur with depth. The sub-layer values of resilient modulus are adjusted by way of suitable model and recomputed stresses. The process is repeated until the values of resilient modulus for all layers are compatible with the computed stress. This procedure takes no account of variation of stress in the horizontal direction. KENLAYER computer program used to analyse the model pavement structure in this study employs this approach.
2. Use of the finite element approach. There are a number of finite element analysis programs that have been developed specially for the pavement problem. These include SENOL (SEcant modulus NOn-Linear analysis) (Brownand Pappin, 1981) and FENLAP (Finite Element Non-linear Analysis for Pavements) (Brunton and d'Almeida, 1992) developed at Nottingham, and GT-PAVE (Tutumluer and Barksdale, 1995) from Georgia Institute of Technology. The problem of the tendency for horizontal tensile stresses to be computed at the bottom of the granular layer appears in finite element programs too. Since unbound materials have negligible tensile strength, aside from that induced by suction and particle interlock, adjustments to the computational procedures are usually applied to avoid false failure conditions. A number of finite element programs differ in the manner in which such stresses are redistributed.

KENLAYER computer program

KENLAYER is based on an elastic multilayer system under a circular loaded area. Solutions are applied iteratively for non-linear layers. KENLAYER employs the M_r-Θ model for computing the stress-dependent resilient modulus described as,

$$M_r = k_1\Theta^{k_2}$$

in which k_1 and k_2 are experimentally described constants and Θ is the sum of three normal stresses, σ_x, σ_y, and σ_z, or sum of three principal stresses, σ_1, σ_2, and σ_3. Including the weight of a layered system gives,

$$\Theta = \sigma_x + \sigma_y + \sigma_z + \gamma z(1 + 2K_0)$$

in which γ is the average unit weight, z is the distance below surface at which the modulus is to be determined, and K_0 is the coefficient of earth pressure at rest. Two methods have been incorporated in KENLAYER for non-linear analysis. In method 1, the non-linear granular layer is subdivided into a number of layers and the stresses at the mid-depth of each layer are used to determine the modulus. If the horizontal stresses, including the geostatic stress, is negative or in tension, it is set to zero. This stress modification is necessary to avoid negative Θ. In method 2, all the granular layers are considered as a single layer and an appropriate point, usually between the upper quarter and the upper third of the layer, is selected to compute the modulus. Because the point is at the upper part of the layer, the chance of negative Θ is rare, so no stress modification is needed. If Θ turns out to be negative, an arbitrary minimum modulus is assigned. Method 1 was used for analysis in this study. The 150 mm base was sub-divided into 6 layers and the 150 mm subbase into 3 layers.

Comparison was first made between KENLAYER and ELSYM5 analysis programs in order to identify any significant differences between results obtained with the two programs. The stiffness values for the base and subbase layers used in ELSYM5 are average values of those computed from the M_r-stress relation from KENLAYER.

Table 7.4 Details of model pavement structure.

Traffic loading
Tyre load: 40 kN, dual 350 mm spacing Tyre pressure: 520 kPa
Base, 150mm
$\gamma = 2210$ kg/m^3 Kenlayer, M_r-Θ model, $k_1 = 60$ MPa , $k_2 = 0.272$, $\nu = 0.35$ Elsym5, E = 340 MPa
Subbase, 150mm
$\gamma = 2160$ kg/m^3 Kenlayer, M_r-Θ model, $k_1 = 42$ MPa , $k_2 = 0.272$, $\nu = 0.35$ Elsym5, E = 150 MPa
Subgrade Linear elastic, Mr = 100 MPa

Stress-strain analysis results follow in the next paragraphs, while full results are given in **Appendix B.** Figure 7.10 shows a graphical comparison of results of vertical and radial stresses under the centre of one of the dual tyres from KENLAYER and

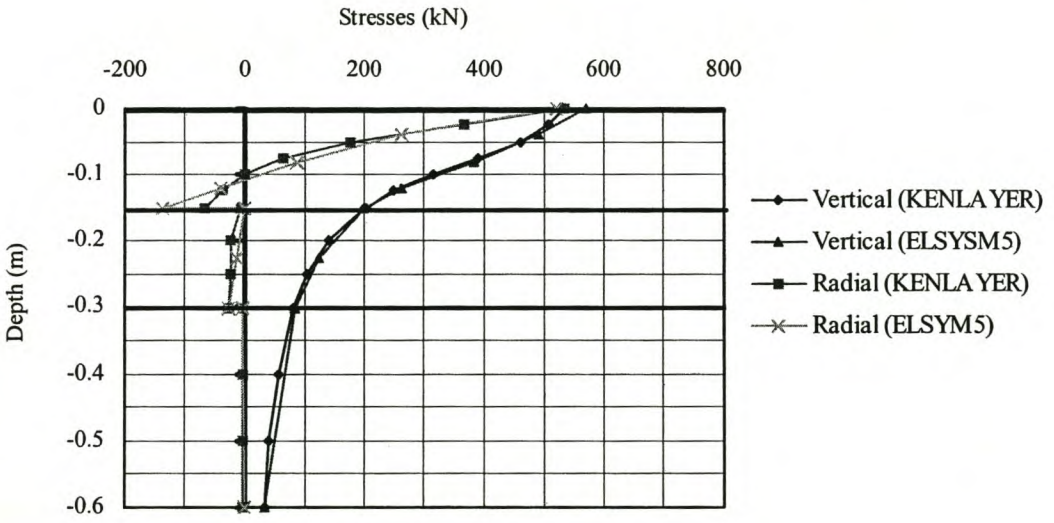

ELSYM5.

Figure 7.10 Comparison between Kenlayer and Elsym5 - Vertical and horizontal stresses under one tyre of the dual wheel.

Vertical stresses under one of the dual tyres match closely for ELSYM5 and KENLAYER. On the other hand, there is an appreciable difference in the horizontal stresses from the two programs. Both programs predict tensile stresses at the bottom of the base and subbase layers. Whether ELSYM5 or KENLAYER predicts a higher tensile stress at the bottom of the base will depend on the relative ratio of the layer moduli. In this case, ELSYM5 predicts a higher tensile stress at the bottom of the base compared to KENLAYER. It is accepted that granular layers can take limited tensile stresses but no definite figures are available on the magnitude of tensile stresses that can be supported.

Figure 7.11 shows the variation of failure factor (F) in pavement cross-section under one of the dual tyres from KENLAYER results.

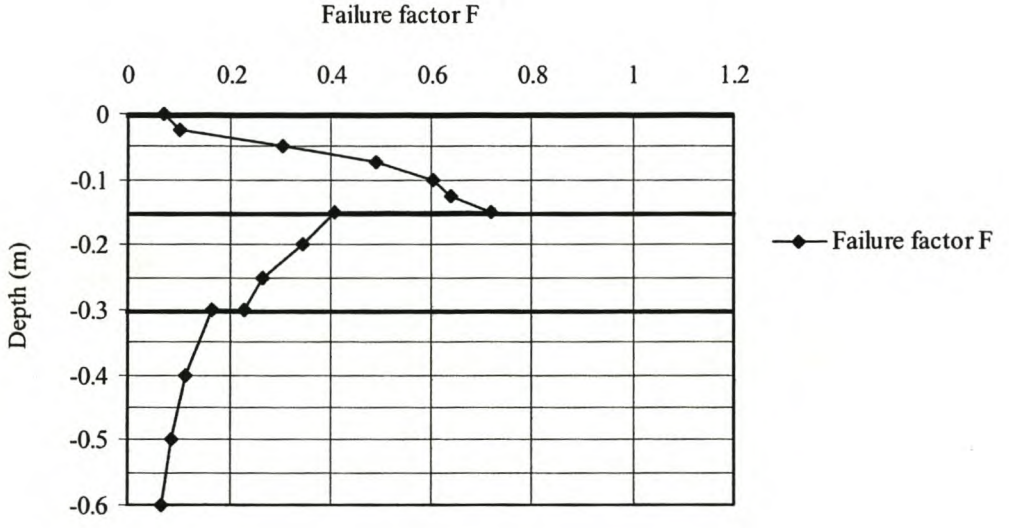

Figure 7.11 Variation of the failure factor F in pavement cross-section under one tyre of the dual wheel.

The results from the above graph show that the most 'highly stressed' point, in terms of higher values of failure factor, occurs at the bottom of the base. In computing the failure factor F, no adjustment was made to the tensile stresses. The Möhr circle representation of such a case is as shown in Figure 7.12(a). In computing the safety factor for designing of granular bases in the South African Mechanistic Pavement

Design Analysis Method (SAMPDAM) (82), the minor principle stress is set to zero and the major principle stress is adjusted under the condition that the deviator stress remain constant as illustrated in Figure 7.12(b). In this study, it was found inappropriate to make such an adjustment because it was assumed that limited tensile stresses are possible in the granular layers. The modified Möhr circle as illustrated in Figure 6.9 and the formulas in Section 7.4 were used for computing the failure factor F.

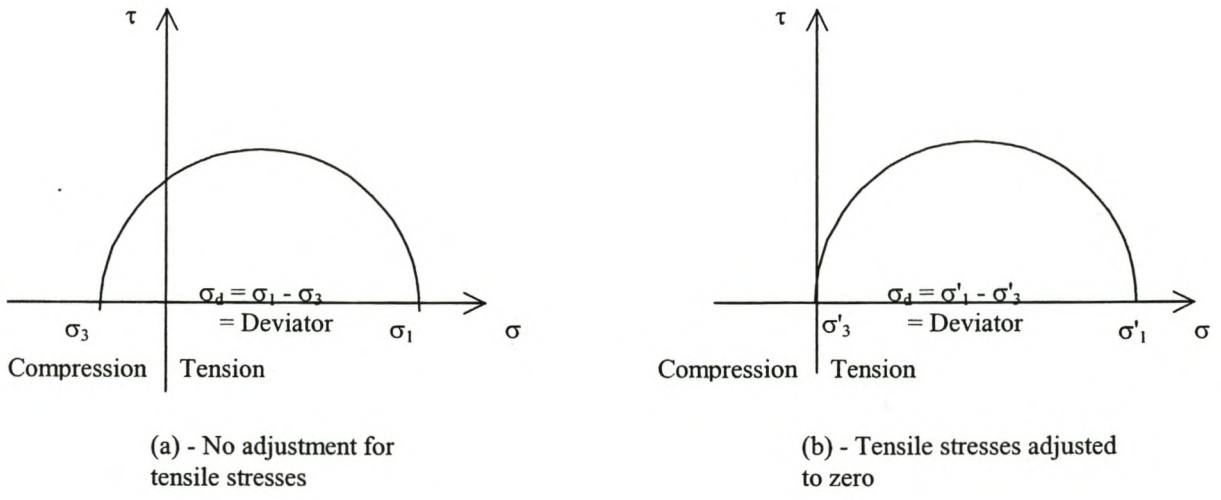

(a) - No adjustment for tensile stresses

(b) - Tensile stresses adjusted to zero

Figure 7.12 Möhr circle representation of stress state (after Theyse (82).

A comparison was made of stresses at a point between the dual tyres (Point 1) and stresses at a point under one of the tyres (Point 2) of the dual wheel.

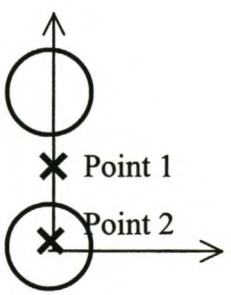

Figure 7.13 shows a comparison of KENLAYER results for vertical and radial stresses under one of the tyres and in between the two tyres of the dual wheel. Figure 7.14 shows the variation of failure factor (F) for the same points.

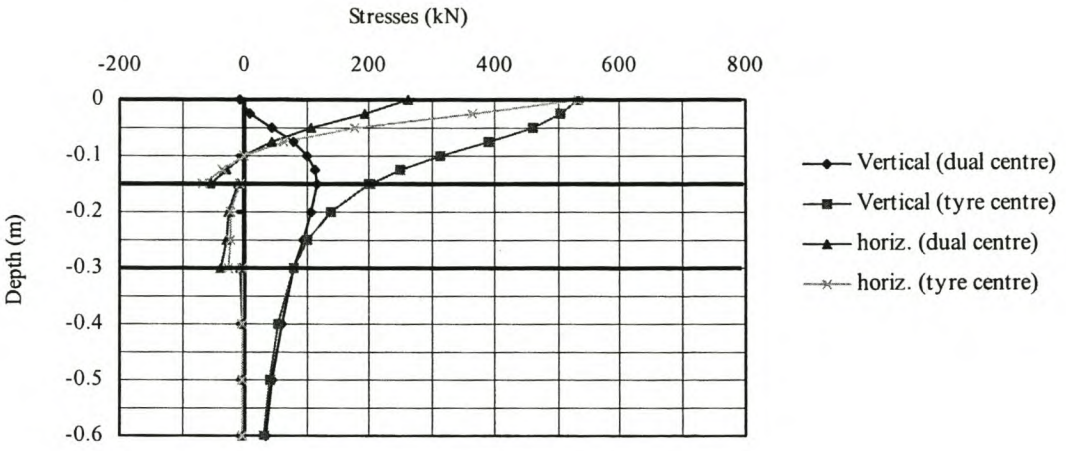

Figure 7.13 Comparison of vertical and horizontal stresses at point between the tyres and under one of the tyres of dual wheel.

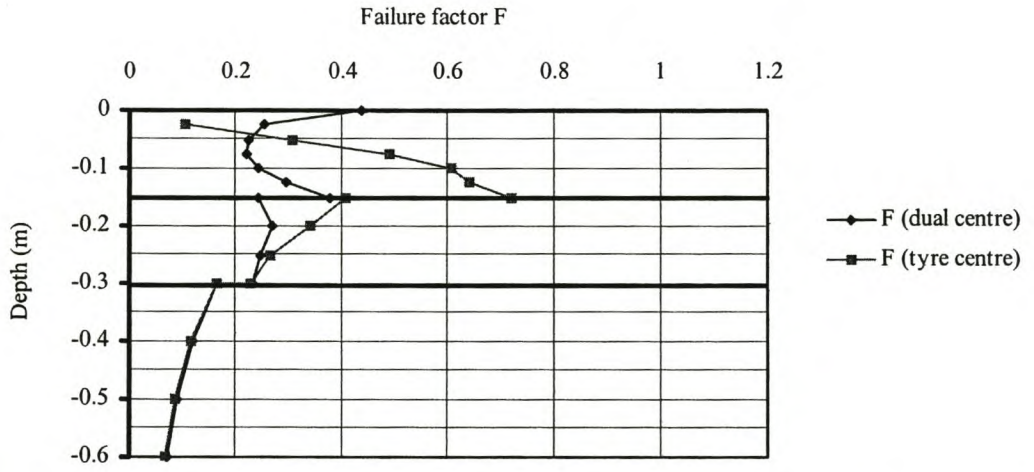

Figure 7.14 Comparison of failure factor F at point between the tyres and under one of the tyres of dual wheel.

It is clear from the above diagrams that in terms of the vertical stress going down to the subgrade there is no significant difference for the two points. However, in the upper layers the point directly under one of the dual tyres (Point 2) appears to be the

more highly 'stressed' because of higher values of failure factor (F). Therefore, all further analysis of stresses in the pavement layers has been done at the point directly under one of the dual tyres.

Figure 7.15 shows the variation of the stress-dependent resilient modulus in the pavement cross-section from KENLAYER results.

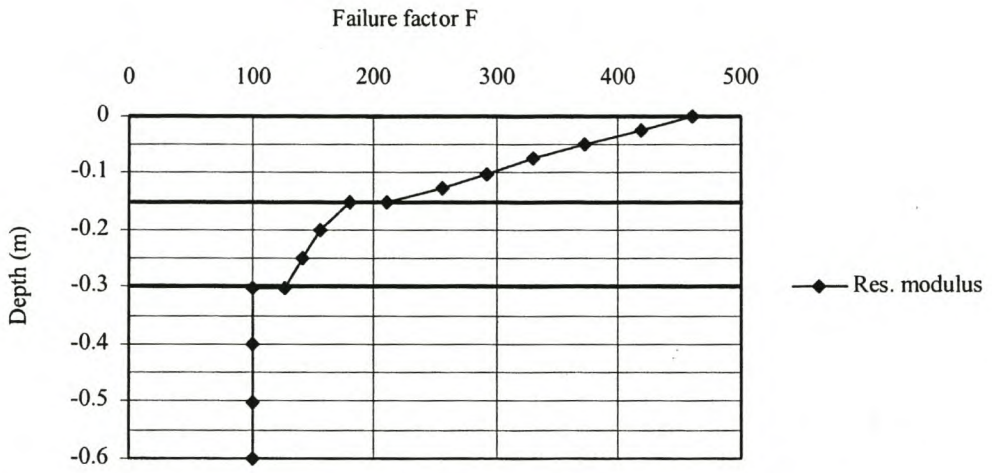

Figure 7.15 Variation of stress-dependent resilient modulus in pavement cross-section under one tyre of dual wheel.

In order to investigate the effect of change in various design parameters, further stress-strain analysis was carried out with KENLAYER as follows:

1. The dual wheel load varied from 40 kN, 50 kN and 60 kN.
2. Tyre pressure varied from 520 kPa, 600 kPa and 700 kPa.
3. Change in subgrade modulus from 100 MPa to 50 MPa.
4. Resilient modulus model parameter k_2 varied.
5. Poisson's ratio varied from 0.35 to 0.5.
6. Variation in layer thicknesses.
7. Dual wheel replaced by single wheel for loads of 40 kN, 50 kN and 60 kN and tyre pressure of 700kPa.

1. The dual wheel load varied from 40 kN, 50 kN and 60 kN.

Figure 7.16 shows vertical and radial stresses for different dual wheel loads of 40 kN, 50 kN and 60 kN from KENLAYER results, while Figure 7.17 shows variation of failure factor F in pavement cross-section.

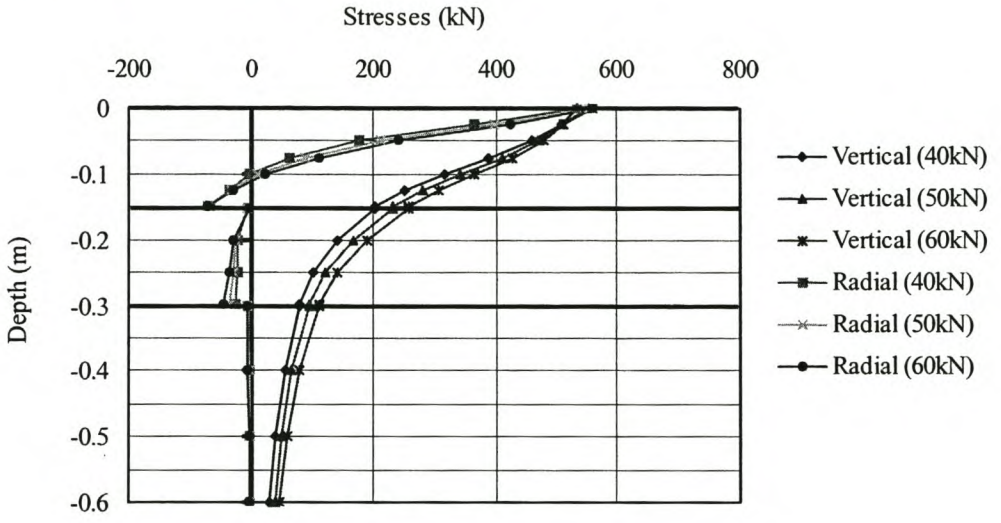

Figure 7.16 Vertical and radial stresses under one tyre of dual wheel - Axle load varied from 40 kN, 50 kN and 60 kN.

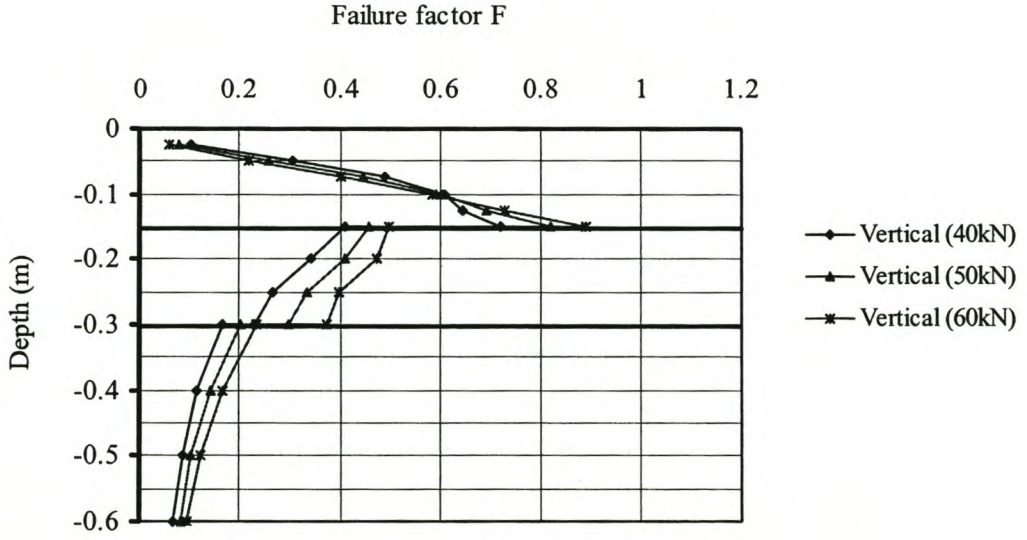

Figure 7.17 Failure factor F under one tyre of dual wheel - Axle load varied from 40 kN, 50 kN and 60 kN.

2. *Tyre pressure varied from 520 kPa, 600 kPa and 700 kPa for a wheel load of 40 kN.*

Figure 7.18 shows vertical and radial stresses for different tyre pressures of 520kPa, 600kPa and 700 kPa from KENLAYER results, while Figure 7.19 shows variation of failure factor F in pavement cross-section.

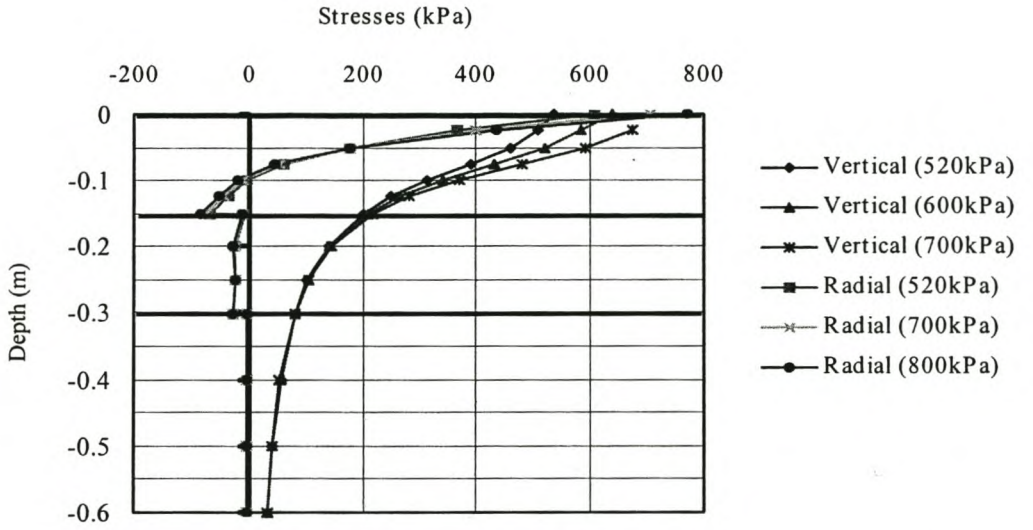

Figure 7.18 Vertical and radial stresses under one tyre of dual wheel - Tyre pressure varied from 520 kPa to 600 kPa and 700 kPa.

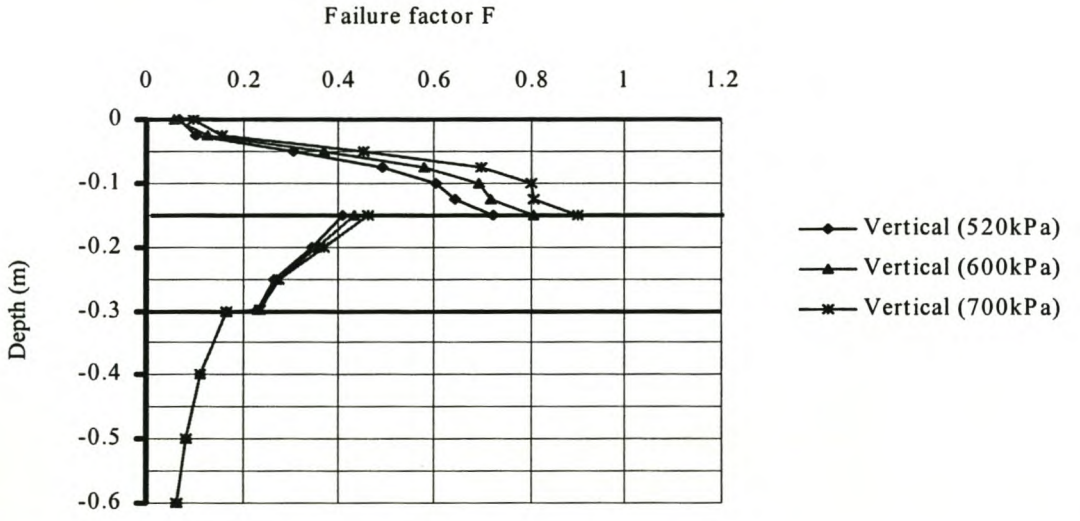

Figure 7.19 Failure factor F under one tyre of dual wheel - Tyre pressure varied from 520 kPa to 600 kPa and 700 kPa.

3. Change in subgrade modulus from 100 MPa to 50 MPa.

Figure 7.20 shows vertical and radial stresses when subgrade modulus is changed from 100 kPa to 50 kPa from KENLAYER results, while Figure 7.21 shows variation of failure factor F in pavement cross-section.

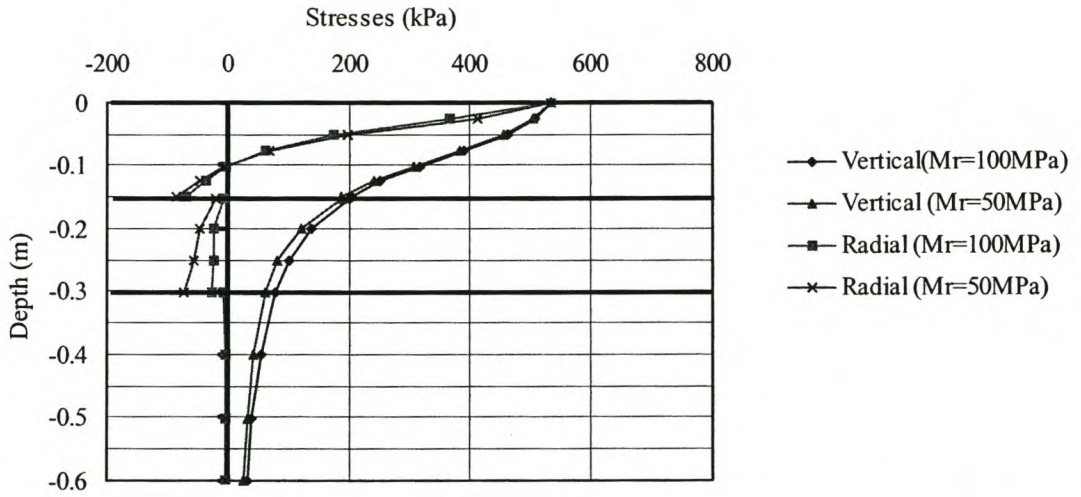

Figure 7.20 Vertical and radial stresses under one tyre of dual wheel - Subgrade modulus changed from 100 MPa to 50 MPa.

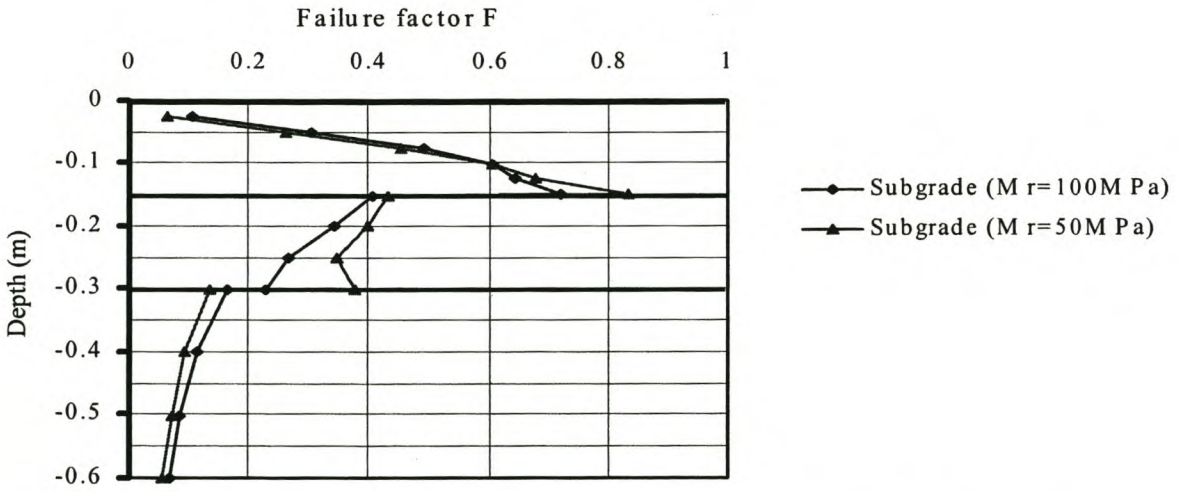

Figure 7.21 Failure factor F under one tyre of dual wheel - Subgrade modulus changed from 100 MPa to 50 MPa.

4. Resilient modulus model parameter k_2 varied.

Figure 7.22 shows KENLAYER vertical and radial stress results when the resilient modulus model parameter k_2 for the base layer is changed from 0.27 to 0.4, while Figure 7.23 shows variation of failure factor F in pavement cross-section.

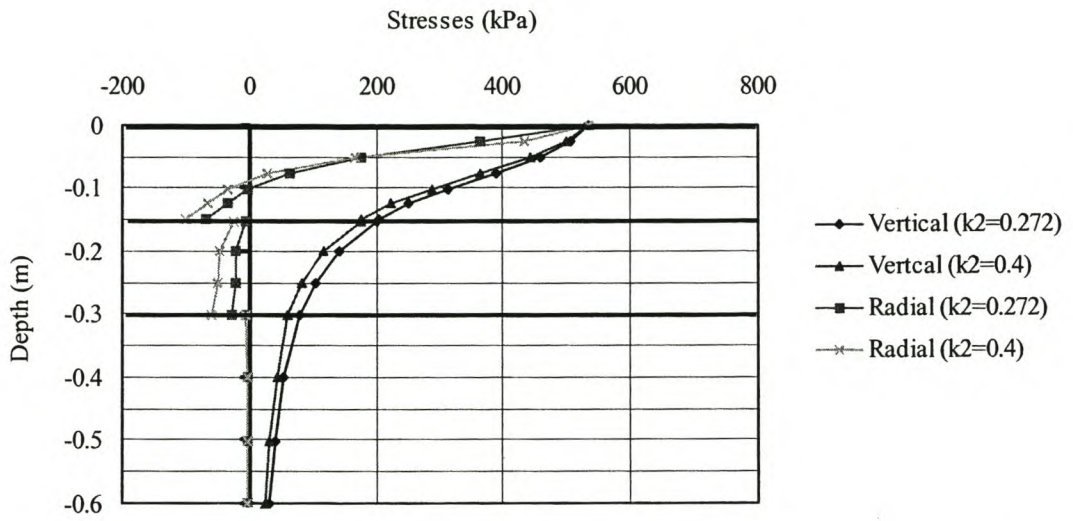

Figure 7.22 Vertical and radial stresses under one tyre of dual wheel - Resilient modulus model parameters k_2 for base layer changed from 0.27 to 0.4.

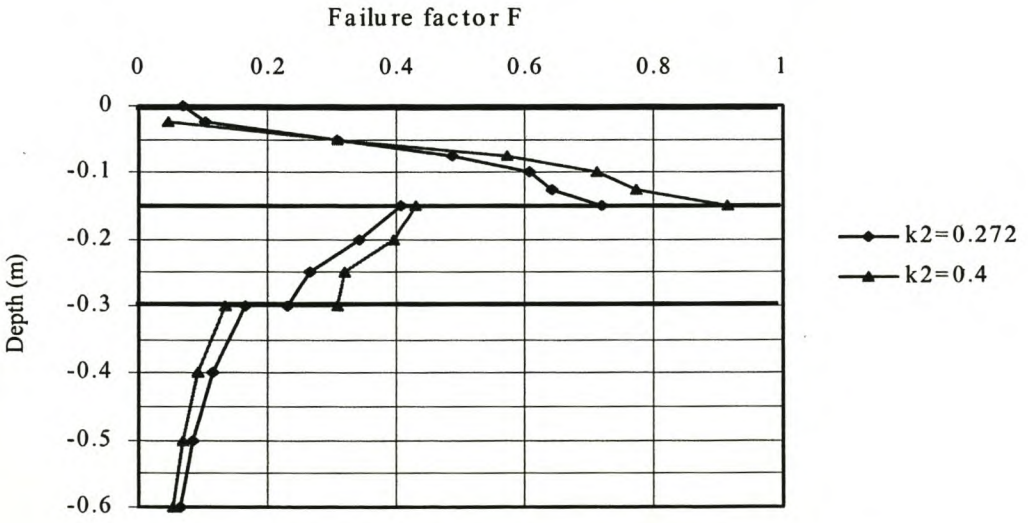

Figure 7.23 Failure factor F under one tyre of dual wheel - Resilient modulus model parameters k_2 for base layer changed from 0.27 to 0.4.

5. Poisson's ratio varied from 0.35 to 0.5.

Figure 7.24 shows KENLAYER vertical and radial stress results when the Poisson's ratio of the base and subbase layers is changed from 0.35 to 0.5, while Figure 7.25 shows variation of failure factor F in pavement cross-section.

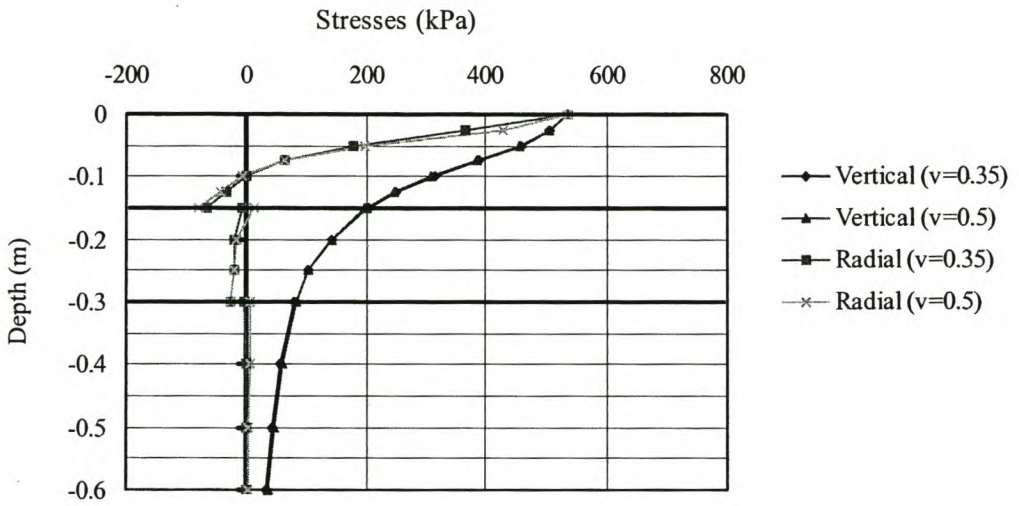

Figure 7.24 Vertical and radial stresses under one tyre of dual wheel - Poisson's ratio for base and subbase layers changed from 0.35 to 0.5.

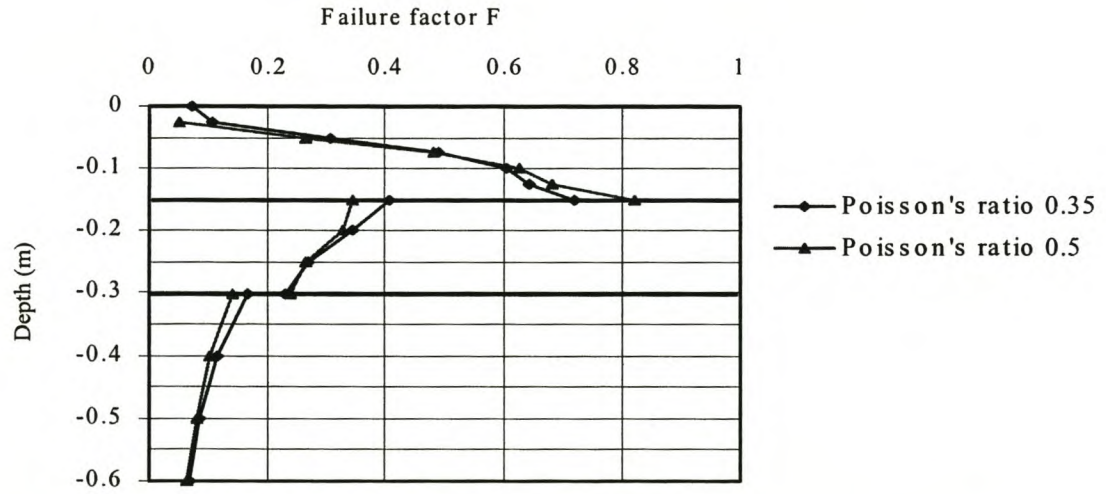

Figure 7.25 Failure factor F under one tyre of dual wheel - Poisson's ratio for base and subbase layers changed from 0.35 to 0.5.

6. *Variation in layer thicknesses.*

Figure 7.26 shows KENLAYER vertical and radial stress results for variation in base and subbase layer thicknesses, while Figure 7.27 shows variation of failure factor F in pavement cross-section.

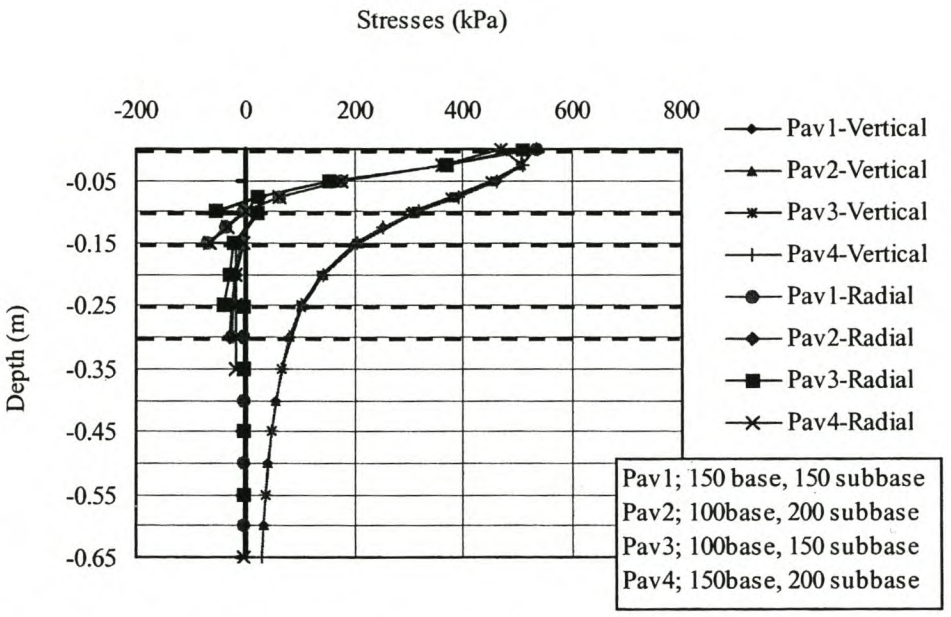

Figure 7.26 Vertical and radial stresses under one tyre of dual wheel - Changes in layer thicknesses.

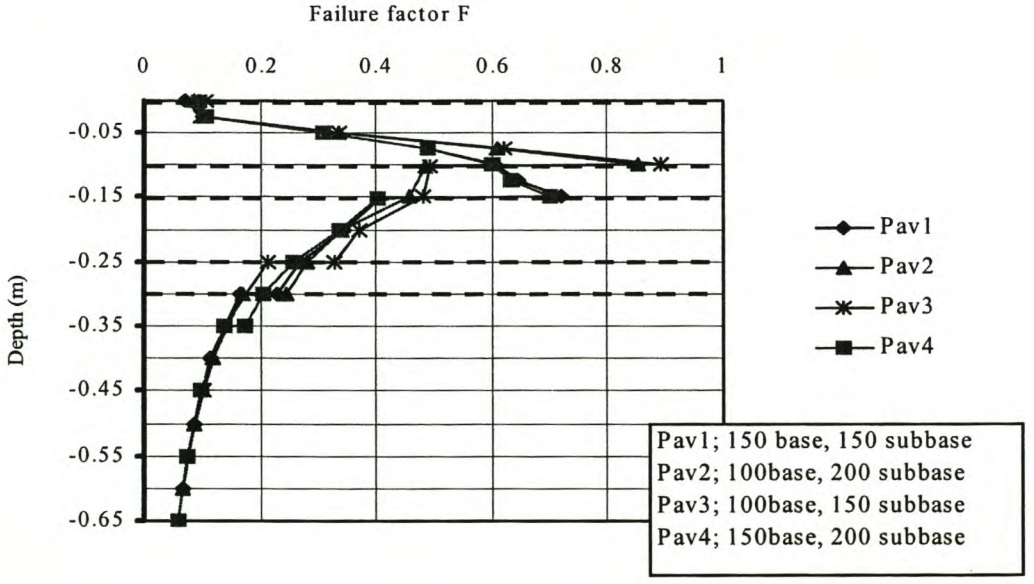

Figure 7.27 Failure factor F under one tyre of dual wheel - Changes in layer thicknesses.

7. Dual tyre replaced by single tyre for wheel loads of 40 kN, 50 kN and 60 kN.

Figure 7.28 shows KENLAYER vertical and radial stress results for analysis carried out by replacing the dual wheel with a single wheel with loads of 40kN, 50kN and 60kN for a tyre pressure of 700 kN, while Figure 7.29 shows variation of failure factor F in pavement cross-section.

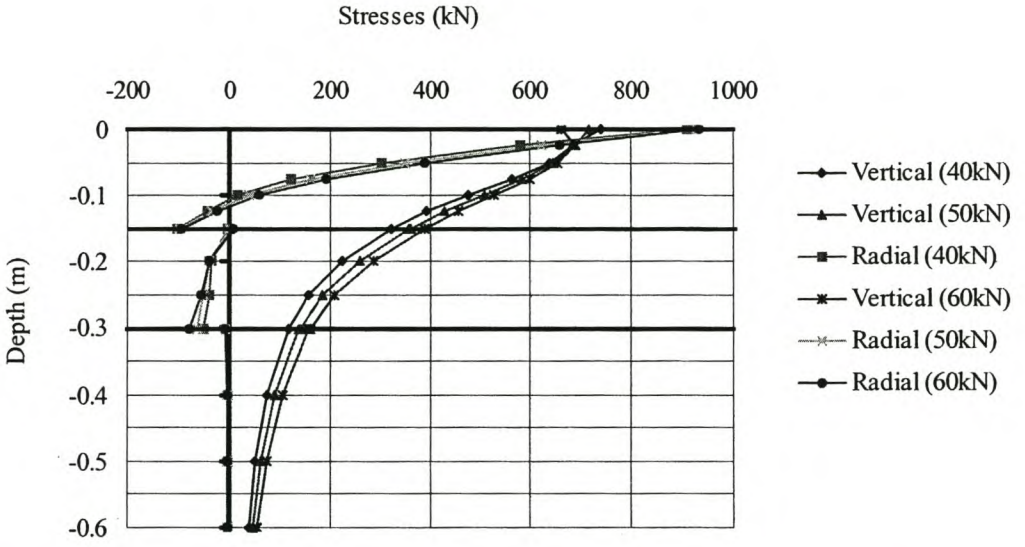

Figure 7.28 Vertical and radial stresses under centre of single wheel - 40kN, 50kN and 60kN wheel loads.

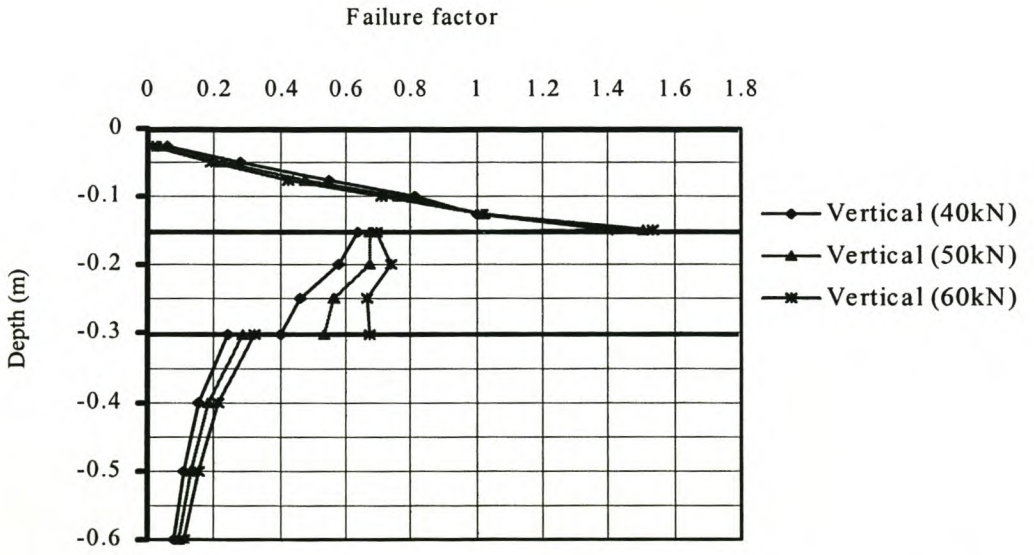

Figure 7.29 Failure factor F under centre of single wheel - 40kN, 50kN and 60kN wheel loads.

The following conclusions can be made from the above graphs:

1) ELSYM5 computer program, based on linear elastic analysis, and KENLAYER which incorporates non-linear analysis, give similar results for the vertical stress in the pavement system, but results differ for the horizontal stresses, Figure 7.10.
2) The highest value of failure factor (F) in the pavement system occurs at the bottom of the base, Figure 7.11. For the bottom third of the base the values for safety factor are higher than the critical 60 % necessary to prevent shear deformation.
3) The most highly 'stressed' point under a dual wheel, in terms of high values of failure factor (F), occurs under one of the tyres, while in terms of vertical stress at the top of the subgrade, both the points under one of the tyres and that in between the tyres give similar results, Figures 7.13 and 7.14.
4) Increased axle loads cause the most change in stresses in the subbase and subgrade layers compared to that caused by all other design parameters, Figures 7.16 and 7.17. On the other hand increased tyre pressures only affect stresses in the upper layers (base) of the pavement, Figures 7.18 and 7.19.
5) Changes in subgrade modulus and resilient- modulus-model parameters have the effect of changing the relative ratio of moduli for the layers, causing appreciable changes in stress distributions, Figures 7.20 - 7.23.
6) Changes in Poisson's ratio of base and subbase layers from 0.35 to 0.5 caused little changes in stress distribution of all layers, Figure 7.24 and 7.25.
7) Figure 7.26 and 7.27 reveal that for a given subgrade strength the vertical stress at a point a particular height from the pavement surface is almost the same irrespective of the relative thickness of the overlying base and subbase. This introduces an important principle that can be used to estimate the required amount of cover required above a subgrade of given strength in order to limit the strain on top of the subgrade.
8) A single wheel load compared to a dual wheel load gave very high stresses in the base and subbase layers. The values for failure factor are particularly very high in the bottom part of the base, Figures 7.28 and 7.29.

7.6.3 Permanent deformation

The permanent deformation in the pavement layers is determined by integrating the vertical plastic strain over the depth of the layers using the permanent deformation model developed in Section 7.5 as follows,

$$Rut(N) = \int_{depth} \varepsilon_p(N) \qquad \text{where, } \varepsilon_p(N) = 0.0018 \times 10^{3.21F} \log N$$

F = failure factor

N = number of load repetitions

This model was developed at the following material characteristics for the laterite gravel tested: 75 - 80 % saturation, 96 % Mod. ASSHTO compaction, c = 146 kPa and $\phi = 32°$. It was developed at a confining stress of 50 kN due to the length of the test. The assumption is that for any stress state the value of the failure factor F controls the deformation. However, the model only applies to stress states with value of failure factor F below the critical 60 % value (region 1 in Figure 7.30). Cyclic triaxial test specimens with failure factor F more than 60 % (region 2), failed after a few load repetitions.

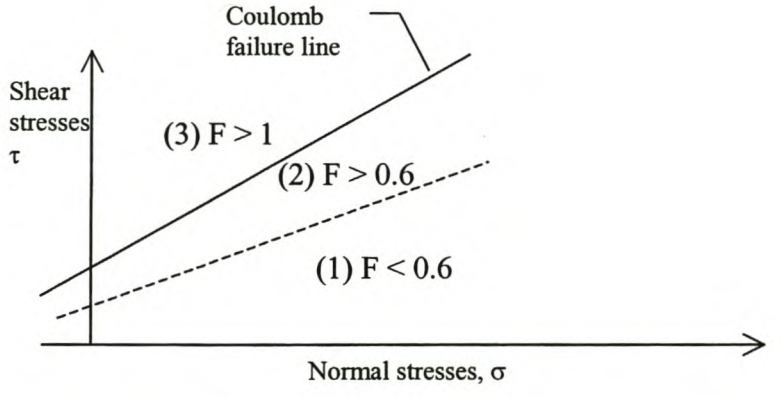

Figure 7.30 Möhr-Coulomb diagram showing safe region.

Unfortunately, the results of stress-strain analysis from the Section 7.6.2, Figure 7.11, show that the failure factor F in the lower third of the base has a value more than 60 %. This means such a model developed from laboratory cyclic load triaxial testing will have limited applications in pavements structures with a granular base over a thin surfacing. The permanent strain at failure in laboratory cyclic triaxial testing for the laterite gravel tested was less than 0.5 %. Deformations encountered in cyclic triaxial testing are thus obviously to small to account for deformation in real pavement structures, which should then be caused by shear failure deformation (region 2 and 3 in Figure 7.30). Therefore, realistic models for this material can only be developed from Accelerated Pavement Testing (APT) on real pavement structures or observations on in service pavements. An example of permanent defornmation model for granular materials developed from HVS testing on a wide range of pavement structures has been described by Wolff and Visser (1994).

Pavement life is determined by the permanent deformation or rut in the base and subbase layers. This should be considered in conjunction with subgrade deformation. Excessive deformation in the subgrade is usually controlled by limiting the vertical strain on top of the subgrade. In applying any permanent deformation model account should also be taken of any relevant variables that might influence the relationship between the accumulation of plastic strain and applied stress like moisture content, gradation and degree of compaction.

8 CONCLUSIONS & RECOMMENDATIONS

A number of conclusions and recommendations came from this study.

8.1 Conclusions

1) The method of pre-test drying and the amount of manipulation during testing were found to affect the Atterberg limits of the lateritic gravel tested. The gradation was relatively unaffected by the method of pre-test drying.
2) The resilient modulus of the lateritic gravel tested was found to be affected by moisture and degree of compaction, apart from the stress level. The Uzan model was found to be the best resilient modulus model for the lateritic gravel investigated. This model takes into account both the effects of deviator stress and confining stress.
3) The treated gravel, both foamed-bitumen and cement treated gravel, also displayed stress-dependent resilient modulus behaviour with a noted increase in resilient modulus with increase in deviator stress.
4) The concept of failure factor, which describes the ratio of the working shear stress to the maximum safe shear stress, was introduced as a critical distress parameter in the model pavement design. It was found that in thinly surfaced granular base pavements, the critical failure factor F in the bottom third of the base is more than the critical 60 %. This means development of permanent strains taking place with increasing number of load repetitions is due to gradual shear.
5) Results of stress strain analysis show that increased axle loading is the foremost likely cause of distress in light pavement structures having granular base and subbase, with effects going down to the subgrade.
6) Testing has shown that the resilient modulus alone, as measured using cyclic load triaxial testing, might not be truly reflective of capacity of granular layers in a

pavement to carry traffic because it does not give information on the potential for plastic deformation development under repeated loads.

8.2 Recommendations

1) Accelerated pavement testing, APT, or observation on in-service pavements is required to develop performance prediction models for thinly surfaced granular base pavements. APT could also be used to validate laboratory developed models and to develop relationships between properties of granular materials determined in the laboratory and actual field performance.
2) Current pavement stress-strain analysis programs, including finite element programs, give tensile stresses at the bottom of the base and subbase layers. There is need to develop ways to better resolve tensile stresses in granular layers to get a better reflection of the true stress state in the granular layers.
3) With the use of mechanistic design methods, making designs at higher axle loads would give more realist designs in cases where overloading is prevalent rather than use load equivalence.

REFERENCES

1. "AASHTO Interim Guide for the Design of Pavement Structures", American Association of State Highway and Transportation Officials, Washington, D.C., 1974.

2. "AASHTO Guide for the Design of Pavement Structures", American Association of State Highway and Transportation Officials, Washington, D.C., 1993.

3. ASSHTO T 274-92, "Standard method of test for resilient modulus of subgrade soils", American Association of State Highway and Transportation Officials, Washington, D.C.

4. Ackroyd, L.W., "The correlation between engineering and pedological soil classification systems in Western Nigeria and its application", 1 Proc. 3rd Regional Conf. for Africa on Soil Mech. and Found. Engineering, Salisbury, pp 47-51, 1963.

5. Ackroyd, L.W., "The engineering classification of some western Nigerian soils and their qualities in road making", British Road Research Laboratory, Overseas bulletin, 10, 32 pp, 1959.

6. Akpokodje, E.G., Hudec, P.P., "The influence of petrology and fabric on the engineering properties of concretionary laterite gravel aggregates", Quart. Journ. Engineering Geology, 27, pp 39-50, 1994.

7. Akpokodje, E.G., Hudec, P.P., "Quality control tests and acceptance specifications for concretionary laterite gravel aggregates", Engineering Geology, 32:255-267, 1992.

8. Alexander, L.T., Cady, J.G., "Genesis and hardening of laterites in soils", U.S. Dept. Agric., Tech. Bull., 1962.

9. Arulanandan, K., "Classification, engineering properties and behaviour of laterite soils", Proc. Spec. 7th Int. Conf. Soil Mech. Found. Engng,, Mexico, 2, pp 45-57, 1969

10. Australian Standard AS 1289.6.8.1, "Determination of the Resilient Modulus and Permanent Deformation of Granular Unbound Materials", Standards Australia, 1995.

11. Bhatia, H.S., Hammond, A.A., "Durability and strength of laterite gravels of Ghana", Building Road Res. Inst., Kumasi, Ghana, Project Rep. S.M., 15 pp, 1970.

12. Boyce, H.R., "A non-linear model for the elastic behaviour of granular materials under repeated loading", Proc. Int. Symp. On Soils under Cyclic and Transient Loading, Swansea, UK, pp 285-294, 1980.

13. British Standards Institution, "Methods for sampling and testing of mineral aggregates, sand and fillers", British Stand., 812, 84 pp, 1960.

14. Brown, S.F., Pappin, J.W., "Analysis of pavements with granular bases", Transportation Research Record, 810, Transportation Research Board, pp 17 - 22, 1981.

15. Brown, S.F., Pappin, J.W., "Modelling of granular materials in pavements", Transportation Research Record, 1022, pp 45 - 51, 1985.

16. Brown, S.F., Pell, P.S., "An experimental investigation of the stresses, strains, and deflections in a layered pavement structure", Proc. 2nd Int. Conf. on Structural Design of Asphalt Pavements, pp 487 - 504, Ann Arbor, 1967.

17. Brunton, J.M., d'Almeida, J.R., "Modelling of material non-linearity in a pavement backcalculation procedure", Transportation Research Record, 1377, Transportation Research Board, pp 99 - 106, 1992.

18. Buchanan, F., "A journey from Madras through the countries of Mysore, Canara and Malabar, 2" East Indian Company. London, 1807

19. Cartmell, H.S., Bergh, A.O., "Lime stabilization of soils for use as road foundations in Northern Rhodesia", Road Research Laboratory, Overseas Bulletin No. 9, 1969.

20. Claesen, A.I.M., Edwards, J.M., Sommer, P., Ugé, P., "Asphalt Pavement Design - The Shell Method' Proc. 4th Int. Conf. on Structural Design of Asphalt Pavements, Vol. 1: pp 39 -74, 1977.

21. Cocks, G.C., Hamory, G., "Road Construction Using Lateritic Gravel in Western Australia", Proc. 2nd Int. Conf. on Geomechanics in Tropical Soils, 1, pp369-384, 1988.

22. CSIR Transportek, "Foamed Asphalt Mix Design", Website, http:\\foamasph.csir.co.za:81/chap4.htm, 1998.

23. De Graft-Johnson, J.W.S., Bhatia, H.S., Yeboa, S.L., "Influence of geology and physical properties on strength characteristics of laterite gravels for road pavements", Highway Res. Board, Rec. 405 pp 87-104, 1972.

24. De Graft-Johnson, "Laterite soils in road construction", Proc. 6th Regional Conf. for Africa on Soil Mech. and Found. Engineering, 1, pp 89-98, 1975.

25. De Graft-Johnson, J.W.S., Bhatia, H.S., Gidigasu, M.D., "The engineering characteristics of laterite gravels of Ghana", Proc. Special Session on Eng. Properties of Laterite soils, Vol 1, Asian Inst. of Technology, Bangkok, pp 117-128, 1969.

26. D'Hoore, J.L., "Studies on the accumulation of sesquioxides in tropical soils", Nat. Inst. Agron. Belg. Congo, Sci. Ser., 62: 132 pp, 1954.

27. Donaldson, G.W., General Report Proc. 4th Regional Conf. for Africa on Soil Mech. and Found. Engineering 2, pp 334-342, 1967.

28. Draft TRH4, "Structural Design of Flexible Pavements for Interurban and Rural Roads", DOT, Pretoria, S.Africa, 1996.

29. Draft TRH13, "Cementitious stabilizers in road construction" DOT, Pretoria, South Africa, 1986.

30. Draft TRH14, "Guidelines for road construction materials" DOT, Pretoria, South Africa, 1985.

31. Warren, H., Dieckmann, W.L., "Numerical computation of stresses and strains in a multiple-layer asphalt pavement system", Internal report, Chevron Res. Corp., California, 1963.

32. "Especificacóes GeraisPara Obras Rodoviárias", (in Portuguese), Departamento Nacional de Estradas de Rodagem, Rio de Janeiro, Brazil, 1971.

33. Evans, E.A., "A laboratory investigation of six lateritic gravels from Uganda", British Road Research Laboratory, Note 3241, 20 pp, (unpublished), 1958.

34. Ferreira-Novais, H., Discussion Proc. 5th Regional Conf. for Africa on Soil Mech. and Found. Engineering 2, 44 pp.

35. Gidigasu, M.D., "Mode of formation and geotechnical characteristics of laterite materials of Ghana in relation to soil forming factors", Engineering Geology, 6, pp 79 - 150, 1972.

36. Gidigasu, M.D., "Degree of weathering in the identification of laterite materials for engineering purposes - A review", Engineering Geology, 8, pp 213 - 266, 1974.

37. Gidigasu, M.D., "Laterite Soil Engineering", Elsevier, New York, 1976.

38. Gidigasu, M.D., "Development of acceptance specifications for tropical gravel paving materials", Engineering Geology, 19, pp 213-240, 1982/83.

39. Government of the Republic of Zambia. Roadsip II Inception Report, 1998.

40. Grace, H., " Investigations in Kenya and Malawi using as-dug laterite as bases for bituminous surfaced roads", Geotechnical and Geological Engineering, 9, pp 183-195, 1991.

41. Harty et al, Thompson, M.R., "Lime reactivity of tropical and sub-tropical soils. Highway Research Record, 442, pp 102 - 112, 1973.

42. Heukelom, W., Klomp, A.J.G., "Dynamic testing as a means of controlling pavements during and after construction", Proc. 1st International Conference on Structural Design of Flexible Pavements, Vol. 1, pp 667 - 679, Ann Arbor, 1962.

43. "Highway Materials, Part 1: Specifications", 10th ed., American Association of State Highway Officials, Washington, D.C., 1971.

44. Huang, Y.H., "Pavement Analysis and Design', Prentice Hall, New Jersey, 1993.

45. Jenkins, K.J., van de Ven, M.F.C., de Groot, J.L.A., "Characterization of Foamed Bitumen", Proc. 7th Conf. on Ashalt Pavements for Southern Africa, Victoria Falls, Zimbabwe, 1999.

46. Jong, D.L. de, Peutz, M.G.F, Korswagen, A., "Computer Program Bisar. Layered systems under normal and tangential surface loads", External report AMSR.0006.731, Koninklijke/Shell-Laboratorium, Amsterdam, 1973.

47. Lekarp, F., Isacsson, U., Dawson, A., " Mechanical properties of unbound granular materials - State of the Art I", American Soc. Civil Eng'rs J'n'l Transp. Eng., Vol 126, No 1, pp 66 - 75, 2000.

48. Lundgren, R., "Field performance of laterite soils", Gen. Report Spec. Sess. Laterite soils. Proc. 7th Int. Conf. Soil Mech. Found. Engng,, Mexico, 2, pp 45-57, 1969.

49. Lyon Associates Inc., "Laterites and Lateritic Soils and Other Problem Soils of Africa", U.S.AI.D. 2164, Baltimore, Maryland, 1971.

50. Mahalinga-Iyer, U., Williams, D.J., "Engineering properties of a lateritic soil profile", Engineering Geology, 31, pp 45 - 58, 1991.

51. Maignien, R., "Review of Research on Laterites", Nat. Resour. Res. IV. UNESCO, Paris, 1966.

52. Maree, J.H., "Die laboratoriumbepaling van die elastiese parameters, die skiufsterkteparameters en die gedrag onder herhaalde belasting van klipslagkroonlaagmateriale: toetsmetodes en apparaatbeskrywing", (in Afrikaans), NITRR, CSIR, S.Africa, Tegniese Verslag RP/11/78, 1979

53. Maree, J.H., "Die resulte an eenmalige belasting en herhaalde belasting drie-assige skuiftoetse op 'n reeks klipslag en gebreekte klip kroonlaagmateriale", (in Afrikaans), NITRR, CSIR, S.Africa, Tegniese Verslag RP/12/78, 1979

54. McFarlane, MJ.J., "Laterites", In: Gouldie, A.S., Pye, K. (eds) "Chemical Sediments and Geomorphology", Academic, London, pp 7 - 58, 1983.

55. Millard, R.S., "Road building in the tropics", J. Appl. Chem., London, 12, pp 342-357, 1962.

56. Millard, M.S., O'Reilly, M.P., "Standards of road building practice in the tropics", Proc. 2nd Conf. Road Res. Board, Australian Road Research Board, Melborne, Australia, pp 830 - 854, 1965.

57. Morin, W.J., Tudor, P.C., "Laterites and Lateritic Soils and Other Problem Soils of Africa", U.S.AI.D. 3682, Lyon Associates Inc., Baltimore, Maryland, 1975.

58. Mountain, M.J., General Report Proc. 5th Regional Conf. for Africa on Soil Mech. and Found. Engineering 2, pp 40 - 48, 1973.

59. Mountain, M.J., "Pedogenic materials, their engineering properties and distribution in S. Africa and S.W. Africa", Proc. 4th Regional Conf. for Africa on Soil Mech. and Found. Engineering 2, pp 65-70, 1967.

60. Nanda, R.L., Krishnamachari, R., "Study of soft aggregates from different parts of India with a view of their use in road construction, 2. Laterites, Central Res. Inst., Road Res. Paper, 15:, 32 pp,1958.

61. Nascimento, U., De Castro, E., Rodrigues, M., "Swelling and petrification of lateritic soils", Nat. Eng. Lab., Lisbon, Tech. Paper, 215, 19 pp, 1964.

62. Netterberg, F., Discussion Proc. 6th Regional Conf. for Africa on Soil Mech. and Found. Engineering 2, 195 pp, 1975

63. Niekerk, A.A. van, Huurman, M., "Establishing the complex behaviour of unbound road building materials from simple material testing", Report 7-95-200-16, Road and Railroad Research Laboratory, Delft Univ of Technology, 1995.

64. Niekerk, A.A. van, Poot, M.R., "Fundamental Behaviour of a Ghanaian Laterite from Triaxial Testing", Delf University of Technology, the Netherlands, 1995.

65. Nixon, I.K., Skipp, B.O., "Airfield construction on overseas soils. 5, Laterite", Proc. Brit. Inst. Civ. Eng., London, 8, pp 253 - 292, 1957.

66. Nogami, J.S., Villibor, D.F., "Use of lateritic fine grained soils in road pavement base courses", Geotechnical and Geological Engineering, 9, pp167-182, 1991.

67. Pannekoek, A.J., and Straaten, L.M.J.U. van, "Algemene geologie", Wolters Noordhoff, Groningen, The Netherlands, 1982.

68. Paute, J.L., Hornych, P., Beraben, J.P., "Repeated load triaxial testing of granular materials on the French network of Laboratoires des Ponts et Chaussées", Flexible Pavements, Balkema, pp 53 - 64, 1993.

69. Powell, W.D., Potter, J.F., Mayhew, H.C., Nunn, M.E., "The structural design of bituminous roads", Laboratory Report 1132, Transport and Road Research Laboratory, Crowthorne, 1984.

70. Queiroz, C., Carapetis, S., Grace, H., Paterson, W., "Observed Behaviour of Bituminous Surfaced Low-Volume laterite Pavements", Transportation Research Record, 1291, pp 126 - 136.

71. "Recommendations on Road Design Standards: Volume 1, Pavement Design Guide", Roads Department, Lusaka, Zambia, 1994.

72. "Recommendations on Road Design Standards: Volume 2, Geometric Design of Rural Roads", Roads Department, Lusaka, Zambia, 1994.

73. Remillon, A., "Les recherches entreprise en Afrique d'expression française", Ann. Inst. Techn. Batiment Trav. Publ., pp 231 - 232; pp 366 - 388.

74. "Road Note 31, A guide to the structural design of bitumen surfaced roads in tropical and sub-tropical countries", Transport and Road Research Laboratory, London, 1977.

75. Ruenkrairergsa, T., "Proposed specifications of soil aggregates for low-volume roads", Transp. Res. Rec. 1106, pp 268-280, 1987.

76. Sabita Manual 21, "The design and use of emulsion treated bases", Sabita, South Africa, 1999.

77. SABS Method 842, "10 % Fines Aggregate Crushing Value (FACT) of coarse aggregate", South African Bureau of Standards.

78. "Standard Specifications for Roads and Bridges", Roads Department, Lusaka, Zambia, 1994.

79. "Standard specifications for transportation materials and methods for sampling and testing. Part 2. Methods for sampling and testing. American Association of State Highway and Transportation Officials, Washington, D.C., 1978

80. Sweere, G.T.H., Galjaard, P.J., Tjong Tjin Joe H., " Engineering behaviour of laterites in road construction", Proc. 2nd Int Conf. Geomechanics in tropical soils, Singapore, 1988.

81. Sweere, G.T.H., "Unbound granular bases for roads", Doctoral Thesis, Technical University of Delft, the Netherlands, 1990.

82. Theyse, H.L., de Beer, M., Rust, F.C., "Overview of the South African Mechanistic Pavement Design Analysis Method", Divisional Publication DP-96/005, CSIR, Transportek, Pretoria, S.Africa, 1996.

83. TMH1, "Standard methods of testing road construction materials", CSIR, Pretoria, S. Africa, 1985.

84. Townsend, F.C., " Geotechnical Characteristics of Residual Soils", Journal of Geotechnical Engineering, Vol 111, No 1, 77-93, 1984

85. Tutumluer, E, Barksdale, R.D., "Behaviour of pavements with granular bases - prediction and performance", in Unbound Aggregates in Roads, University of Nottingham, pp. 173 - 183, 1995.

86. "Use of soil-cement mixtures for base courses", Wartime road problems No. 7, Highway Research Board, 1943.

87. Uzan, J., Witczak, M.W., Schullion, T., Lytton, R.L., "Development and validation of realistic pavement response models", 7th Int. Conf. Struct. Design of Asphalt Pavements, Nottingham, U.K, Vol. 1, pp 334-350, 1992.

88. Vallerga, B.A., Schuster, J.A., Love, A.L., Van Til, C.J., "Engineering Study of Laterite and Lateritic Soils in Connection with Construction of Roads, Highways and Airfields", U.S.AI.D, Rep. AID/CSD-1810, 1969.

89. Van der Merwe, C.P., Bate, I.C., "The properties and use of laterites in Rhodesia", Proc. 5th Regional Conf. for Africa on Soil Mech. and Found. Engineering 2, pp 7-14, 1971.

90. Verbal communications with engineers at Zulu Burrow Development Consultants, involved in design and supervision of roads works in Zambia, Dec. 1998.

91. Visser, A.T., Queiroz, C.A.V., Hudson, W.R., "Study of the resilient characteristics of tropical soils for use in low-volume pavement design", Transportation Research Record 898, Transportation Research Board, Washington D.C., pp 133 - 140, 1983.

92. Vuong, B.T., "Bridging the gaps between research and practical applications - Improved characterization of unbound pavement materials", Technical report to APRG, 1999.

93. Weinert, H.H., "The natural road construction materials of Southern Africa", Academica, Cape Town, 1980.

94. Winterkorn, F.H., Chandrasekharan, E.C., "Laterites and their stabilization", Highway Research Board, Washingtion, Bull. 44, pp 10 - 29, 1951.

95. Gidigasu, M.D., Yeboa, S.M., " Significance of pre-testing preparations in evaluating index properties of laterite materials", Highway Research Record, 405, pp 105 - 116, Washington, 1972.

96. "State of the art: Lime stabilization", Transportation Research Circular, No. 180, 1976.

97. Cabrera, J.G., Nwakanma, C.A., "Pozzolonic activity and mechanism of red tropical soil-lime systems", Transportation Research Record, 702, TRB, pp 199 - 207, 1979.

98. Laboratôrio Nacional de Engenharia Civil, Laboratôrio de Engenharia de Angola, Laboratôrio de Engenharia de Mocambique, Junta Autonoma de Estradas de Angola, "Portugues studies on engineering properties of lateritic soils", Proc. 7th Int. Conf. Soil Mech. Fndn, Engng., Special session Engng. Props. Lat. Soils, Mexico City, 1, pp 85 - 96, 1969. LNEC Memória No 143, Lisboa,1972.

99. Road Note 29. A guide for the structural design of pavements for new roads. HMSO, London, 1977.

100. Shell Pavement Design Manual. Shell International Petroleum Company, London, 1978.

101. MS-1, "Thickness Design - Asphalt Pavements for Highways and Streets"' the Asphalt Institute, Maryland, 1981.

102. Correia, A.G. (ed.), "Flexible pavements", Proc. of the European Symposium Euroflex, Lisbon, Portugal, 1993.

103. Sabita Manual 14, "GEMS - The design and use of granular emulsion mixes", Sabita, South Africa, 1993.

104. Uzan, J., "Characterization of granular materials", TRR 1022, Transportation Research Board, 1985, pp. 52-59, Washington, D.C., 1985.

105. Wolff, H., Visser, A.T., "Incorporating elasto-plasticity in granular layer pavement design", Proc. Inst. Civ. Engrs. Transp., 105, pp. 259-272, 1994.

106. Barksdale, R.D., "Laboratory evaluation of rutting in base course materials", Proc. 3rd Int. Conference on Structural Design of Asphalt Pavements, pp. 161 - 174, London, U.K., 1972.

APPENDIX A

Regression results

A1. Regression analysis results for resilient modulus models

1. K-Θ model

$M_r = k_1 \Theta^{k_2}$

Regression eqn: $\log M_r = \log k_1 + k_2 \log \Theta$

A1.1 Computational Tableau for logMr vs logΘ : K-Θ model

Θ (kPa)	Mr (MPa)	Log Θ x_i	Log Mr y_i	$x_i y_i$	x_i^2	y_i^2	$y_i' = \alpha+\beta x_i$	y_i-y_i'	$(y_i-y')_i^2$
220	195	2.34242	2.29003	5.364229	5.486944	5.24426	2.35352	-0.0635	0.0040302
270	213	2.43136	2.32838	5.6611378	5.91153	5.42135	2.37771	-0.0493	0.0024334
370	268	2.5682	2.42813	6.23594	6.59566	5.89584	2.41493	0.01321	0.0001745
470	312	2.6721	2.49415	6.6646251	7.140107	6.22081	2.44319	0.05097	0.0025979
570	326	2.75587	2.51322	6.9261132	7.594846	6.31626	2.46597	0.04725	0.0022322
620	312	2.79239	2.49415	6.9646566	7.797451	6.22081	2.4759	0.01825	0.0003331
720	335	2.85733	2.52504	7.2148926	8.164349	6.37585	2.49357	0.03148	0.0009909
820	358	2.91381	2.55388	7.4415397	8.490311	6.52232	2.50893	0.04495	0.0020209
920	379	2.96379	2.57864	7.6425395	8.784038	6.64938	2.52252	0.05612	0.0031493
1020	382	3.0086	2.58206	7.7683963	9.051675	6.66705	2.53471	0.04735	0.0022425
1220	313	3.08636	2.49554	7.7021478	9.525617	6.22774	2.55586	-0.0603	0.0036377
1270	326	3.1038	2.51322	7.8005341	9.633598	6.31626	2.5606	-0.0474	0.0022453
1320	337	3.12057	2.52763	7.887656	9.737982	6.38891	2.56516	-0.0375	0.0014088
1370	348	3.13672	2.54158	7.9722239	9.839016	6.45963	2.56956	-0.028	0.0007827
1420	355	3.15229	2.55023	8.0390551	9.936922	6.50366	2.57379	-0.0236	0.0005551
Σ 12600	4759	42.9056	37.4159	107.2857	123.6900	93.4301			0.0288346
Avrg.=		2.8604	2.49439						
n=	15								
β=	0.27198		s^2y	0.0071524					
α=	1.71641		s^2y|x	0.002218					
			r^2	0.6898894					

2. K-σ_3 model

$M_r = k_1 \sigma_3^{k_2}$

Regression eqn: $\log M_r = \log k_1 + k_2 \log \sigma_3$

A1.2 Computational Tableau for Mr vs confining stress

σ_3	Mr (MPa)	Log σ_3 x_i	Log Mr y_i	$x_i y_i$	x_i^2	y_i^2	$y_i' = \alpha+\beta x_i$	y_i-y_i'	$(y_i-y')_i^2$
50	195	1.69897	2.29003	3.8907001	2.886499	5.24426	2.42741	-0.1374	0.0188708
50	213	1.69897	2.32838	3.9558471	2.886499	5.42135	2.42741	-0.099	0.0098062
50	268	1.69897	2.42813	4.1253282	2.886499	5.89584	2.42741	0.00073	5.314E-07
50	312	1.69897	2.49415	4.2374938	2.886499	6.22081	2.42741	0.06675	0.0044554
50	326	1.69897	2.51322	4.2698813	2.886499	6.31626	2.42741	0.08581	0.0073637
150	312	2.17609	2.49415	5.427508	4.735373	6.22081	2.50379	-0.0096	9.286E-05
150	335	2.17609	2.52504	5.4947279	4.735373	6.37585	2.50379	0.02125	0.0004517
150	358	2.17609	2.55388	5.5574825	4.735373	6.52232	2.50379	0.05009	0.0025092
150	379	2.17609	2.57864	5.6113542	4.735373	6.64938	2.50379	0.07485	0.0056023
150	382	2.17609	2.58206	5.6188055	4.735373	6.66705	2.50379	0.07827	0.0061266
300	313	2.47712	2.49554	6.1817659	6.13613	6.22774	2.55198	-0.0564	0.0031855
300	326	2.47712	2.51322	6.2255447	6.13613	6.31626	2.55198	-0.0388	0.0015029
300	337	2.47712	2.52763	6.2612458	6.13613	6.38891	2.55198	-0.0244	0.0005931
300	348	2.47712	2.54158	6.2958	6.13613	6.45963	2.55198	-0.0104	0.0001083
300	355	2.47712	2.55023	6.3172249	6.13613	6.50366	2.55198	-0.0018	3.084E-06
Σ 2500	4759	31.7609	37.4159	79.4707	68.7900	93.4301			0.0606722
Avrg.=		2.1174	2.49439						
n=	15								
β=	0.1601		s^2y	0.0071524					
α=	2.15541		s^2y|x	0.0046671					
			r^2	0.3474822					

3. Uzan's model

$$M_r = k_1 \Theta^{k_2} \tau_{oct}^{\ k_3}$$

Regression eqn: $\log M_r = \log k_1 + k_2 \log \Theta + k_3 \log \tau_{oct}$

A1.3 Computational Tableau for Mr vs confining/deviator stress: Uzan's model

Θ (kPa)	σ_s (kPa)	τ_{oct} (kPa)	Mr (MPa)	logΘ	logτ_{oct}	logMr							y'	
220	50	40.8	195	2.342	1.611	2.29	0.268	0.546	0.383	0.105	0.15	0.041	2.295	2E-05
270	100	81.7	213	2.431	1.912	2.328	0.184	0.192	0.188	0.071	0.073	0.028	2.368	0.002
370	200	163	267	2.568	2.213	2.427	0.085	0.019	0.04	0.02	0.009	0.004	2.445	3E-04
470	300	245	312	2.672	2.389	2.494	0.035	0.002	-0.007	3E-05	-7E-06	3E-08	2.491	9E-06
570	400	327	326	2.756	2.514	2.514	0.011	0.027	-0.017	-0.002	0.003	4E-04	2.524	1E-04
620	150	122	312	2.792	2.088	2.494	0.005	0.068	0.018	-7E-06	-3E-05	1E-08	2.431	0.004
720	250	204	335	2.857	2.31	2.525	9E-06	0.002	1E-04	-9E-05	-0.001	9E-04	2.485	0.002
820	350	286	358	2.914	2.456	2.553	0.003	0.011	0.006	0.003	0.006	0.004	2.522	0.001
920	450	367	379	2.964	2.565	2.578	0.011	0.046	0.022	0.009	0.018	0.007	2.549	8E-04
1020	550	449	382	3.009	2.652	2.582	0.022	0.092	0.045	0.013	0.027	0.008	2.572	1E-04
1220	300	245	313	3.086	2.389	2.495	0.051	0.002	0.009	2E-04	3E-05	6E-07	2.517	5E-04
1270	350	286	326	3.104	2.456	2.513	0.059	0.011	0.026	0.005	0.002	3E-04	2.534	4E-04
1320	400	327	337	3.121	2.514	2.527	0.068	0.027	0.043	0.009	0.005	0.001	2.548	4E-04
1370	450	367	348	3.137	2.565	2.542	0.076	0.046	0.06	0.013	0.01	0.002	2.56	3E-04
1420	500	408	355	3.152	2.611	2.55	0.085	0.068	0.076	0.016	0.015	0.003	2.572	5E-04
				42.91	35.25	37.41	0.964	1.159	0.89	0.262	0.318	0.1	37.41	0.012
				2.86	2.35	2.494								
n=	15			0.964	b1	0.89	b2	0.262						
m=	2			0.89	b1	1.159	b2	0.318						
				b1	0.064		sy^2	0.007		r^2	0.863			
				b2	0.225		sy|x^2	1E-03						
				b0	1.782									

$0.964\beta_1 + 0.89\beta_2 = 0.262$
$0.89\beta_1 + 1.159\beta_2 = 0.318$

A2. Regression analysis results for deformation model

$\varepsilon_p = a_i + b_i \log N$ $\quad a_i, b_i = f\{\text{failure factor F}\}$

A2.1 Computational Tableau for Curve 1: $\sigma_{dev} = 200$ kPa, F = 0.31

Deform. (mm)	ε_p (%) y_i	Load rep. (N)	LogN x_i	$x_i y_i$	x_i^2	y_i^2	$y_i' = \alpha+\beta x_i$	$y_i - y_i'$	$(y_i-y')_i^2$
0	0.0000	100	2	0	4	0	-0.0082	0.00824	6.79204E-05
0.029	0.0104	500	2.69897	0.02795	7.28444	0.00011	0.00958	0.00078	6.04051E-07
0.039	0.0139	1000	3	0.04179	9	0.00019	0.01726	-0.0033	1.10662E-05
0.059	0.0211	2000	3.30103	0.06956	10.8968	0.00044	0.02493	-0.0039	1.48916E-05
0.068	0.0243	3000	3.47712	0.08444	12.0904	0.00059	0.02942	-0.0051	2.6362E-05
0.088	0.0314	5000	3.69897	0.11625	13.6824	0.00099	0.03508	-0.0036	1.33072E-05
0.117	0.0418	10000	4	0.16714	16	0.00175	0.04275	-0.001	9.33141E-07
0.137	0.0489	20000	4.30103	0.21044	18.4989	0.00239	0.05043	-0.0015	2.24508E-06
0.156	0.0557	30000	4.47712	0.24944	20.0446	0.0031	0.05492	0.0008	6.36222E-07
0.176	0.0629	50000	4.69897	0.29536	22.0803	0.00395	0.06057	0.00228	5.21718E-06
0.186	0.0664	75000	4.87506	0.32384	23.7662	0.00441	0.06506	0.00137	1.86548E-06
0.205	0.0732	100000	5	0.36607	25	0.00536	0.06825	0.00497	2.46615E-05
Σ =1.26	0.4500	296600	45.5283	1.9523	182.344	0.02329			0.0016971
Avrg.	0.0375		3.79402						
n	12								
β	0.0255		s^2_y	0.00058					
α	-0.0592		$s^2_{y\|x}$	1.7E-05					
			r^2	0.9709					

A2.2 Computational Tableau for Curve 2: $\sigma_{dev} = 300$ kPa, S.F. = 0.47

Deform. (mm)	ε_p (%) y_i	Load rep. (N)	LogN x_i	$x_i y_i$	x_i^2	y_i^2	$y_i' = \alpha+\beta x_i$	$y_i - y_i'$	$(y_i-y')_i^2$
0	0.0000	100	2	0	4	0	0.0122	-0.0122	0.000148853
0.156	0.0557	500	2.69897	0.15037	7.28444	0.0031	0.05749	-0.0018	3.16547E-06
0.224	0.0800	1000	3	0.24	9	0.0064	0.077	0.003	8.9996E-06
0.283	0.1011	2000	3.30103	0.33364	10.8968	0.01022	0.09651	0.00456	2.0837E-05
0.332	0.1186	3000	3.47712	0.41229	12.0904	0.01406	0.10792	0.01065	0.00011351
0.361	0.1289	5000	3.69897	0.4769	13.6824	0.01662	0.12229	0.00664	4.40308E-05
0.41	0.1464	10000	4	0.58571	16	0.02144	0.1418	0.00463	2.14273E-05
0.459	0.1639	20000	4.30103	0.70506	18.4989	0.02687	0.16131	0.00262	6.87676E-06
0.469	0.1675	30000	4.47712	0.74992	20.0446	0.02806	0.17272	-0.0052	2.72155E-05
0.508	0.1814	50000	4.69897	0.85253	22.0803	0.03292	0.18709	-0.0057	3.20806E-05
0.557	0.1989	75000	4.87506	0.96979	23.7662	0.03957	0.1985	0.00043	1.80962E-07
0.557	0.1989	100000	5	0.99464	25	0.03957	0.2066	-0.0077	5.88378E-05
Σ=4.316	1.5414	296600	45.5283	6.47085	182.344	0.23883			0.000486015
Avrg.	0.1285		3.79402						
N	12								
β	0.0648		s^2_y	0.00371					
α	-0.1174		$s^2_{y\|x}$	4.9E-05					
			r^2	0.98691					

A2.3 Computational Tableau for Curve 3: σ_{dev} = 400 kPa, S.F. = 0.63

Deform. (mm)	ε_p (%) y_i	Load rep. (N)	LogN x_i	$x_i y_i$	x_i^2	y_i^2	$y_i' = \alpha+\beta x_i$	y_i-y_i'	$(y_i-y')_i^2$
0	0.0000	100	2	0	4	0	0.00199	-0.002	3.94066E-06
0.518	0.1850	500	2.69897	0.49931	7.28444	0.03423	0.18027	0.00473	2.23857E-05
0.716	0.2557	1000	3	0.76714	9	0.06539	0.25705	-0.0013	1.78732E-06
1	0.3571	2500	3.39794	1.21355	11.546	0.12755	0.35855	-0.0014	1.98622E-06
Σ=2.234	0.7979	4100	11.0969	2.48	31.8304	0.22717			3.00999E-05
Avrg.	0.1995		2.77423						
N	4								
β	0.2550		s^2_y	0.02267					
α	-0.5081		$s^2_{y\|x}$	3E-06					
			r^2	0.99987					

Relationship between constant b in permanent deformation model and failure factor F.

$b = c10^{d*F}$ where c,d = constants

Regression eqn: logb = logc + d*F

A2.4 Computational Tableau for Curve1/Curve2/Curve3 to obtain conts. c and d

b_i	$Logb_i$ y_i		F x_i	$x_i y_i$	x_i^2	y_i^2	$y_i' = \alpha+\beta x_i$	y_i-y_i'	$(y_i-y')_i^2$
0.0255	-1.5935		0.35335	-0.5631	0.12486	2.5393	-1.6097	0.01622	0.000263082
0.0648	-1.1884		0.49469	-0.5879	0.24472	1.41236	-1.156	-0.0324	0.001052326
0.20605	-0.686		0.63603	-0.4363	0.40453	0.47062	-0.7022	0.01622	0.000263082
Σ=0.296	-3.4680	0	1.48407	-1.5873	0.77411	4.42228			0.001578489
Avrg.	-1.1560		0.49469						
n	3								
β	3.21035		s^2_y	0.20668					
α	-2.7441		$s^2_{y\|x}$	0.00016					
			r^2	0.99924					

APPENDIX B

Stress-strain analysis results

Full stress-strain analysis results for the model pavement design in Chapter 7. Results from Elsym5 and Kenlayer analysis program are presented.

Details of pavement structure used in analysis:

Traffic loading
Tyre load: 40 kN, dual wheel at 350 mm spacing Tyre pressure: 520 kPa
Base, 150mm
γ = 2210 kg/m3 Elsym5: Average Mr = 340 MPa Kenlayer: K-Θ model, k_1 = 60 MPa , k_2 = 0.272, ν = 0.35
Subbase, 150mm
γ = 21600 kg/m3 Elsym5: Average Mr = 280 MPa Kenlayer: K-Θ model, k_1 = 42 MPa , k_2 = 0.272, ν = 0.35
Subgrade Linear elastic, Mr = 100 Mpa

Orientation of dual wheel to co-ordinate axis.

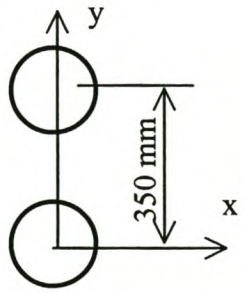

B1. Elsym5 Results.

S1, S2, S3 = principal stresses

P1, P2, P3 = principal strains

Sign convention {tension negative, compression positive}

Depth (mm)	Xout (mm)	Yout (mm)	S1	S2	S3	Vertical displ. (mm)	P1	P2	P3
1	0	0	5.70E+02	5.29E+02	5.20E+02	6.69E-01	5.97E-04	4.35E-04	3.98E-04
1	0	175	1.83E+02	1.33E+01	5.13E+00	5.38E-01	5.18E-04	-1.54E-04	-1.87E-04
1	0	525	1.03E+02	5.06E+00	-3.66E+00	3.78E-01	3.01E-04	-8.72E-05	-1.22E-04
1	0	700	3.02E+01	-1.26E+00	-2.35E+01	2.41E-01	1.14E-04	-1.07E-05	-9.88E-05
1	0	875	1.56E+01	3.68E+00	-1.33E+01	1.74E-01	5.58E-05	8.51E-06	-5.90E-05
1	0	1050	6.66E+00	-9.47E-01	-1.11E+01	1.35E-01	3.20E-05	1.74E-06	-3.84E-05
40	0	0	4.89E+02	2.78E+02	2.62E+02	6.43E-01	8.82E-04	4.44E-05	-1.87E-05
40	0	175	1.55E+02	1.05E+02	2.24E+01	5.47E-01	3.25E-04	1.27E-04	-2.02E-04
40	0	525	9.98E+01	6.06E+01	-1.44E+01	3.83E-01	2.46E-04	9.03E-05	-2.08E-04
40	0	700	2.21E+01	5.27E+00	-5.64E+00	2.41E-01	6.53E-05	-1.43E-06	-4.47E-05
40	0	875	1.07E+01	5.36E-01	-6.20E+00	1.74E-01	3.72E-05	-3.03E-06	-2.98E-05
40	0	1050	6.23E+00	6.46E-02	-4.89E+00	1.35E-01	2.33E-05	-1.20E-06	-2.09E-05
80	0	0	3.84E+02	9.16E+01	8.64E+01	6.05E-01	9.47E-04	-2.15E-04	-2.36E-04
80	0	175	1.46E+02	7.68E+01	3.62E+01	5.51E-01	3.12E-04	3.87E-05	-1.23E-04
80	0	525	1.40E+02	2.37E+01	-2.42E+01	3.85E-01	4.12E-04	-4.95E-05	-2.40E-04
80	0	700	2.23E+01	1.34E+01	-2.62E+00	2.42E-01	5.44E-05	1.91E-05	-4.44E-05
80	0	875	7.94E+00	4.93E+00	-4.37E-01	1.74E-01	1.87E-05	6.77E-06	-1.45E-05
80	0	1050	5.16E+00	8.16E-01	-1.59E-01	1.35E-01	1.45E-05	-2.75E-06	-6.61E-06
120	0	0	2.65E+02	-1.63E+01	-3.93E+01	5.69E-01	8.35E-04	-2.80E-04	-3.71E-04
120	0	175	1.10E+02	9.07E+01	-2.99E+01	5.44E-01	2.60E-04	1.85E-04	-2.94E-04
120	0	525	1.32E+02	-1.16E+01	-2.00E+01	3.82E-01	4.22E-04	-1.50E-04	-1.83E-04
120	0	700	3.78E+01	5.17E+00	-3.36E-01	2.43E-01	1.06E-04	-2.33E-05	-4.52E-05
120	0	875	1.41E+01	5.34E+00	1.17E-01	1.74E-01	3.59E-05	1.04E-06	-1.97E-05
120	0	1050	5.95E+00	4.11E+00	4.94E-02	1.35E-01	1.32E-05	5.91E-06	-1.02E-05
150	0	0	2.01E+02	-9.96E+01	-1.35E+02	5.45E-01	8.33E-04	-3.61E-04	-5.02E-04
150	0	175	1.17E+02	6.46E+01	-8.29E+01	5.35E-01	3.62E-04	1.55E-04	-4.30E-04
150	0	525	1.10E+02	-1.65E+00	-3.96E+01	3.78E-01	3.65E-04	-7.69E-05	-2.28E-04
150	0	700	4.81E+01	1.68E+00	-6.33E-01	2.43E-01	1.41E-04	-4.40E-05	-5.32E-05
150	0	875	2.08E+01	3.47E+00	3.94E-01	1.75E-01	5.71E-05	-1.16E-05	-2.38E-05
150	0	1050	9.79E+00	3.35E+00	8.82E-02	1.36E-01	2.52E-05	-3.16E-07	-1.33E-05
151	0	0	2.00E+02	1.52E+01	4.31E-01	5.43E-01	1.30E-03	-3.66E-04	-4.99E-04
151	0	175	1.17E+02	6.28E+01	-1.64E+00	5.34E-01	6.34E-04	1.51E-04	-4.29E-04
151	0	525	1.06E+02	5.05E-01	-6.61E+00	3.77E-01	7.18E-04	-2.28E-04	-2.92E-04
151	0	700	3.26E+01	2.32E+00	-3.00E+00	2.43E-01	2.19E-04	-5.37E-05	-1.02E-04
151	0	875	1.21E+01	2.10E+00	-9.77E-01	1.75E-01	7.79E-05	-1.19E-05	-3.96E-05
151	0	1050	5.19E+00	1.62E+00	-3.43E-01	1.36E-01	3.16E-05	-4.92E-07	-1.82E-05
225	0	0	1.22E+02	1.57E+00	-1.21E+01	4.68E-01	8.40E-04	-2.47E-04	-3.70E-04
225	0	175	1.02E+02	2.15E+01	-1.30E+01	4.85E-01	6.59E-04	-6.40E-05	-3.74E-04

Contd. / Elsym5 Results

Depth (mm)	Xout (mm)	Yout (mm)	S1	S2	S3	Vertical displ. (mm)	P1	P2	P3
225	0	525	8.06E+01	-6.48E+00	-6.78E+00	3.53E-01	5.68E-04	-2.15E-04	-2.18E-04
225	0	700	3.49E+01	-1.25E+00	-2.29E+00	2.41E-01	2.41E-04	-8.43E-05	-9.37E-05
225	0	875	1.59E+01	5.30E-01	-4.21E-01	1.76E-01	1.06E-04	-3.26E-05	-4.12E-05
225	0	1050	8.11E+00	8.97E-01	-1.15E-01	1.36E-01	5.23E-05	-1.27E-05	-2.18E-05
300	0	0	8.25E+01	-1.33E+01	-2.72E+01	4.15E-01	6.45E-04	-2.18E-04	-3.43E-04
300	0	175	8.16E+01	-3.97E+00	-2.80E+01	4.38E-01	6.19E-04	-1.52E-04	-3.68E-04
300	0	525	5.82E+01	-4.98E+00	-1.51E+01	3.29E-01	4.35E-04	-1.34E-04	-2.25E-04
300	0	700	3.28E+01	7.03E-01	-4.61E+00	2.37E-01	2.28E-04	-6.10E-05	-1.09E-04
300	0	875	1.84E+01	5.68E-01	-8.50E-01	1.75E-01	1.23E-04	-3.71E-05	-4.98E-05
300	0	1050	1.06E+01	2.52E-01	1.41E-01	1.37E-01	6.95E-05	-2.33E-05	-2.43E-05
301	0	0	8.26E+01	4.56E+00	-3.65E+00	4.14E-01	8.23E-04	-2.31E-04	-3.42E-04
301	0	175	8.14E+01	1.19E+01	-3.99E+00	4.37E-01	7.86E-04	-1.52E-04	-3.66E-04
301	0	525	5.92E+01	-5.23E-01	-1.86E+00	3.28E-01	6.00E-04	-2.06E-04	-2.24E-04
301	0	700	3.13E+01	-1.95E-01	-7.59E-01	2.37E-01	3.16E-04	-1.09E-04	-1.16E-04
301	0	875	1.60E+01	4.06E-01	-5.48E-01	1.75E-01	1.60E-04	-4.99E-05	-6.28E-05
301	0	1050	8.56E+00	5.16E-01	-4.14E-01	1.37E-01	8.53E-05	-2.34E-05	-3.59E-05
600	0	0	3.34E+01	7.26E-02	-1.59E+00	2.64E-01	3.39E-04	-1.11E-04	-1.33E-04
600	0	175	-3.54E+01	3.74E-01	-1.77E+00	2.75E-01	3.59E-04	-1.14E-04	-1.43E-04
600	0	525	2.79E+01	-4.21E-01	-1.21E+00	2.34E-01	2.84E-04	-9.75E-05	-1.08E-04
600	0	700	2.07E+01	-5.93E-01	-7.36E-01	1.97E-01	2.12E-04	-7.59E-05	-7.79E-05
600	0	875	1.44E+01	-3.58E-01	-5.47E-01	1.62E-01	1.47E-04	-5.21E-05	-5.46E-05
600	0	1050	9.74E+00	-1.18E-01	-4.42E-01	1.33E-01	9.94E-05	-3.37E-05	-3.81E-05

B2. Kenlayer Results.

S1, S2, S3 = principal stresses

P1, P2, P3 = principal strains

Sign convention {tension negative, compression positive}

Depth (m)	Yout (m)	Vert. displ. (m)	Vert. stress (kPa)	S1	S2	S3	Vert. strain	P1	P2	P3
0.001	0	6.62E-04	5.34E+02	6.56E+02	6.08E+02	5.34E+02	2.08E-04	5.84E-04	2.08E-04	4.36E-04
0.025	0	6.53E-04	5.06E+02	5.06E+02	3.92E+02	3.65E+02	5.49E-04	5.49E-04	1.15E-04	1.15E-04
0.05	0	6.35E-04	4.60E+02	4.60E+02	1.83E+02	1.76E+02	8.43E-04	8.44E-04	-1.24E-04	-1.23E-04
0.075	0	6.11E-04	3.89E+02	3.90E+02	6.92E+01	6.22E+01	9.69E-04	9.70E-04	-2.78E-04	-2.78E-04
0.1	0	5.85E-04	3.16E+02	3.16E+02	1.47E+01	-1.44E+00	9.83E-04	9.85E-04	-3.71E-04	-3.71E-04
0.125	0	5.60E-04	2.52E+02	2.52E+02	-1.37E+01	-3.53E+01	9.48E-04	9.52E-04	-4.20E-04	-4.20E-04
0.15	0	5.37E-04	2.03E+02	2.04E+02	-4.14E+01	-6.70E+01	9.11E-04	9.16E-04	-4.69E-04	-4.69E-04
0.151	0	5.36E-04	2.02E+02	2.03E+02	9.69E+00	-6.50E+00	1.16E-03	1.17E-03	-4.68E-04	-4.68E-04
0.2	0	4.87E-04	1.40E+02	1.42E+02	-4.93E+00	-2.18E+01	8.62E-04	8.76E-04	-4.04E-04	-4.04E-04
0.25	0	4.47E-04	1.03E+02	1.05E+02	-7.88E+00	-2.25E+01	7.14E-04	7.32E-04	-3.58E-04	-3.58E-04
0.3	0	4.13E-04	7.98E+01	8.16E+01	-1.28E+01	-2.63E+01	6.35E-04	6.52E-04	-3.45E-04	-3.45E-04
0.301	0	4.12E-04	7.95E+01	8.17E+01	3.85E+00	-4.39E+00	7.89E-04	8.19E-04	-3.43E-04	-3.43E-04
0.4	0	3.47E-04	5.53E+01	5.72E+01	1.76E+00	-2.94E+00	5.50E-04	5.76E-04	-2.36E-04	-2.36E-04
0.5	0	2.99E-04	4.11E+01	4.26E+01	5.61E-01	-2.16E+00	4.12E-04	4.32E-04	-1.73E-04	-1.73E-04
0.6	0	2.63E-04	3.19E+01	3.30E+01	-3.02E-02	-1.67E+00	3.22E-04	3.36E-04	-1.32E-04	-1.32E-04
0.001	0.175	5.38E-04	-7.62E+00	2.11E+02	-7.62E+00	-1.04E+01	-1.77E-04	4.94E-04	-1.85E-04	-1.85E-04
0.025	0.175	5.43E-04	9.90E+00	1.51E+02	1.38E+02	9.90E+00	-2.08E-04	2.26E-04	-2.08E-04	1.87E-04
0.05	0.175	5.47E-04	4.31E+01	1.84E+02	8.17E+01	4.31E+01	-1.26E-04	3.55E-04	-1.26E-04	5.65E-06
0.075	0.175	5.49E-04	7.83E+01	1.63E+02	7.83E+01	3.08E+01	2.97E-05	3.52E-04	-1.52E-04	-1.52E-04
0.1	0.175	5.45E-04	1.02E+02	1.23E+02	1.02E+02	-3.57E+00	1.90E-04	2.80E-04	-2.60E-04	-2.60E-04
0.125	0.175	5.39E-04	1.14E+02	1.14E+02	8.58E+01	-2.58E+01	3.27E-04	3.27E-04	-3.37E-04	-3.37E-04
0.15	0.175	5.29E-04	1.16E+02	1.16E+02	6.10E+01	-4.51E+01	4.19E-04	4.19E-04	-4.06E-04	-4.06E-04
0.151	0.175	5.28E-04	1.16E+02	1.16E+02	6.07E+01	-8.20E+00	5.66E-04	5.66E-04	-4.06E-04	-4.06E-04
0.2	0.175	4.99E-04	1.08E+02	1.08E+02	2.73E+01	-2.10E+01	6.10E-04	6.10E-04	-3.94E-04	-3.94E-04
0.25	0.175	4.67E-04	9.39E+01	9.39E+01	7.83E+00	-2.33E+01	6.31E-04	6.31E-04	-3.74E-04	-3.74E-04
0.3	0.175	4.35E-04	8.08E+01	8.08E+01	-3.73E+00	-2.71E+01	6.26E-04	6.26E-04	-3.70E-04	-3.70E-04
0.301	0.175	4.34E-04	8.05E+01	8.05E+01	1.11E+01	-4.79E+00	7.83E-04	7.83E-04	-3.68E-04	-3.68E-04
0.4	0.175	3.66E-04	6.00E+01	6.00E+01	4.04E+00	-3.30E+00	5.97E-04	5.97E-04	-2.57E-04	-2.57E-04
0.5	0.175	3.14E-04	4.52E+01	4.52E+01	1.35E+00	-2.40E+00	4.56E-04	4.56E-04	-1.87E-04	-1.87E-04
0.6	0.175	2.74E-04	3.49E+01	3.49E+01	2.66E-01	-1.83E+00	3.55E-04	3.55E-04	-1.42E-04	-1.42E-04
0.001	0.525	3.79E-04	-2.85E+00	1.19E+02	-2.71E+00	-1.74E+01	-8.74E-05	2.87E-04	-1.32E-04	-1.32E-04
0.025	0.525	3.81E-04	5.03E+00	8.66E+01	7.71E+01	-9.30E+00	-1.08E-04	1.43E-04	-1.52E-04	6.98E-05
0.05	0.525	3.83E-04	2.18E+01	1.29E+02	4.92E+01	-1.55E+01	-6.96E-05	2.96E-04	-1.97E-04	2.38E-05
0.075	0.525	3.84E-04	3.97E+01	1.44E+02	2.13E+01	-1.80E+01	6.19E-06	4.02E-04	-2.14E-04	-6.39E-05
0.1	0.525	3.83E-04	5.19E+01	1.39E+02	2.25E+00	-1.80E+01	8.52E-05	4.57E-04	-2.13E-04	-1.27E-04
0.125	0.525	3.80E-04	5.82E+01	1.27E+02	-1.04E+01	-1.56E+01	1.53E-04	4.79E-04	-1.99E-04	-1.74E-04
0.15	0.525	3.75E-04	6.01E+01	1.11E+02	-8.82E+00	-2.12E+01	2.00E-04	4.60E-04	-2.16E-04	-2.16E-04
0.151	0.525	3.75E-04	6.01E+01	1.09E+02	-2.84E+00	-1.08E+01	2.75E-04	6.59E-04	-2.78E-04	-2.16E-04
0.2	0.525	3.61E-04	5.69E+01	8.93E+01	-9.22E+00	-1.03E+01	3.03E-04	5.56E-04	-2.22E-04	-2.22E-04

Contd. / Kenlayer Results

Depth (m)	Yout (m)	Vert. displ. (m)	Vert. stress (kPa)	S1	S2	S3	Vert. strain	P1	P2	P3
0.25	0.35	3.44E-04	5.10E+01	7.21E+01	-7.59E+00	-1.22E+01	3.21E-04	5.02E-04	-2.21E-04	-2.21E-04
0.3	0.525	3.28E-04	4.53E+01	5.79E+01	-5.09E+00	-1.46E+01	3.27E-04	4.43E-04	-2.26E-04	-2.26E-04
0.301	0.525	3.27E-04	4.52E+01	5.88E+01	-8.89E-01	-2.29E+00	4.15E-04	6.00E-04	-2.26E-04	-2.26E-04
0.4	0.525	2.90E-04	3.60E+01	4.42E+01	-4.60E-01	-1.81E+00	3.40E-04	4.50E-04	-1.71E-04	-1.71E-04
0.5	0.525	2.59E-04	2.91E+01	3.44E+01	-4.22E-01	-1.49E+00	2.79E-04	3.51E-04	-1.34E-04	-1.34E-04
0.6	0.525	2.34E-04	2.40E+01	2.76E+01	-4.61E-01	-1.25E+00	2.33E-04	2.82E-04	-1.07E-04	-1.07E-04
0.001	0.7	2.41E-04	2.07E+00	3.91E+01	2.07E+00	-2.39E+01	-7.40E-06	1.06E-04	-8.72E-05	-8.72E-05
0.025	0.7	2.41E-04	3.83E-01	3.10E+01	1.80E+00	-8.89E+00	-1.79E-05	7.61E-05	-4.63E-05	-4.20E-05
0.05	0.7	2.42E-04	1.28E+00	2.16E+01	1.28E+01	-3.47E+00	-2.30E-05	4.62E-05	-3.92E-05	1.82E-07
0.075	0.7	2.42E-04	2.78E+00	2.41E+01	1.39E+01	-2.78E+00	-2.42E-05	5.70E-05	-4.54E-05	1.83E-05
0.1	0.7	2.43E-04	4.64E+00	3.19E+01	7.99E+00	-2.36E+00	-2.18E-05	9.47E-05	-5.16E-05	-7.44E-06
0.125	0.7	2.43E-04	6.66E+00	3.68E+01	3.56E+00	-1.80E+00	-1.59E-05	1.28E-04	-5.62E-05	-3.07E-05
0.15	0.7	2.44E-04	8.62E+00	4.06E+01	1.83E-01	-9.49E-01	-8.71E-06	1.55E-04	-5.76E-05	-5.19E-05
0.151	0.7	2.44E-04	8.70E+00	3.41E+01	1.65E+00	-3.43E+00	2.55E-06	2.01E-04	-9.21E-05	-5.24E-05
0.2	0.7	2.43E-04	1.21E+01	3.63E+01	-1.51E+00	-2.34E+00	2.87E-05	2.18E-04	-8.39E-05	-7.75E-05
0.25	0.7	2.41E-04	1.47E+01	3.50E+01	-1.25E+00	-3.28E+00	5.79E-05	2.32E-04	-9.59E-05	-9.59E-05
0.3	0.7	2.37E-04	1.62E+01	3.27E+01	5.29E-01	-4.50E+00	8.04E-05	2.33E-04	-1.10E-04	-1.10E-04
0.301	0.7	2.37E-04	1.62E+01	3.14E+01	-3.40E-01	-8.09E-01	1.13E-04	3.18E-04	-1.17E-04	-1.10E-04
0.4	0.7	2.25E-04	1.69E+01	2.78E+01	-6.53E-01	-7.34E-01	1.36E-04	2.83E-04	-1.02E-04	-1.01E-04
0.5	0.7	2.11E-04	1.62E+01	2.40E+01	-6.55E-01	-7.51E-01	1.40E-04	2.45E-04	-8.93E-05	-8.93E-05
0.6	0.7	1.97E-04	1.50E+01	2.06E+01	-5.97E-01	-7.52E-01	1.35E-04	2.11E-04	-7.76E-05	-7.76E-05
0.001	0.875	1.75E-04	-2.63E-02	1.69E+01	-2.63E-02	-1.83E+01	1.06E-06	5.32E-05	-5.52E-05	-5.52E-05
0.025	0.825	1.75E-04	-5.42E-02	1.48E+01	-1.17E-02	-1.01E+01	-3.93E-06	4.18E-05	-3.48E-05	-3.47E-05
0.05	0.825	1.75E-04	2.57E-01	1.14E+01	1.06E+00	-2.71E+00	-7.72E-06	3.02E-05	-1.78E-05	-1.51E-05
0.075	0.825	1.75E-04	5.90E-01	8.43E+00	5.64E+00	-6.95E-01	-1.10E-05	1.89E-05	-1.59E-05	3.38E-06
0.1	0.825	1.75E-04	1.02E+00	1.03E+01	6.01E+00	-3.68E-01	-1.33E-05	2.63E-05	-1.92E-05	8.05E-06
0.125	0.825	1.76E-04	1.54E+00	1.38E+01	4.11E+00	-1.88E-01	-1.45E-05	4.38E-05	-2.28E-05	-2.27E-06
0.15	0.825	1.76E-04	2.12E+00	1.68E+01	2.70E+00	-6.54E-04	-1.50E-05	6.00E-05	-2.58E-05	-1.20E-05
0.151	0.825	1.76E-04	2.14E+00	1.30E+01	2.13E+00	-7.60E-01	-1.23E-05	7.22E-05	-3.49E-05	-1.24E-05
0.2	0.825	1.77E-04	3.36E+00	1.62E+01	8.11E-01	-2.63E-01	-7.64E-06	9.25E-05	-3.59E-05	-2.75E-05
0.25	0.825	1.77E-04	4.57E+00	1.76E+01	1.14E-01	-1.76E-01	3.13E-07	1.12E-04	-4.04E-05	-4.04E-05
0.3	0.825	1.76E-04	5.61E+00	1.83E+01	5.48E-01	-8.39E-01	8.64E-06	1.26E-04	-5.09E-05	-5.09E-05
0.301	0.825	1.76E-04	5.63E+00	1.62E+01	3.75E-01	-5.03E-01	1.99E-05	1.62E-04	-6.29E-05	-5.10E-05
0.4	0.825	1.73E-04	7.14E+00	1.63E+01	-2.69E-02	-5.62E-01	4.13E-05	1.65E-04	-6.26E-05	-5.54E-05
0.5	0.825	1.68E-04	8.02E+00	1.56E+01	-2.51E-01	-5.62E-01	5.67E-05	1.58E-04	-5.92E-05	-5.50E-05
0.6	0.825	1.62E-04	8.36E+00	1.44E+01	-3.65E-01	-5.36E-01	6.57E-05	1.47E-04	-5.45E-05	-5.21E-05
0.001	1.050	1.36E-04	1.46E+00	1.03E+01	1.46E+00	-1.10E+01	3.87E-06	3.10E-05	-3.44E-05	-3.44E-05
0.025	1.050	1.36E-04	2.15E-01	8.59E+00	2.15E-01	-7.95E+00	-1.76E-08	2.57E-05	-2.51E-05	-2.51E-05
0.05	1.050	1.36E-04	7.97E-02	6.92E+00	1.06E-01	-3.16E+00	-3.14E-06	2.02E-05	-1.42E-05	-1.41E-05
0.075	1.050	1.36E-04	1.53E-01	5.48E+00	1.06E+00	-3.00E-01	-5.59E-06	1.47E-05	-7.31E-06	-3.84E-06
0.1	1.050	1.36E-04	2.76E-01	4.27E+00	3.78E+00	-4.67E-02	-7.68E-06	9.36E-06	-9.06E-06	5.92E-06
0.125	1.050	1.36E-04	4.37E-01	6.00E+00	3.29E+00	1.70E-02	-9.41E-06	1.71E-05	-1.14E-05	4.17E-06
0.15	1.050	1.37E-04	6.28E-01	7.93E+00	2.57E+00	6.46E-02	-1.08E-05	2.66E-05	-1.37E-05	-8.54E-07
0.151	1.050	1.37E-04	6.36E-01	5.80E+00	1.79E+00	-1.72E-01	-1.00E-05	3.03E-05	-1.64E-05	-1.04E-06
0.2	1.050	1.37E-04	1.08E+00	8.17E+00	1.19E+00	-2.40E-03	-1.05E-05	4.48E-05	-1.90E-05	-9.64E-06
0.25	1.050	1.38E-04	1.58E+00	9.55E+00	6.33E-01	8.76E-02	-9.31E-06	5.90E-05	-2.21E-05	-1.74E-05
0.3	1.050	1.38E-04	2.08E+00	1.06E+01	2.39E-01	1.58E-01	-7.06E-06	7.14E-05	-2.48E-05	-2.41E-05

APPENDIX C

Specifications

C1.1 AASHTO criteria for Base and Subbase courses: (43)

	Base
Plasticity index	<6
Liquid limit	<25
Los Angeles abrasion loss	<50 %
Percent passing 0.075 mm sieve	<67 % passing 0.425 mm sieve

Sieve size mm	-Percent by weight passing-					
	Grade A	Grade B	Grade C	Grade D	Grade E	Grade F
50	100	100	-	-	-	-
25	-	75-95	100	100	100	100
9.5	30-60	40-75	50-85	60-100	-	-
No. 4 (4.75)	25-55	30-60	35-65	50-85	55-100	70-100
No. 10 (2.00)	15-40	20-45	25-50	40-70	40-100	55-100
No. 40 (0.425)	8-20	15-30	15-30	25-45	20-50	30-70
No. 200 (0.075)	2-8	5-20	5-15	5-20	6-20	8-25

C1.2 Brazilian National Highway Department (DNER) (32)

Criteria	Traffic classification	
	Heavy	Light
CBR	≥80	≥60
Liquid limit	<35	<40
Plasticity index	<10	<12
Los Angeles abrasion loss (%)	<65	<65
Swell from CBR test (%)	<0.2	<0.2

Grain size distributions of soil aggregates for base courses of the DNER are identical to those of AASHTO as shown in Table C1, except the grades E and F soil aggregates are not employed by the DNER.

C1.3 Zambian specifications for gravel base and subbase materials (78)

Sieve size	-Percent by weight passing-			
	Base		Sub-base	
Mm	0/30	0/40	0/40	0/60
75				100
63	100	100	100	95-100
37.5	100	90-100	90-100	75-95
31.5	95-100	80-95	80-95	65-90
25	80-95	- -	- -	- -
16	62-85	52-80	50-80	40-75
8	42-70	35-65	30-67	25-60
4	30-55	26-50	22-55	18-50
2	22-40	20-40	15-45	12-40
1	15-30	15-30	8-35	7-30
0.5	10-23	10-23	6-27	5-25
0.25	7-17	7-17	3-22	2-20
0.125	5-13	5-13	2-16	1-13
0.075	4-10	4-10	0-12	0-10

	Base	Sub-base
California Bearing Ratio (CBR)	>90% at 98% Mod. AASHTO	>25% at 96% Mod. AASHTO

	Base		Sub-base	
Material class	A	B	C	D
Los Angeles Abrasion, Max. %	40	45	45	50
Sodium Sulphate Soundness, Max. %	12	12	20	20
Flakiness Index, Max.	30	30	35	35
Crushing Ratio, Min. %	80	60	30	-
Plasticity Index, Max. %	6	6	8	10

C1.4 Road Note 31, specifications for gravel base and subbase materials (74)

Sieve size	-Percent by weight passing-			
	Nominal maximum size			
mm	37.5mm	20mm	10mm	5mm
37.5	100	- -	- -	- -
20	80-100	100	- -	- -
10	55-80	80-100	100	- -
5	40-60	50-75	80-100	100
2.36	30-50	35-60	50-80	80-100
1.18	- -	- -	40-65	50-80
0.6	15-30	15-35	- -	30-60
0.3	- -	- -	20-40	20-45
0.075	5-15	5-15	10-25	10-25

	Base
Plasticity index	<6
Liquid limit	<25
Linear shrinkage	<4%
California Bearing Ratio	80 @ 100% BS Comp. (2.5kg)

APPENDIX D

Zambian Pavement Design Related Information

A1. Metric road map.

A2. Summarised traffic counts data for the six trunk roads measured in 1995

A3. Typical gravel characteristics: Extract from materials report on rehab. of trunk road T2 between Kafue and Monze, 1999.

A4. Zambian Pavement Design Guide Catalogue

*Information courtesy of Roads department, Lusaka.

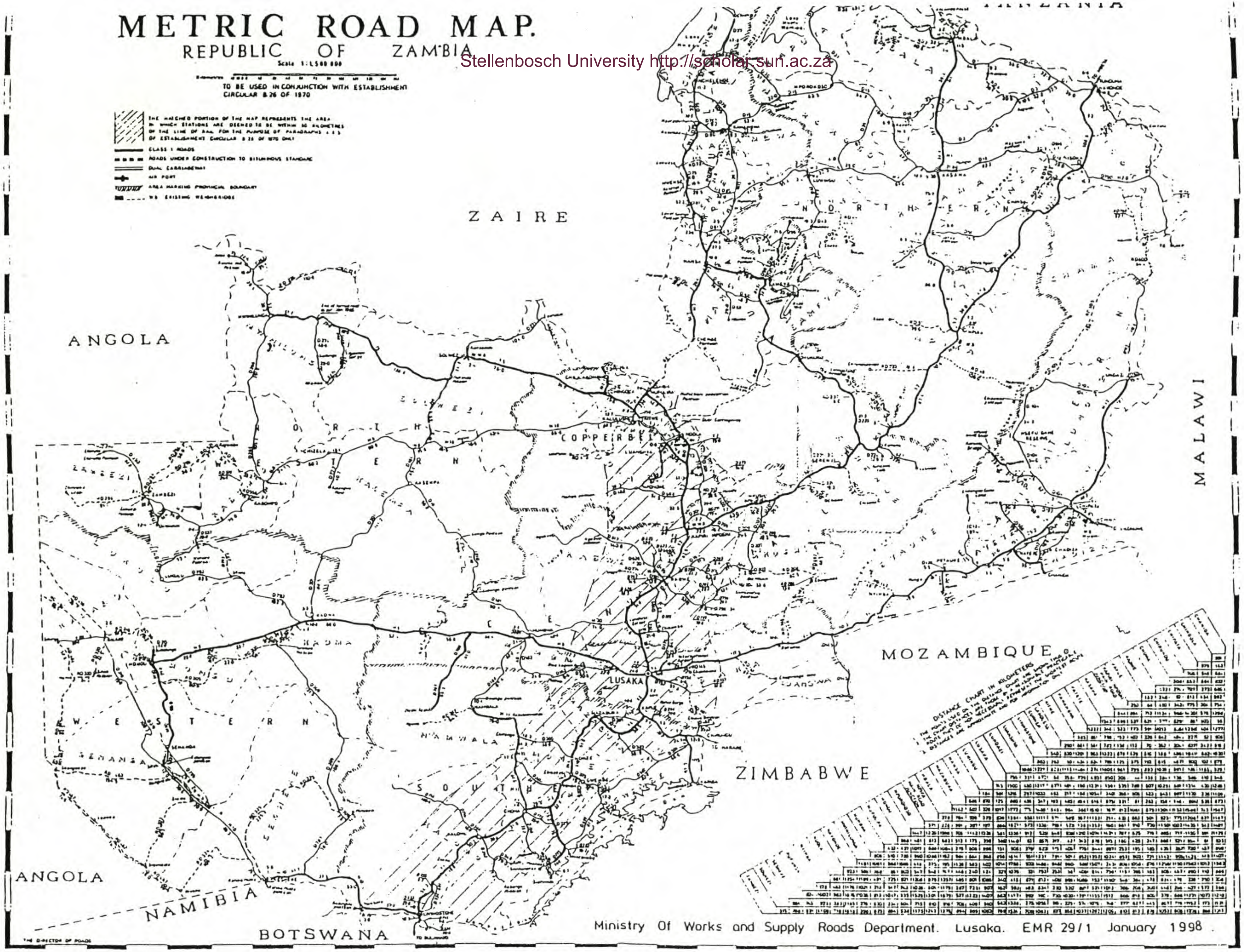

A2. Traffic count data for the six trunk roads.

Traffic Count Data for T_001		Livingstone - T002 Start km 0.000								
Count year 1995						Length = 428.3 km				
Location	STA0000+2.500	STA0000+7.300	STA0000+75 000	STA0000+19 5.000	STA0000+21 5.000	STA0000+28 5.000	STA0000+32 5.000	STA0000+35 3.200	STA0000+41 8.000
	All counts reduced to AADT								
Motorcycle and Scooter	5	10	1	2	2	2	3	5	3
Passenger Car	150	300	100	150	120	130	170	260	210
Micro Bus	30	55	18	25	21	23	26	35	30
Light Delivery Vehicle	120	250	85	125	102	111	155	250	200
Medium Delivery Vehicle	25	50	18	25	20	23	26	35	30
Mini Bus	20	40	13	13	16	17	31	50	45
Big Bus	15	20	9	9	10	11	13	15	15
Rigid Truck (2 axles)	30	50	26	26	29	31	58	85	85
Rigid Truck (3 and 4 axles)	5	10	5	5	5	6	6	5	5
Rigid Truck and Drawbar Trailer	10	15	10	10	11	12	15	18	18
Horse + Semi Trailer (3 & 4 axles)	4	7	4	4	4	5	7	10	10
Horse + Semi Trailer (5 & 6 axles)	15	30	15	15	17	18	39	60	60
Horse + Semi Trailer (7 axles)	0	0	0	0	0	0	0	0	0
Horse + Two Semi Trailers	10	20	10	10	11	12	18	25	25
Other Vehicles	5	10	0	3	0	0	1	4	2

Traffic Count Data for T_002			Chirundu-Nakonde				Start km 0.000					Length = 1147 km		
Count year 1995														
Location	STA0000+13 300	STA0000+53 000	STA0000+81 000	STA0000+95 000	STA0000+12 6.000	STA0000+13 1.000	STA0000+15 0.000	STA0000+20 4.000	STA0000+23 5.000	STA0000+27 2.000	STA0000+34 0.000	STA0000+35 0.135	STA0000417 335	STA0000507 735
						All counts reduced to AADT								
Motorcycle and Scooter	1	2	5	6	20	40	6	1	1	10	5	4	2	1
Passenger Car	106	184	535	731	2360	4800	535	490	457	880	440	125	80	44
Micro Bus	34	47	111	152	435	850	177	82	49	220	110	27	23	13
Light Delivery Vehicle	101	149	409	558	1425	2800	656	513	398	840	422	183	116	61
Medium Delivery Vehicle	11	16	38	53	120	250	180	92	107	200	98	39	20	11
Mini Bus	3	8	62	213	330	500	156	135	123	215	107	11	11	9
Big Bus	20	22	21	41	80	120	105	72	41	160	79	19	19	16
Rigid Truck (2 axles)	10	21	153	205	285	430	330	151	68	250	166	48	40	30
Rigid Truck (3 and 4 axles)	4	12	35	43	45	65	157	37	22	70	47	19	15	13
Rigid Truck and Drawbar Trailer	5	6	17	21	32	50	112	41	38	70	46	15	15	110
Horse + Semi Trailer (3 & 4 axles)	2	7	20	25	21	30	156	24	16	50	33	11	11	7
Horse + Semi Trailer (5 & 6 axles)	79	89	97	120	130	190	357	170	172	210	138	44	44	30
Horse + Semi Trailer (7 axles)	2	2	2	2	20	30	10	6	0	5	0	0	0	0
Horse + Two Semi Trailers	23	26	44	54	46	70	195	77	19	125	82	17	17	11
Other Vehicles	4	0	4	1	13	25	6	2	2	10	6	6	6	4

Traffic Count Data for T_003		Kapiri-Kasumbalesa Start km 0.000												
Count year 1995						Length = 263.4 km								
Location	STA0000+0.500	STA0000+79 500	STA0000+80 500	STA0000+10 5.000	STA0000+12 9.000	STA0000+13 2.000	STA0000+17 1.000	STA0000+18 5.000	STA0000+18 8.000	STA0000+21 7.000	STA0000+24 3.000	STA0000+24 4.000	STA0000257 000
	All counts reduced to AADT												
Motorcycle and Scooter	10	2	4	4	1	1	4	4	3	6	18	27	4
Passenger Car	390	472	398	1450	367	286	1140	590	536	1070	351	520	200
Micro Bus	58	65	45	240	61	75	300	140	127	250	183	270	24
Light Delivery Vehicle	380	408	336	1130	284	295	1180	570	519	1030	342	510	96
Medium Delivery Vehicle	72	54	29	90	22.5	91.5	360	65	52	100	159	230	33
Mini Bus	80	92	58	380	127	129	380	220	187	280	157	190	11
Big Bus	52	44	25	65	21.5	57	170	60	50	75	80	100	80
Rigid Truck (2 axles)	122	132	98	310	104	139	415	190	167	250	159	200	85
Rigid Truck (3 and 4 axles)	32	35	10	60	20	54	160	30	26	40	79	100	5
Rigid Truck and Drawbar Trailer	46	51	42	35	11.5	34.5	100	8	3	5	81	100	5
Horse + Semi Trailer (3 & 4 axles)	36	26	15	40	13.5	45.5	130	20	14	20	55	70	9
Horse + Semi Trailer (5 & 6 axles)	158	146	100	190	64	110	330	145	125	180	115	140	140
Horse + Semi Trailer (7 axles)	8	15	1	15	5	8	20	3	2	3	10	13	3
Horse + Two Semi Trailers	54	56	19	90	29.5	95.5	280	35	30	45	87	110	48
Other Vehicles	8	3	1	4	1	0.5	2	1	0	1	8	12	2

Traffic Count Data for T_004		Lusaka-Chipata				Start km 0.000		
Count year 1995						Length = 593 km		
Location	STA0000+44.000	STA0000+100.000	STA0000+187.000	STA0000+345.000	STA0000+435.000	STA0000+550.000	STA0000+567.000	STA0000+585.000
	All counts reduced to AADT							
Motorcycle and Scooter	18	0	0	0	0	0	0	0
Passenger Car	197	60	68	68	68	68	140	85
Micro Bus	42	18	7	7	7	7	15	9
Light Delivery Vehicle	198	59	42	42	42	42	85	50
Medium Delivery Vehicle	21	4	9	9	9	9	15	11
Mini Bus	115	31	27	27	27	27	40	20
Big Bus	18	17	15	15	15	15	20	10
Rigid Truck (2 axles)	71	30	28	17	17	17	25	13
Rigid Truck (3 and 4 axles)	4	6	9	6	6	6	9	4
Rigid Truck and Drawbar Trailer	8	12	14	9	9	9	14	7
Horse + Semi Trailer (3 & 4 axles)	11	6	12	8	8	8	12	6
Horse + Semi Trailer (5 & 6 axles)	24	22	22	14	14	14	21	11
Horse + Semi Trailer (7 axles)	0	0	0	0	0	0	0	0
Horse + Two Semi Trailers	6	8	13	8	8	8	12	6
Other Vehicles	0	0	0	5	5	5	10	3

Traffic Count Data for T_005		Chingola-Jimbe				Start km 0.000		
Count year 1995						Length = 543.8 km		
Location	STA0000+3.500	STA0000+40.000	STA0000+168.000	STA0000+185.000	STA0000+350.000			
	All counts reduced to AADT							
Motorcycle and Scooter	5	2	2.5	3	1			
Passenger Car	150	79	120	67	6			
Micro Bus	35	17	25	0	1			
Light Delivery Vehicle	250	134	200	50	9			
Medium Delivery Vehicle	30	11	20	7	1			
Mini Bus	50	24	40	1	0			
Big Bus	10	5	7	5	3			
Rigid Truck (2 axles)	150	55	120	10	3			
Rigid Truck (3 and 4 axles)	25	2	20	6	1			
Rigid Truck and Drawbar Trailer	15	8	15	3	0			
Horse + Semi Trailer (3 & 4 axles)	12	9	12	0	0.5			
Horse + Semi Trailer (5 & 6 axles)	15	11	12	2	0			
Horse + Semi Trailer (7 axles)	2	0	2	0	0			
Horse + Two Semi Trailers	3	5	2	1	0			
Other Vehicles	3	0	3	0	0			

Traffic Count Data for T_006	Katete-Chanida					Start km 0.000		
Count year 1995						Length = 55.1 km		
Location	STA0000+1.000	STA0000+10.000						
	All counts reduced to AADT							
Motorcycle and Scooter	0	0						
Passenger Car	34	15						
Micro Bus	4	2						
Light Delivery Vehicle	21	10						
Medium Delivery Vehicle	5	2						
Mini Bus	14	5						
Big Bus	21	3						
Rigid Truck (2 axles)	27	12						
Rigid Truck (3 and 4 axles)	6	1.5						
Rigid Truck and Drawbar Trailer	9	3						
Horse + Semi Trailer (3 & 4 axles)	6	3						
Horse + Semi Trailer (5 & 6 axles)	12	3						
Horse + Semi Trailer (7 axles)	0	0						
Horse + Two Semi Trailers	6	3						
Other Vehicles	6	3						

TABLE 1

CLASSIFICATION TESTS

Kafue - Monze Road

MATERIALS SOURCE	ST KM	DESCRIPTION	% PASSING 3/4	7	36	200	ATTERBERG LL	PI	LIN. SHRINKAGE %	CLASSIFICATION
NATURAL GRAVEL:										
GS 1	47	Quartz gravel and laterite gravel								
GS 2	52	Quartz gravel and laterite gravel	100	29	12	9	26	9	4.7	A-2-4
GS 3	58	Decomposed rock, gravel and stones in a matrix of red soil	79	31	24	23	30	12	6.0	A-2-6
GS 4	60	Laterite gravel	100	39	36	33	21	6	3.3	A-2-4
GS 5	67	Laterite gravel					SP	SP	0.7	A-2-4
GS 6	106	A) Laterite gravel, fine	95	78	72	40	25	9	5.3	A-4
		B) Laterite gravel, coarse	61	35	19	11	24	7	4.0	A-2-4
		C) Quartz gravel	100	79	38	22	25	7	4.0	A-2-4
GS 7	112	Broken, decomposed limestone								
GS 8	140	Quartz and laterite, gravel	100	84	57	47	25	7	3.3	A-4
GS 9	147.5	Quartz gravel	91	28	15	11	Sp	Sp	1.3	A-1-a
GS 10	152.5	A) Laterite gravel	100	31	27	18	24	7	3.3	A-1-b
		B) Laterite and quartz gravel	100	58	54	45	Sp	Sp	1.3	A-4
		Gravel used for potholes	100	94	51	35	30	11	6.0	A-2-6
		Existing stabilized base	97	68	59	37	NP	NP	-	A-4
RIVER SAND:										
SS 1	42.5	Sand	96	76	24	6				A-1-b
			96	10	7	-				
SS 2	133	Sand	86	64	27	11				A-1-b

A4. Catalogue to Zambian Pavement Design Guide.

STANDARD DESIGN GUIDE

CHART NO: 1

PAVEMENT TYPE: FLEXIBLE

COURSE	MATERIAL	LEGEND	LAYER COEFF.	h min. (mm)	h max (mm)
BASE	NATURAL OR CRUSHED GRAVEL		a_2 = 0.12(1)	125	200
SUBBASE	NATURAL GRAVEL		a_3 = 0.11	100	250

	T4	T3	T2	T1
S2	27 — 42 SD h_1=20 a_1=0	59 — 82 SD h_1=20 a_1=0	69 — 96 AC h_1=80 a_1=0,35	80 — 109 AC h_1=100 a_1=0,35
S3	24 — 34 SD h_1=20 a_1=0	54 — 76 SD h_1=20 a_1=0	64 — 89 AC h_1=80 a_1=0,35	74 — 101 AC h_1=100 a_1=0,35
S4	21 — 29 SD h_1=20 a_1=0	49 — 70 SD h_1=20 a_1=0	59 — 82 AC h_1=50 a_1=0,35	68 — 94 AC h_1=80 a_1=0,35
S5	12 — 21 SD h_1=20 a_1=0	29 — 48 SD h_1=20 a_1=0	37 — 59 AC h_1=50 a_1=0,35	46 — 70 AC h_1=80 a_1=0,35

SUBGRADE	
CLASS	CBR %
S1	2 - 7
S2	8 - 14
S3	12 - 20
S4	18 - 30
S5	> 30

TRAFFIC	
CLASS	ESA x 10^6
T0	> 20
T1	8 - 20
T2	2.5 - 8
T3	0.5 - 2.5
T4	< 0.5

DETERMINATION OF DSN

$$DSN = \frac{SN_D \times SN_W}{\left[\frac{n_W}{12} \times SN_D^{2.8} + \frac{n_D}{12} \times SN_W^{2.8}\right]^{\frac{1}{2.8}}}$$

n_W = NUMBER OF RAINY MONTHS

n_D = NUMBER OF DRY MONTHS

TRAFFIC CLASS T

SUBGRADE CLASS S

SN_D	DSN	SN_W

h_1 SURFACING a_1

h_2 BASE a_2

h_3 SUBBASE a_3

$SN = \sum_i a_i h_i$

T5: LOW TRAFFIC, LESS THAN 150,000 ESA: AS FOR T4 USING h_{min}.

NOTE: (1) a_1=0,13 FOR CRUSHED GRAVEL WITH MIN 40% CRUSHED PARTICLES IN THE FRACTION RETAINED ON THE 2mm SIEVE

PAVEMENT TYPE: FLEXIBLE

COURSE	MATERIAL	LEGEND	LAYER COEFF.	h min. (mm)	h max (mm)
BASE	CRUSHED STONE		$a_2 = 0,14$	125	200
SUBBASE	NATURAL GRAVEL		$a_3 = 0,11$	100	250

	T4	T3	T2	T1
S2	27 / 42	59 / 82	69 / 96	80 / 109
	SD $h_1=20$ $a_1=0$	SD $h_1=20$ $a_1=0$	AC $h_1=50$ $a_1=0.35$	AC $h_1=80$ $a_1=0,35$
S3	24 / 34	54 / 76	64 / 89	74 / 101
	SD $h_1=20$ $a_1=0$	SD $h_1=20$ $a_1=0$	AC $h_1=50$ $a_1=0,35$	AC $h_1=80$ $a_1=0,35$
S4	21 / 29	49 / 70	59 / 82	68 / 94
	SD $h_1=20$ $a_1=0$	SD $h_1=20$ $a_1=0$	AC $h_1=50$ $a_1=0,35$	AC $h_1=80$ $a_1=0,35$
S5	12 / 21	29 / 48	37 / 59	46 / 70
	SD $h_1=20$ $a_1=0$	SD $h_1=20$ $a_1=0$	AC $h_1=50$ $a_1=0,35$	AC $h_1=80$ $a_1=0,35$

SUBGRADE	
CLASS	CBR %
S1	2 - 7
S2	8 - 14
S3	12 - 20
S4	18 - 30
S5	> 30

TRAFFIC	
CLASS	ESA x 10^6
T0	> 20
T1	8 - 20
T2	2.5 - 8
T3	0.5 - 2.5
T4	< 0.5

DETERMINATION OF DSN

$$DSN = \frac{SN_D \times SN_W}{\left[\frac{n_W}{12} \times SN_D^{2.8} + \frac{n_D}{12} \times SN_W^{2.8}\right]^{\frac{1}{2.8}}}$$

n_W = NUMBER OF RAINY MONTHS

n_D = NUMBER OF DRY MONTHS

TRAFFIC CLASS T

SUBGRADE CLASS S

SN_D | DSN | SN_W

h_1 SURFACING a_1

h_2 BASE a_2

h_3 SUBBASE a_3

$SN = \sum a_i h_i$

T5: LOW TRAFFIC, LESS THAN 150.000 ESA: AS FOR T4 USING $h_{min.}$

STANDARD DESIGN GUIDE

CHART NO.:

PAVEMENT TYPE: FLEXIBLE

COURSE	MATERIAL	LEGEND	LAYER COEFF.	h min. (mm)	h max (mm)
BASE	BITUMINOUS DENSE OR SEMI DENSE MACADAM		$a_2 = 0.20$	70	150
SUBBASE	NATURAL GRAVEL		$a_3 = 0.11$	100	250

	T4	T3	T2	T1
S2		59 / 82	69 / 96	80 / 109
		SD h_1=10 a_1=0.20	AC h_1=40 a_1=0.35	AC h_1=80 a_1=0.35
S3		54 / 76	64 / 89	74 / 101
		SD h_1=10 a_1=0.20	AC h_1=40 a_1=0.35	AC h_1=80 a_1=0.35
S4		49 / 70	59 / 82	68 / 94
		SD h_1=10 a_1=0.20	AC h_1=40 a_1=0.35	AC h_1=80 a_1=0.35
S5				46 / 70
				AC h_1=80 a_1=0.35

SUBGRADE	
CLASS	CBR %
S1	2 - 7
S2	8 - 14
S3	12 - 20
S4	18 - 30
S5	> 30

TRAFFIC	
CLASS	ESA x 10^6
T0	> 20
T1	8 - 20
T2	2.5 - 8
T3	0.5 - 2.5
T4	< 0.5

DETERMINATION OF DSN

$$DSN = \frac{SN_O \times SN_W}{\left[\frac{n_W}{12} \times SN_O^{2.8} + \frac{n_D}{12} \times SN_W^{2.8}\right]^{\frac{1}{2.8}}}$$

n_W = NUMBER OF RAINY MONTHS

n_D = NUMBER OF DRY MONTHS

TRAFFIC CLASS T

SUBGRADE CLASS S

SN_O | DSN | SN_W

h_1 SURFACING a_1

h_2 BASE a_2

h_3 SUBBASE a_3

$SN = \sum a_i h_i$

PAVEMENT TYPE: SEMIFLEXIBLE

COURSE	MATERIAL	LEGEND	LAYER COEFF.	: h_{min} (mm)	h_{max} (mm)
BASE	CEMENT TREATED GRAVEL, TYPE B		$a_2 = 0,14$	125	200
SUBBASE	NATURAL GRAVEL		$a_3 = 0,11$	100	250

	T4	T3	T2	T1
S2	27 — 42 h_1=20 SD a_1=0	59 — 82 h_1=20 SD a_1=0	69 — 96 (1)	80 — 109 h_1=100 AC a_1=0,35
S3	24 — 34 h_1=20 SD a_1=0	54 — 76 h_1=20 SD a_1=0	64 — 89 (1)	74 — 101 h_1=100 AC a_1=0,35
S4	21 — 29 h_1=20 SD a_1=0	49 — 70 h_1=20 SD a_1=0	59 — 82 (1)	68 — 94 h_1=100 AC a_1=0,35
S5	12 — 21 h_1=20 SD a_1=0	(2)	37 — 59 (1)	46 — 70 h_1=100 AC a_1=0,35

SUBGRADE	
CLASS	CBR %
S1	2 - 7
S2	8 - 14
S3	12 - 20
S4	18 - 30
S5	> 30

TRAFFIC	
CLASS	ESA x 10^6
T0	> 20
T1	8 - 20
T2	2.5 - 8
T3	0.5 - 2.5
T4	< 0.5

DETERMINATION OF DSN

$$DSN = \frac{SN_D \times SN_W}{\left[\left(\frac{n_W}{12} \times SN_D^{2.8}\right) + \left(\frac{n_D}{12} \times SN_W^{2.8}\right)\right]^{\frac{1}{2.8}}}$$

n_W = NUMBER OF RAINY MONTHS

n_D = NUMBER OF DRY MONTHS

TRAFFIC CLASS T

SUBGRADE CLASS S

SN_D — DSN — SN_W

h_1 SURFACING a_1

h_2 BASE a_2

h_3 SUBBASE a_3

$SN = \sum a_i h_i$

T5: LOW TRAFFIC, LESS THAN 150,000 ESA : AS FOR T4 USING h_{min}.

NOTES: (1) DESIGN SHALL BE AS SHOWN ON CHART NO. 7

(2) DESIGN SHALL BE AS SHOWN ON CHART NO. 5

PAVEMENT TYPE: SEMIFLEXIBLE

COURSE	MATERIAL	LEGEND	LAYER COEFF.	h_{min} (mm)	h_{max} (mm)
BASE	CEMENT TREATED GRAVEL TYPE A		$a_2 = 0.18$	125	175
SUBBASE	NATURAL GRAVEL		$a_3 = 0.11$	100	250

	T4	T3	T2	T1
S2	27 — 42 SD $h_1 = 20$ $a_1 = 0$	59 — 82 SD $h_1 = 20$ $a_1 = 0$	69 — 96 (1)	80 — 109 AC $h_1 = 100$ $a_1 = 0.35$
S3	24 — 34 SD $h_1 = 20$ $a_1 = 0$	54 — 76 SD $h_1 = 20$ $a_1 = 0$	64 — 89 (1)	74 — 101 AC $h_1 = 100$ $a_1 = 0.35$
S4	21 — 29 SD $h_1 = 20$ $a_1 = 0$	49 — 70 SD $h_1 = 20$ $a_1 = 0$	59 — 82 (1)	68 — 94 AC $h_1 = 100$ $a_1 = 0.35$
S5	12 — 21 SD $h_1 = 20$ $a_1 = 0$	29 — 48 SD $h_1 = 20$ $a_1 = 0$	37 — 59 (1)	46 — 70 AC $h_1 = 100$ $a_1 = 0.35$

SUBGRADE	
CLASS	CBR %
S1	2 - 7
S2	8 - 14
S3	12 - 20
S4	18 - 30
S5	> 30

TRAFFIC	
CLASS	ESA $\times 10^6$
T0	> 20
T1	8 - 20
T2	2.5 - 8
T3	0.5 - 2.5
T4	< 0.5

DETERMINATION OF DSN

$$DSN = \frac{SN_D \times SN_W}{\left[\frac{n_W}{12} \times SN_D^{2.8} + \frac{n_D}{12} \times SN_W^{2.8}\right]^{\frac{1}{2.8}}}$$

n_W = NUMBER OF RAINY MONTHS

n_D = NUMBER OF DRY MONTHS

TRAFFIC CLASS T

SUBGRADE CLASS S

SN_D | DSN | SN_W

h_1 SURFACING a_1

h_2 BASE a_2

h_3 SUBBASE a_3

$SN = \sum a_i h_i$

T5 LOW TRAFFIC, LESS THAN 150,000 ESA: AS FOR T4 USING h_{min}

NOTE: (1) DESIGN SHALL BE AS SHOWN ON CHART NO. 8

STANDARD DESIGN GUIDE

CHART NO: 6

PAVEMENT TYPE: FLEXIBLE

COURSE	MATERIAL	LEGEND	LAYER COEFF.	h min. (mm)	h max (mm)
BASE	CRUSHED STONE		$a_2 = 0.18$	125	200
SUBBASE	CEMENT OR LIME TREATED MATERIAL, TYPE C		$a_3 = 0.12$	100	200

	T4	T3	T2	T1
S2		59 / 82 — SD, h_1=20, a_1=0	69 / 96 — AC, h_1=50, a_1=0.35	80 / 109 — AC, h_1=80, a_1=0.35
S3		54 / 76 — SD, h_1=20, a_1=0	64 / 89 — AC, h_1=50, a_1=0.35	74 / 101 — AC, h_1=80, a_1=0.35
S4		49 / 70 — SD, h_1=20, a_1=0	59 / 82 — AC, h_1=50, a_1=0.35	68 / 94 — AC, h_1=80, a_1=0.35
S5		24 / 43 — SD, h_1=20, a_1=0	32 / 54 — AC, h_1=50, a_1=0.35 (1)	41 / 65 — AC, h_1=80, a_1=0.35 (1)

SUBGRADE	
CLASS	CBR %
S1	2 - 7
S2	8 - 14
S3	12 - 20
S4	18 - 30
S5	> 30

TRAFFIC	
CLASS	ESA × 10^6
T0	> 20
T1	8 - 20
T2	2.5 - 8
T3	0.5 - 2.5
T4	< 0.5

DETERMINATION OF DSN

$$DSN = \frac{SN_D \times SN_W}{\left[\frac{n_W}{12} \times SN_D^{2.8} + \frac{n_D}{12} \times SN_W^{2.8}\right]^{\frac{1}{2.8}}}$$

n_W = NUMBER OF RAINY MONTHS

n_D = NUMBER OF DRY MONTHS

TRAFFIC CLASS T

SUBGRADE CLASS S

SN_D	DSN	SN_W

h_1 SURFACING a_1

h_2 BASE a_2

h_3 SUBBASE a_3

$$SN = \sum_i a_i h_i$$

NOTE: (1) CEMENT TREATED SUBGRADE WHERE REQUIRED

PAVEMENT TYPE : FLEXIBLE

COURSE	MATERIAL	LEGEND	LAYER COEFF.	h_{min} (mm)	h_{max} (mm)
BASE	BITUMINOUS DENSE OR SEMI DENSE MACADAM		$a_2 = 0.20$	70	150
SUBBASE	CEMENT OR LIME TREATED MATERIAL TYPE C		$a_3 = 0.12$	100	220

	T4	T3	T2	T1
S2		59 — 82 SD $h_1 = 10$ $a_1 = 0.20$ (1) ($a_4 = 0.10$)	69 — 96 AC $h_1 = 40$ $a_1 = 0.35$ (1) ($a_4 = 0.10$)	80 — 109 AC $h_1 = 80$ $a_1 = 0.35$ (1) ($a_4 = 0.10$)
S3		54 — 76 SD $h_1 = 10$ $a_1 = 0.20$ (1) ($a_4 = 0.10$)	64 — 89 AC $h_1 = 40$ $a_1 = 0.35$ (1) ($a_4 = 0.10$)	74 — 101 AC $h_1 = 80$ $a_1 = 0.35$ (1) ($a_4 = 0.10$)
S4		49 — 70 SD $h_1 = 10$ $a_1 = 0.20$ (1)	59 — 82 AC $h_1 = 40$ $a_1 = 0.35$ (1)	68 — 94 AC $h_1 = 80$ $a_1 = 0.35$ (1)
S5		24 — 43 SD $h_1 = 10$ $a_1 = 0.20$ (2)	32 — 54 AC $h_1 = 40$ $a_1 = 0.35$ (2)	41 — 65 AC $h_1 = 80$ $a_1 = 0.35$ (2)

SUBGRADE	
CLASS	CBR %
S1	2 - 7
S2	8 - 14
S3	12 - 20
S4	18 - 30
S5	> 30

TRAFFIC	
CLASS	ESA $\times 10^6$
T0	> 20
T1	8 - 20
T2	2.5 - 8
T3	0.5 - 2.5
T4	< 0.5

DETERMINATION OF DSN

$$DSN = \frac{SN_D \times SN_W}{\left[\frac{n_W}{12} \times SN_D^{2.8} + \frac{n_D}{12} \times SN_W^{2.8}\right]^{\frac{1}{2.8}}}$$

n_W = NUMBER OF RAINY MONTHS

n_D = NUMBER OF DRY MONTHS

TRAFFIC CLASS T

SUBGRADE CLASS S

SN_D	DSN	SN_W

h_1 SURFACING a_1

h_2 BASE a_2

h_3 SUBBASE a_3

$SN = \sum a_i h_i$

NOTES: (1) GRANULAR SUBBASE BELOW STABILIZED MATERIAL WHERE REQUIRED

(2) CEMENT TREATED SUBGRADE WHERE REQUIRED

PAVEMENT TYPE SELECTABLE

COURSE	MATERIAL	LEGEND	LAYER COEFF.	h min. (mm)	h max (mm)
BASE	BITUMINOUS SEMI DENSE MACADAM		$a_2 = 0.20$	70	150
SUBBASE	CEMENT TREATED GRAVEL TYPE B		$a_3 = 0.16$	100	200

	T4	T3	T2	T1
S2			69 / 96	80 / 108
S3			64 / 89	74 / 101
S4			59 / 82	68 / 94
S5			32 / 54	41 / 65

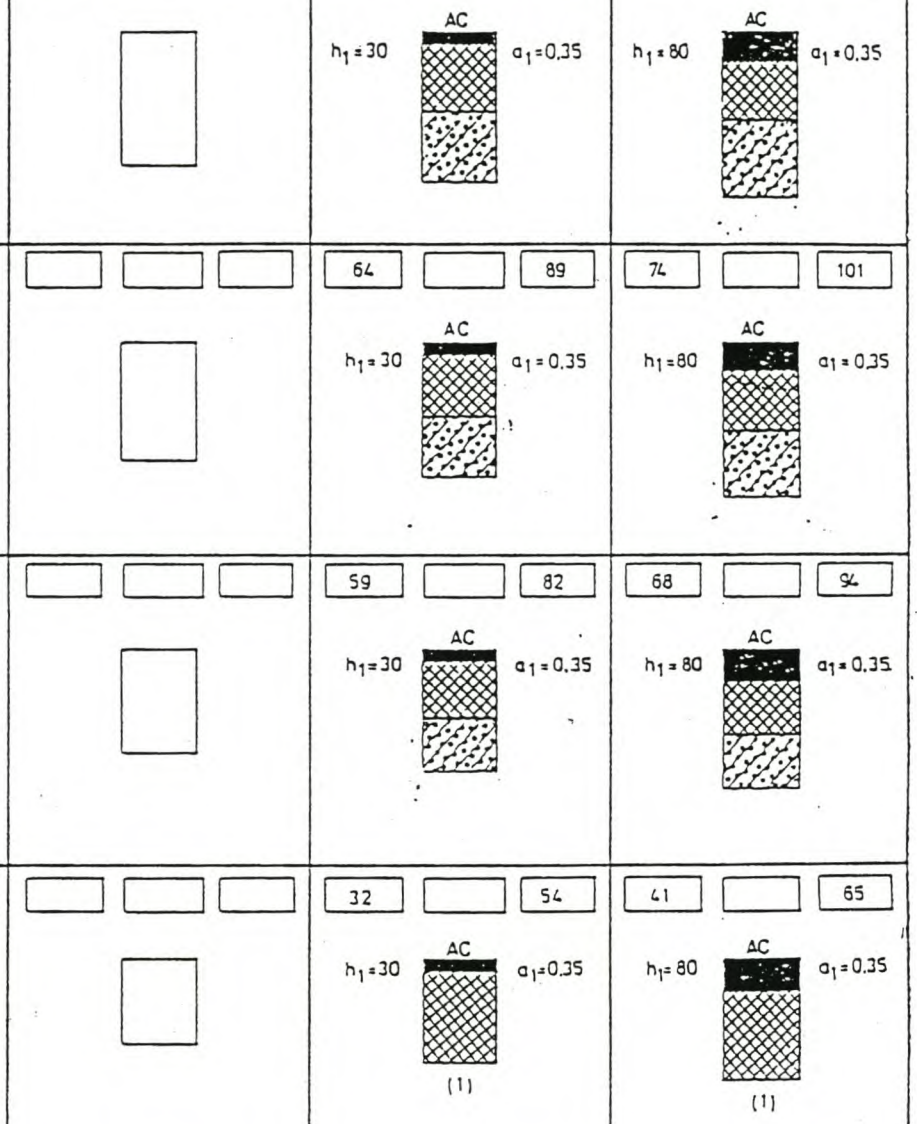

SUBGRADE	
CLASS	CBR %
S1	2 - 7
S2	8 - 14
S3	12 - 20
S4	18 - 30
S5	> 30

TRAFFIC	
CLASS	ESA x 10^6
T0	> 20
T1	8 - 20
T2	2.5 - 8
T3	0.5 - 2.5
T4	< 0.5

DETERMINATION OF DSN

$$DSN = \frac{SN_O \times SN_W}{\left[\frac{n_W}{12} \times SN_O^{2.8} + \frac{n_O}{12} \times SN_W^{2.8}\right]^{\frac{1}{2.8}}}$$

n_W = NUMBER OF RAINY MONTHS

n_O = NUMBER OF DRY MONTHS

TRAFFIC CLASS T

SUBGRADE CLASS S

SN_O | OSN | SN_W

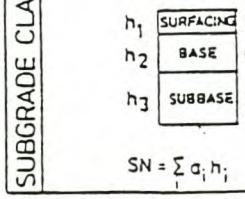

$SN = \sum a_i h_i$

NOTE : (1) CEMENT TREATED SUBGRADE WHERE REQUIRED